Effects of the Over-Expression of Neuronal Glutamate Dehydrogenase (GLUD1) on Mouse Brain Mitochondrial Function

By

Laura Anguiano

Submitted to the graduate degree program in Pharmacology and Toxicology and the Graduate Faculty of the University of Kansas in partial fulfillment of the requirements for the degree of Doctor of Philosophy.

_____

Dr. Elias K. Michaelis

_____

Dr. Mary L. Michaelis

_____

Dr. Rick T. Dobrowsky

_____

Dr. Honglian Shi

_____

Dr. Robert S. Cohen

July 13th 2012

The Dissertation Committee for Laura Anguiano

certifies that this is the approved version of the following dissertation:

Effects of the Over-Expression of Neuronal Glutamate Dehydrogenase (GLUD1) on Mouse Brain Mitochondrial Function

_____

Dr. Elias K. Michaelis

Date approved: July 13th 2012

ABSTRACT

Glutamate has been shown to lead to neurotoxicity and subsequent neurodegeneration through changes in synaptic function, loss of glutamatergic neurons, synapses, and dendrites. All of these characteristics are also observed during aging or in age-associated neurodegenerative diseases. To probe the effects of excess glutamate and determine if these effects might contribute to the morphological and functional changes associated with aging, our laboratory generated a transgenic mouse model that over-expresses the mitochondrial glutamate dehydrogenase 1 (GLUD1) gene. This transgene was only expressed in neurons through the use of the neuron-specific enolase promoter. The Glud1 Tg mouse model generated in our laboratory demonstrated significantly increased GLUD1 levels, GLUD activity, extracellular glutamate levels, and increased glutamate release after stimulation as compared to wild type (wt). There were also many significant morphological changes observed in the Tg mice including cell layer thinning in the hippocampus, cortex, and striatum, accompanied by synapse, neuronal, and dendrite losses. It was noted that the morphological changes observed were within specific brain regions; for example, the cerebellum showed no changes despite the fact that *Glud1* was over-expressed in all neuronal cells. In addition, the morphological changes in the various brain regions of the Tg mice were further exacerbated by advancing age.

Selective neuronal vulnerability has also been observed in many neurodegenerative diseases and has been found to occur in the cerebral cortex, hippocampus, and amygdala neurons of those with Alzheimer's disease. Therefore, the Glud1 Tg mice

may be used to probe the molecular and cellular pathways involved in selective neuronal vulnerability as it may relate to excess extracellular glutamate.

The studies presented in this dissertation focused on investigating the role of mitochondria in inducing region specific neuronal degeneration under the conditions of the combined effects of aging and excess glutamate activity in the central nervous system. Specifically, I have focused on whether there are changes in mitochondrial bioenergetics (Chapter 2), mitochondrial Ca^{2+} regulation (Chapter 3), and mitochondrial reactive oxygen species generation (Chapter 4) during the aging process in different brain regions in wild type and *Glud1* Tg mice.

Our studies demonstrated that there are altered mitochondrial electron transport system activities, mitochondrial calcium dishomeostasis, mitochondrial membrane potential, and generation of reactive oxygen species in the Tg as compared to wt mice. Complex I of the electron transport system is significantly lower in the Tg as compared to wt mice at 9 months in the cerebellum. In addition, the membrane potential in the Tg mice as compared to wt mice is 2-fold higher and the same results were demonstrated for the levels of superoxide. Mitochondrial calcium uptake in the Tg mice is 2-fold higher than wt mice at 9 months and significantly decreases across advances age. Taken together, these data suggest some adaptive and compensatory mechanisms might be taken place in the Tg mice as a result of the over-expression of the *Glud1* gene i.e. down-regulated complex I activity and decreased calcium uptake across age.

ACKNOWLEDGEMENTS

First and foremost, I would like to thank Dr. Elias K. Michaelis for his guidance and support throughout my graduate career. Thank you for not only taking a chance on me once, but twice. Your understanding and patience as my mentor immensely impacted my ability to continue on with motivation and confidence. I would also like to thank Dr. Mary Lou Michaelis for the countless times she listened to my seminars and laboratory presentations and continued to provide support and feedback. The remaining members of my committee: Drs. Rick Dobrowsky; Robert Cohen, and Honglian Shi, thank you for all your time and continued feedback and support. I would also like to thank the entire department of Pharmacology and Toxicology for your investment in my future.

To Dr. Ranu Pal, thank you for not only being a colleague, but a trusted friend and smiling face. Thank you for never letting me give up and for your faith in my abilities. To Drs. Xinkun Wang and Dongwei Hui, thank you for all of your guidance and patience in dealing with the many questions I continuously bombarded you with. Thank you to the members of Dr. Mary Lou Michaelis's lab, Jennifer Bean, Misty Bechtel, and Dr.Lei Jiang for all of your help and support. In addition, thank you to Dr.Abdul Baki Agbas for being a crucial and motivational person in my life at the beginning of such a long journey.

To my dear lab friend Dr.Heather Menchen who continuously gave me hope and support not only on an intellectual, but personal level. Thank you. To the entire Leary family, Cynthia, Steve, Ryan, and Camden. Thank you for giving me hope that honest

and good people still do exist and for being such an inspiring group of people for me and my daughters.

To my friends Jennifer Tyler and Sarah Harness. Thank you for pushing me and believing in me at times that I did not believe in myself. You two are the true definition of a friend that will drop everything to come to the aide of another friend. For that and for your continued support, I thank you.

To my dear friend Dr. Cibele Pinto. Who would have guessed that our friendship would have outlasted our graduate career when we met in the departmental office at such a young age. You have been one of the strongest and uplifting influences that I have had in my life and for that no words will ever be able to express my gratitude. Thank you for being there for me and calling me more than a friend, but a sister.

To my cousins Patricia Rodriguez, Mirta Chavez, Nora Rodriguez, and Oscar Rodriguez. You all are the true embodiment of family and it is through your constant support and guidance that I found myself out of some of the hardest times in my life. Thank you for being a part of my life and for continuing to instill in me the morals and values our families raised us with.

To my Aunt Martha Rodriguez and Uncle Oscar Rodriguez. You two were my knights in shining armor that continuously reminded me that there is a light at the end of the tunnel and that more importantly, “God never gives us more than we can handle”. Thank you for reminding me to stay close to my faith and always follow my heart and dreams.

To my mother, Margaret Anguiano. Thank you for instilling in me something to this day that I cannot even describe, but know I owe my successes and

accomplishments in life to. Thank you for always making me feel as if I can do no wrong and for always being my number one cheerleader and more importantly for always stressing the importance of an education to me.

Last and most importantly to my daughters, Alexandria and Abbygail. Thank you for dealing with me these last few years in a time of stress and a bit of chaos. Thank you for the many, many times Mommy had to study and could not devote that time to my girls. Your patience and understanding and support drove me continue and press on at times I wanted to give up. I hope that life awards you two the many blessings and opportunities that I have been cherished to receive, but more importantly that you remember that the best things in life must be worked for.

Throughout my college career I was faced with the same question over and over by a multitude of people. “How do you do it?” At the time I did not have an answer for such a question, but now I know that the answer is a very simple and short one. The answer is, “Family, Friends, and Faith”.

TABLE OF CONTENTS

List of Tables and Figures

Chapter One: The Role of Glutamate, Glutamate Dehydrogenase, and Mitochondria in the Brain

1. NEUROTRANSMISSION IN THE BRAIN

Neurons communicate to one another by transferring information from the axons of one neuron to the dendrites of another. This process of neurotransmission is not direct and involves the release of chemicals into the space between the axon and dendrite, the synapse. The neurotransmitters bind to receptors located within the cell membranes of dendrites which either inhibit or stimulate an electrical response in the receiving cell's dendrites. See figure 1 for an illustration of the structure. The type of response is dependent on the type of neurotransmitter released.

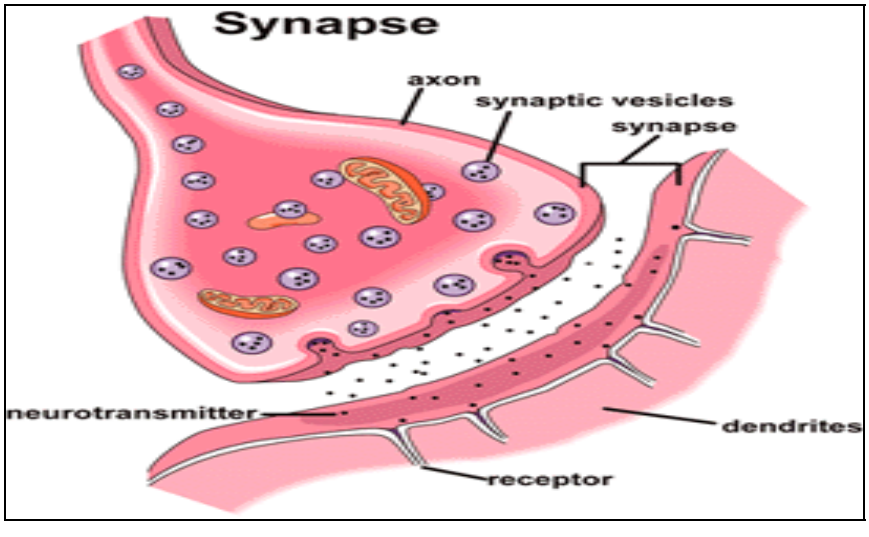

Figure 1 Pre and post synaptic structure illustrating neurotransmitter release.

The neurotransmitters in the brain can be divided into three main groups, amino acids, peptides, and monoamines. The most prevalent neurotransmitter in the brain is glutamate, which functions as an excitatory molecule and is present at well over 90% of excitatory synapses in the human brain (Fonnum 1984).

Glutamatergic System

The role of glutamate in processes such as synaptic transmission, plasticity, and learning has been well established by a multitude of studies (Clark, Magnusson et al. 1997); (Barnes 1979); (Wenk and Barnes 2000); (Levy and Steward 1979; Cotman and Monaghan 1988; Francis, Sims et al. 1993; Laube, Hirai et al. 1997). Excessive glutamate can lead to hyper-activation of glutamate receptors, and this has been demonstrated to lead to increased calcium ions (Ca^{2+}) entering the postsynaptic cell (Pull, McIlwain et al. 1970). The high Ca^{2+}concentration in post-synaptic cells can lead to cell death by activating proteases, lipases, nitric oxide synthase, and enzymes that destroy the cell by necrosis or apoptosis (Olney, Ho et al. 1971) (Meldrum and Garthwaite 1990) (Lipton 1999), resulting in a loss of neuronal structuel and synapses (Palmada and Centelles 1998) (Aarts, Wei et al. 2003) (Peters, Sethares et al. 2008).

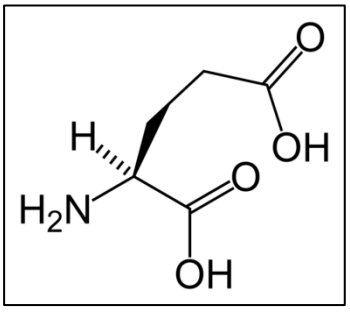

Figure 2 L-glutamate chemical structure

Glutamate is used as the neurotransmitter at fast excitatory synapses in the brain and spinal cord and figure 2 illustrates glutamate's chemical structure. In addition, it is also used at "plastic" synapses, i.e. synapses that are capable of decreasing or increasing in strength. These plastic synapses are thought to be

the main memory storage elements in the brain and therefore glutamate is involved in processes such as memory formation and learning. In addition, glutamatergic neuro-transmission is involved in a wide array of other cellular processes including energy metabolism, protein synthesis, and ammonia metabolism. Due to its multi-purpose role, intracellular glutamate content is high ~10 mmol/kg weight (Francis, Sims et al. 1993) (Debanne, Daoudal et al. 2003).

Biosynthesis

Glutamate is synthesized in the brain through a variety of different reactions involving different enzymes. Major contributors are the mitochondrial enzyme glutaminase which converts glutamine to glutamate (Procter, Palmer et al. 1988) and aspartate aminotransferase which transaminates □-ketoglutarate to produce glutamate in the cytosol. Table 1 shows a listing of these and other metabolic reactions leading to glutamate synthesis.

Table 1 List of chemical reactions leading to glutamate synthesis.

Reactants	Products	Enzymes
Glutamine + H_2O	→ Glutamate+ NH_3	GLS, GLS2
NAcGlu + H_2O	→ Glutamate + Acetate	(unknown)
α-ketoglutarate + NAD(P)H + NH_4^+	→ Glutamate + $NAD(P)^+$ + H_2O	GLUD1, GLUD2
α-ketoglutarate + α-amino acid	→ Glutamate + α-keto acid	transaminase
1-Pyrroline-5-carboxylate + NAD^+ + H_2O	→ Glutamate + NADH	ALDH4A1
N-formimino-L-glutamate + FH_4	→ Glutamate + 5-formimino-FH_4	FTCD

In addition, mitochondrial glutamate dehydrogenase (Glud1) catalyzes an oxidative deamination of glutamate to form α-ketoglutarate (Fig.3).

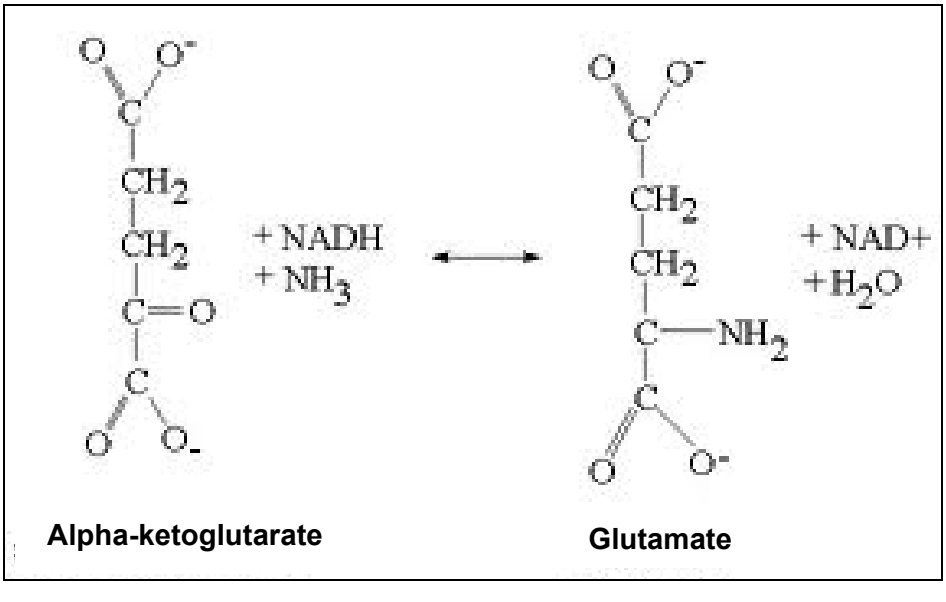

Figure 3 Reversible reaction catalyzed by glutamate dehydrogenase.

The α-ketoglutarate is transported out of mitochondria by the keto-dicarboxylic acid carriers, as mentioned earlier, and is transaminated by aspartate aminotransferase to produce glutamate. This glutamate is stored in synaptic vesicles until nerve impulses trigger release of glutamate from the pre-synaptic cell. Even though a variety of enzymes and reactions are involved in the biosynthesis of glutamate in nerve endings (Table 1), studies have shown that the releasable endogenous glutamate pool in cerebellar neurons is dependent on α-ketoglutarate formed by glutamate dehydrogenase (GLUD) (Palaiologos, Hertz et al. 1989).

Once released from the vesicles, glutamate may be removed from the synapse by rapid reuptake systems located on the pre-and post-synaptic elements and on astrocytes. In astrocytes, it is metabolized to glutamine by glutamine synthase. Glutamine is released by astrocytes and can be taken up by neurons once again for recycling into glutamate (Danbolt 2001). Figure 4 illustrates the pathways of glutamate biosynthesis in nerve endings and the central role of glutamate dehydrogenase in contributing to the pool of releasable glutamate. As illustrated, glutamate plays a pivotal role in cell metabolism being synthesized by the transamination of α-ketoglutarate (also known as 2-oxoglutarate), an intermediate in the Krebs cycle (TCA cycle). The resulting alpha-ketoacid products from this reaction can also contribute as fuel for further metabolic processes.

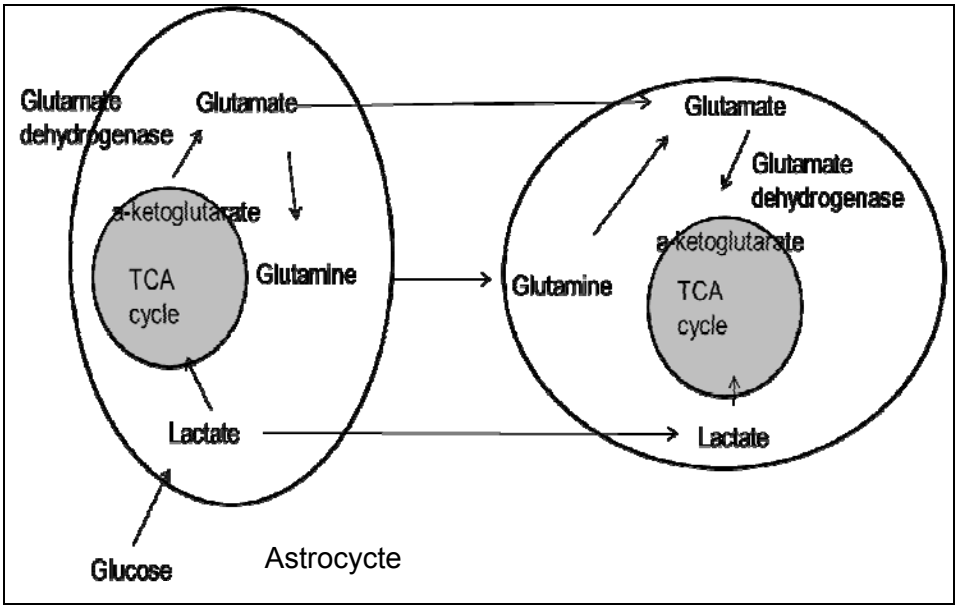

Figure 4 Major pathways of glutamate synthesis at nerve endings.

Glutamate Interaction with its Receptors

Once released from the pre-synaptic cell, glutamate is free to bind to its receptors on the post-synaptic cell. Glutamate receptors exist primarily in the central nervous system and are found on both neuronal and glial cells and both cell types are therefore influenced by this molecule. These receptors are localized on the dendrites of postsynaptic cells (Steinhauser and Gallo 1996) (Palmada and Centelles 1998). Glutamate receptors are divided into two types based on the mechanism by which their activation gives rise to a postsynaptic current (Cotman and Monaghan 1988). These two types include metabotropic and ionotropic receptors (Hollmann and Heinemann 1994) (Sprengel and Seeburg 1993) (Ozawa, Kamiya et al. 1998) and are further divided into sub-types based on specific agonists that bind to the receptor.

Ionotropic Receptors

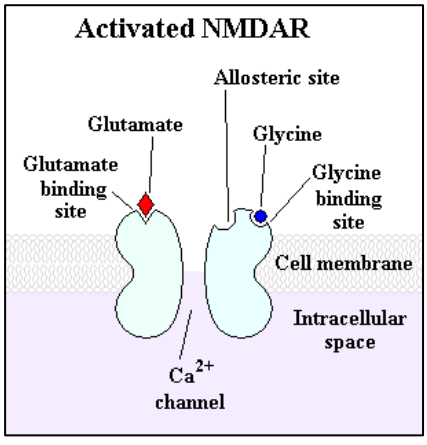

Figure 5 Activated NMDA receptor.

Ionotropic glutamate receptors are ligand-gated nonselective cation channels that allow K+, Na^{+}, and Ca^{2+} ions to flow through once glutamate binds to the receptor (Palmada and Centelles 1998). This ion flow triggers an excitatory postsynaptic current (EPSC) which is a depolarizing current. If the depolarizing current is strong enough and reaches threshold it activates an action potential in the postsynaptic neuron. All three sub-types of ionotropic receptors; N-methyl-D-aspartate (NMDA), α-amino-3-hydroxyl-5-methyl-4-isoxazole-propionate (AMPA), and Kainate bind glutamate. NMDA receptors are permeable to calcium and it is the flow of calcium that is thought to cause long-term potentiation (LTP) by transducing signaling cascades and regulating gene expression (Ozawa, Kamiya et al. 1998). Long term potentiation is the process that underlies learning and memory, a form of synaptic strengthening following brief, high frequency stimulation (Francis 2003) (Baudry 2001). Figure 5 illustrates an example of an activated NMDA receptor with the glutamate and glycine binding sites and the channel which allows for entry of calcium ions. NMDA receptors have also been demonstrated to play a key role in the excitotoxic process. Over-activation of NMDA receptors triggers excessive entry of calcium (Ca^{2+}) initiating a series of nuclear and cytoplasmic processes that promote neuronal cell death, i.e. Ca^{2+} activated proteolytic enzymes, Ca2+/calmodulin kinase II (CaM-KII), and many enzymes are phosphorylated which increases their activity (Del Bigio 2000)

(Otmakhov, Tao-Cheng et al. 2004) (Sanhueza, Fernandez-Villalobos et al. 2011) (Ashpole, Song et al. 2012) and taken together all of these mechanisms can lead to cell damage and/or death (Choi 1992) (Aarts, Wei et al. 2003).

2. ROLE OF THE GLUTAMATERGIC SYSEM IN AGING AND AGE-ASSOCIATED DISEASES

Changes in the glutamatergic system throughout aging have shown that extracellular glutamate levels increase with age in specific brain regions, specifically the hippocampus (Donzanti, Hite et al. 1993) (Freeman and Gibson 1987) (Kaiser, Schuff et al. 2005) (Potier, Billard et al. 2010), but decreasing in regions such as the cerebral cortex (Saransaari and Oja 1995). Therefore, changes in glutamate concentrations with age are region specific. More examples include the striatum where glutamate concentrations increase in the lateral, but not the medial striatum of rats (Donzanti, Hite et al. 1993). Beyond the observed increases in extracellular glutamate with advancing age, there is a steady decline in many cognitive processes, specifically a marked dysfunction of primate prefrontal cortex leading to a decreased ability to perform cognitive tasks (Hedden and Gabrieli 2004). An underlying cause of the decline in these cognitive functions is thought to be due to a loss and/or damage of glutamatergic synapses which has been shown to occur in aging

Image analysis shows synapse losses in normal aging cortex

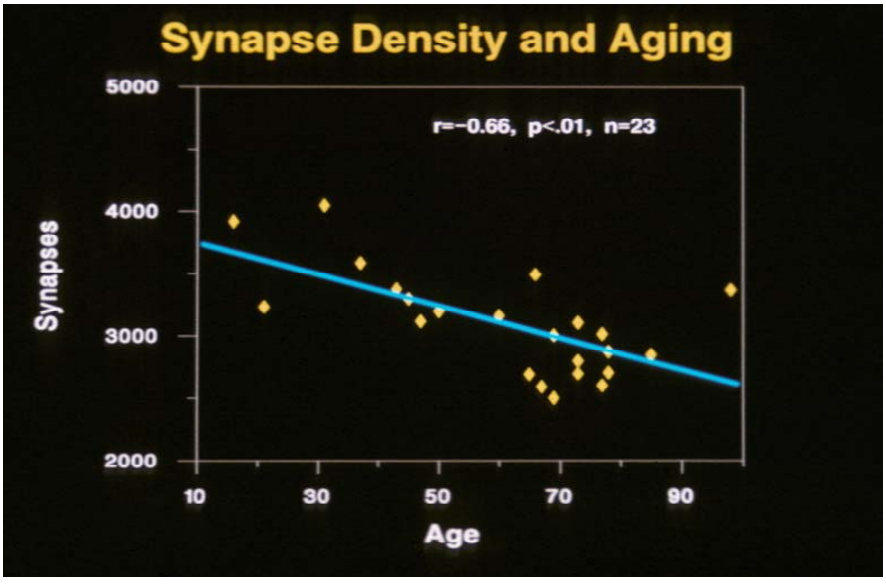

Figure 6 Image analysis showing synapse losses in normal aging cortex.

From: Structure of the Human Brain in Normal Aging and in Alzheimer's Disease.

(Peters, Sethares et al. 2008). Electron microscopic studies have shown that in specific layers of the frontal cortex in rhesus monkeys there is an overall loss of about 30% of excitatory (glutamatergic) synapses with age (Peters, Sethares et al. 2008). In the same study, behavioral tests were carried out to assess the cognitive status of the monkeys and these results showed that there was a strong correlation between excitatory (glutamatergic) synapse loss and cognitive impairment (Peters, Sethares et al. 2008). Figure 6 illustrates the correlation between synapse loss and aging in normal cortex. With an increase in age there is an increase in synapse loss.

Age-associated Diseases

Some of the strongest evidence supporting the role of the glutamatergic system in age-associated diseases comes from histopathological data. In these studies, brains from patients with AD exhibited atrophy in the temporal, frontal, and hippocampal/entorhinal cortex regions (Francis 2003). The atrophy was the result of a loss of pyramidal neurons and their synapses. These changes also correlated with the degree of dementia in the patients suffering from the disease. The highest correlation coefficient among dementia and individual neurochemical and neuroanatomical measures was the correlation between synapse loss and dementia (Fig. 7) (Francis 2003).

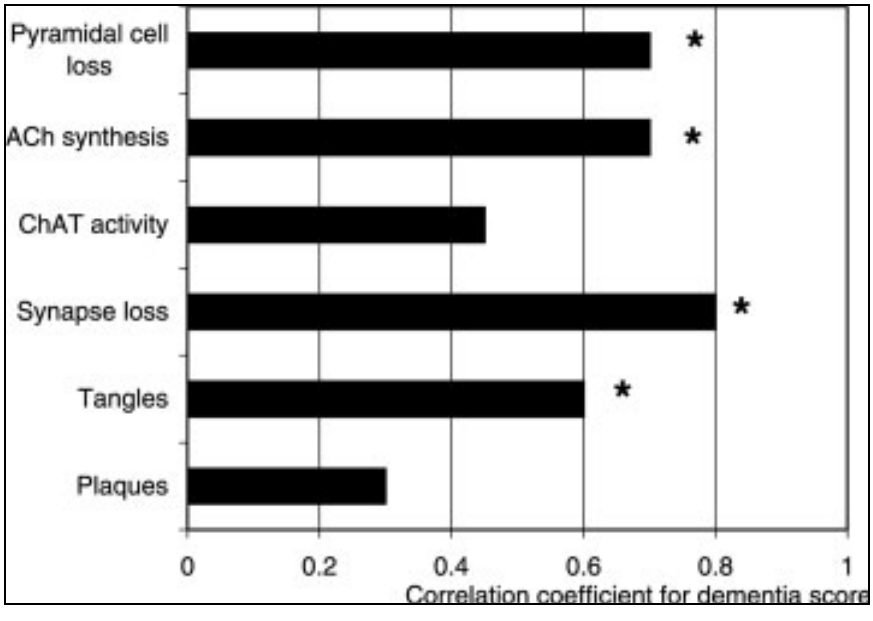

Figure 7 Magnitude of correlations between various markers of the Glutamatergic and cholinergic system and the dementia rating. Asterisks indicate statistically significant relationships. Francis et al. 2003

In 1993 Francis et al. provided biochemical evidence that glutamate is the neurotransmitter used by the cells lost in AD. Therefore, the conclusion was that due to the specific cell and synapse loss, glutamatergic neurons and activity are

decreased in AD (Francis, Sims et al. 1993). This decrease or dysfunction in excitatory neurotransmission might be part of the clinical manifestations seen in Alzheimer's disease, i.e., decreased cognitive abilities such as memory and learning.

Conclusion

To probe the effects of excess glutamate and determine if these effects might contribute to aging, three different types of animal models have been generated to investigate the effects of excess extracellular glutamate concentrations in the brain of organisms. The first two types of animal models generated in excess glutamate in the extracellular space by knocking down the glutamate transporters *Slc1a2* (*Eaat2 or Glt-1*) and *Slc1a3* (*Eaat1 or Glast*) (Matsugami, Tanemura et al. 2006) (Rothstein, Dykes et al. 1996). The third animal model resulted in excess glutamate by knocking down the tuberous sclerosis complex-1 gene (*Tsc1*) (Zeng, Ouyang et al. 2007). All three of these animal models have been shown to lead to an excess accumulation of glutamate with increases between 1.5 and 32-fold the normal levels of extracellular glutamate (Matsugami, Tanemura et al. 2006) (Rothstein, Dykes et al. 1996) (Zeng, Ouyang et al. 2007). Even though the generation of these animal models did lead to an excess accumulation of glutamate, there were limitations in their. The first two animal models resulted in excessive brain damage and embryonic lethality and the third model resulted in dramatic reductions in the life span of the mutant mice. These severe limitations have therefore made these animal

models unsuitable for studying the effects of chronic, aging-related excess glutamate formation and release in the brain. The three animal models described above would not accurately mimic the transient and moderate increases in extracellular glutamate that might occur throughout a prolonged period of the life of an organism. The goal of our laboratory was to generate a mouse model that would result in transient and moderate increases in extracellular glutamate. This model would allow us to probe the molecular changes within neurons in response to the presence of excess extracellular glutamate throughout development and during the aging process.

3. GLUTAMTE DEHYDROGENASE TRANSGENIC MOUSE MODEL

Rationale

Two types of transgenic mice were generated, one over-expressing the cytoplasmic enzyme alanine aminotransferase, and the other the mitochondrial enzyme glutamate dehydrogenase 1 (GLUD1). Both transgenes were expressed only in neurons through the use of the neuron-specific enolase promoter, but only the GLUD1 transgenic line resulted in mice that overproduced and over-released glutamate at the synapse (Bao, Pal et al. 2009).

Glutamate dehydrogenase

The enzyme glutamate dehydrogenase is a mitochondrial matrix enzyme which plays a key role in glutamate metabolism and energy homeostasis. It is present in highest concentrations in the nervous tissue as compared with other tissues. Glutamate dehydrogenase displays an energy sensing mechanism,

which allows enzyme activation under states of low cellular energy. Upon activation in the neuron, it catalyzes the oxidative deamination of glutamate to α-ketoglutarate. The α-ketoglutarate serves as a substrate for the TCA cycle and when transported back into the cytoplasm is converted into glutamate. Therefore, in neurons glutamate dehydrogenase is involved in energy production and the metabolism of glutamate (Palaiologos, Hertz et al. 1989). In the astrocyte it catalyzes the reductive amination of α-ketoglutarate to form glutamate. In addition, it is involved in a major pathway for cerebral ammonia generation. Cooper et al., demonstrated that a small amount of [^{13}N] ammonia in rat brain is incorporated into glutamate indicating that the cerebral glutamate dehydrogenase reaction more likely favors glutamate oxidation (ammonia production) (Cooper 2012). Taken together, these studies demonstrate that in brain an increase in glutamate dehydrogenase activity leads to excess glutamate formation. These studies did not however differentiate between neuronal vs. glial glutamate dehydrogenase activity. The effect of up or down regulation of glutamate dehydrogenase activity in neurons vs. glial cells may have different results. Our goal was to create a transgenic animal model that would over-express the glutamate dehydrogenase gene, specifically in neurons. The neuronal targeted over-expression of glutamate dehydrogenase would lead to excess glutamate and would allow us to probe the effects of excess extracellular glutamate on neurons, specifically, the molecular and cellular pathways that may lead to altered metabolic states, synapse loss, neuronal loss, structural modifications and function.

Generation and characterization of the *Glud1* mouse model

The transgenic mouse model was generated by over-expressing the *Glud 1* gene in central nervous system neurons. Briefly, "Tg mice were generated by microinjecting fertilized oocytes from super-ovulating C57BL6/SJL hybrid mice with linearized DNA containing the cDNA of mouse *Glud1*. The cDNA was placed under the control of the *Nse* promoter." (Bao, Pal et al. 2009). The mouse model was characterized in terms of GLUD1 activity, amino acid concentrations, synaptic glutamate release, stimulus-evoked glutamate release *in vivo,* neuronal structure, effects of age on dendrite structure and neuronal numbers, functional changes in neurons, alterations in spine density and morphology of neurons. The results of these characterizations are illustrated in figure 8.

Biochemical and Cellular Characteristics	Brain Region/Subcellular Fraction	Tg vs. wt (↑-increase; ↓-decrease; →-no change)
GLUD Activity (Biochemical)	Whole brain homogenate	↑
	Whole brain P2	↑↑
	Whole brain synaptosomes	↑↑↑
GLUD Activity (Histochemical)	Hippocampus	↑↑
GLUD Immunoreactivity	Hippocampus	↑↑
	Cortex	↑↑
	Cerebellum	↑↑
	Striatum	↑↑
Glutamate Levels	Striatum	↑
	Hippocampus	↑
Neuronal Loss	CA1 Hippocampus	↓↓
	CA3 Hippocampus	→
	Dentate Gyrus	↓↓
	Motor/Somatosensory Cortex	↓
	Spinal Cord Motorneurons	↓↓
MAP2A Dendrite Labeling	CA1 Hippocampus	↓↓
	CA3 Hippocampus	→
	Motor/Somatosensory Cortex	↓↓
	Striatum	↓↓
Depolarization-induced Glutamate Release	Striatum	↑↑
Synaptic Glutamate Release	CA1 Hippocampus	↑↑↑
Spine Density	CA1 Hippocampus	↓↓
Synaptophysin Labeling of Nerve Terminals	CA1 Hippocampus	↓↓
Transient and Sustained LTP	CA1 Hippocampus	↓↓

Figure 8 Summary of differential characteristics of Glud1 Tg mice compared to with wt C57BL6 mice. Bao, X et al., 2009.

Figure 8 demonstrates that the Tg mice exhibited higher GLUD1 levels and higher enzyme activity (35-40%) as compared with wt littermates. These results were obtained using *in vitro* biochemical assays and *in situ* histochemical detection assays. A magnetic resonance spectroscopy (MRS) approach was used to measure amino acid concentrations in the brains of living mice. The results demonstrated that in both hippocampus and striatum, the concentration of glutamate was significantly increased, but by a relatively modest amount. Having demonstrated the increases in glutamate, our laboratory also examined whether

the Tg mice would have increased glutamate release *in vivo* after stimulus application. A self-referencing multi-electrode array for measuring glutamate release and reuptake *in vivo* was used and the results demonstrated that after stimulus application glutamate release was higher in the Tg mice while glutamate reuptake was not significantly different from that of the wt mice. In addition, the increase of stimulus-evoked glutamate occurred through synaptic release at glutamatergic synpases as the data demonstrated significantly higher increases (5-fold increase) in both frequency and amplitude(2-fold increase) of miniature excitatory postsynaptic currents (mEPSCs) in *Glud1* as compared with wt mice (Bao, Pal et al. 2009).

Many significant morphological differences were observed between the Tg and the wt mice. For example, there was cell layer thinning observed in the Tg mouse hippocampus CA1 pyramidal cell layer (Fig. 9A, B) and the ventral granule cell layer of the dentate gyrus (Fig. 9C, D), and significant decreases in the number of neurons in the CA1 region of the hippocampus of the Tg mice as compared with that of the wt mice (Bao, Pal et al. 2009).

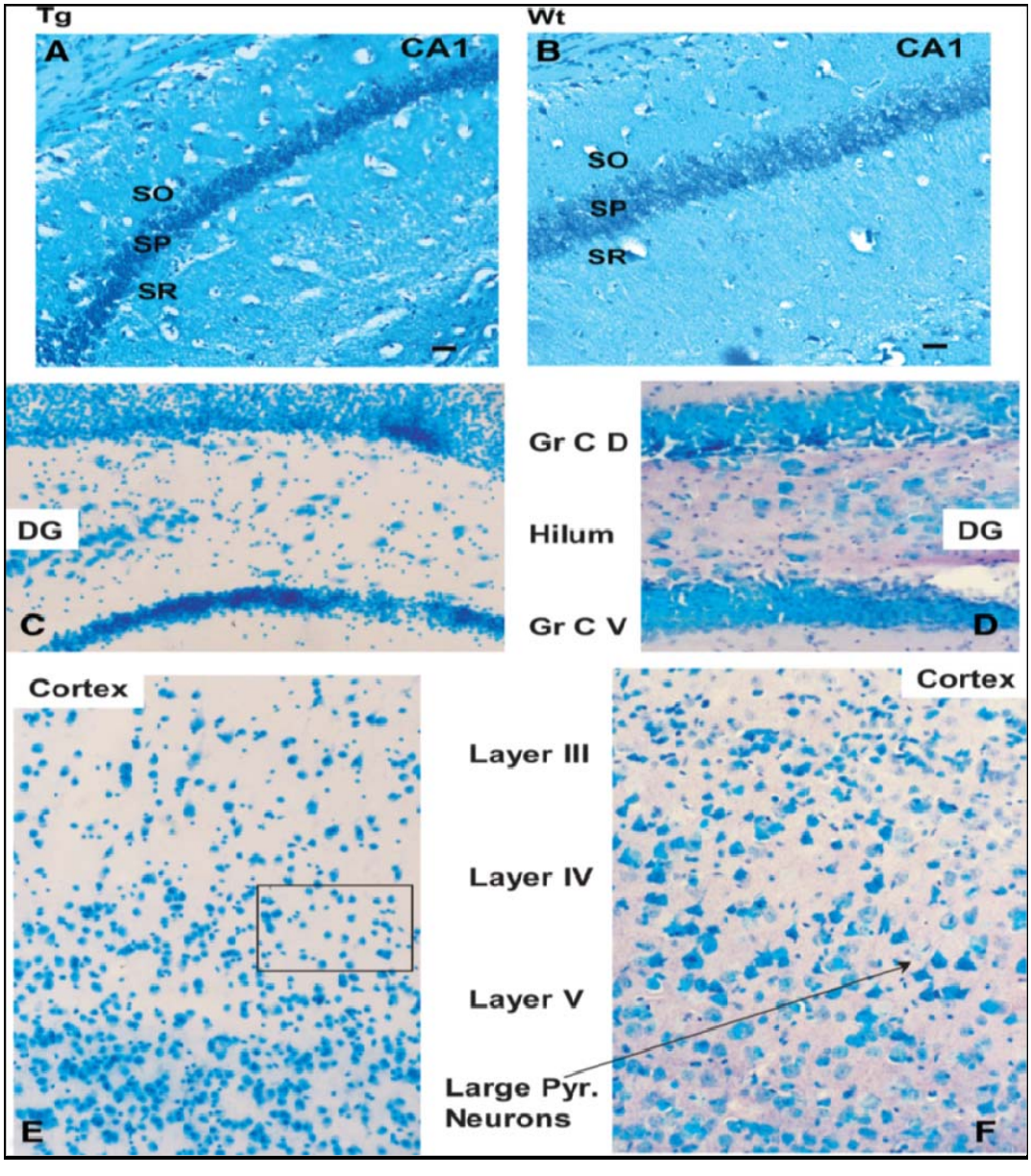

Figure 9 Neuronal structure of Tg Glud1 and wt mice. Histological sections through the hippocampus CA1 (*A*, *B*), dentate gyrus (*C*, *D*), and cerebral cortex (*E*, *F*) of 16-month-old Tg (*A*, *C*, *E*) and wt (*B*,*D*, *F*) mice. Bao, et al., 2009. Sections were stained with methylene blue. N=5

In addition to changes in hippocampus tissue, loss of pyramidal cells was seen in layers III-V of the primary motor/somatosensory cortex of Tg mice (Figure 9E, F). A finding of interest was that despite the significant changes and losses in the Tg mice in cortical and hippocampal regions, the cerebellum did not demonstrate any changes. The morphological changes observed in the Glud1 Tg mice are similar to those observed after acute injections of a glutamate transport inhibitor. These findings may serve as indirect evidence that the observed morphological changes could be a result of altered Glud1 and increased glutamate levels.

In addition to significant changes in neurons, robust changes in dendrite labeling were also observed. There were significant decreases in dendrite labeling by anti-MAP2A antibodies in the CA1 region of the hippocampus in the Tg mice (figure 10), as well as the striatum. The decreases in dendrite labeling by MAP2A are similar to those observed after inhibition of glutamate transporters which results in increases in extracellular glutamate, providing more indirect evidence that these morphological changes are the result of excess extracellular glutamate.

In addition to the significant morphological differences in neuronal elements in the brain between Tg and wt mice, functional changes in neurons were also observed. Specifically, the slope of excitatory postsynaptic potentials fEPSPs in the post-high frequency stimulation period were significantly lower in the Tg mice. A contributing factor to this observation could be the significant decrease in spine density in dendrites of the hippocampus CA1 region neurons observed in Tg mice.

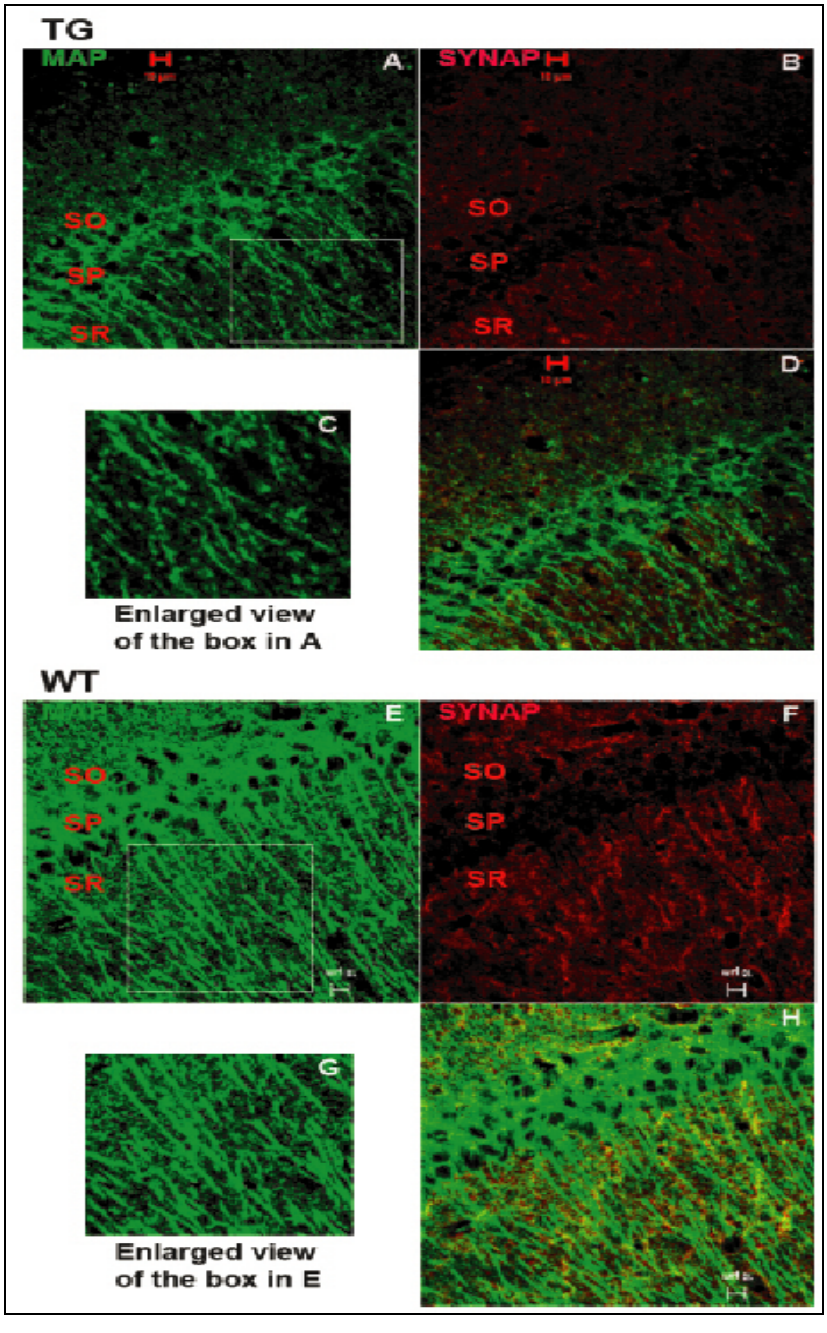

Figure 10 Immune labeling of MAP2A (green) and synaptophysin (red) reactive sites in CA1 of hippocampus of 12-month-old wt (A-D) and Tg (E-H) mice. C,G Enlarged views of dendrite labeling by anti-MAP2A antibodies in the SO of CA1 pyramidal neurons. D,H Superimposed images of MAP2A- and synaptophysin-immunoreactive sites. Scale bars, 10 mm. Bao et al. 2009

Many studies have shown that with age there is a decrease in neurons and synapses (Peters, Sethares et al. 2008) and an increase in extracellular

glutamate (Donzanti, Hite et al. 1993). When dendrite labeling using MAP2A antibodies was measured in the CA1 region of the hippocampus of Tg and wt mice, there was a significant decrease in labeling in Tg, but not in wt, mice across age (Figure 11A). In addition, comparisons between the two genotypes at each age (6, 11, and 20 months) revealed significant differences (Bao, Pal et al. 2009). Cell counts were also performed in the hippocampus CA1 and CA3 regions and demonstrated significant decreases in the Tg mice as compared to wt (Fig 11B) and in every age group.

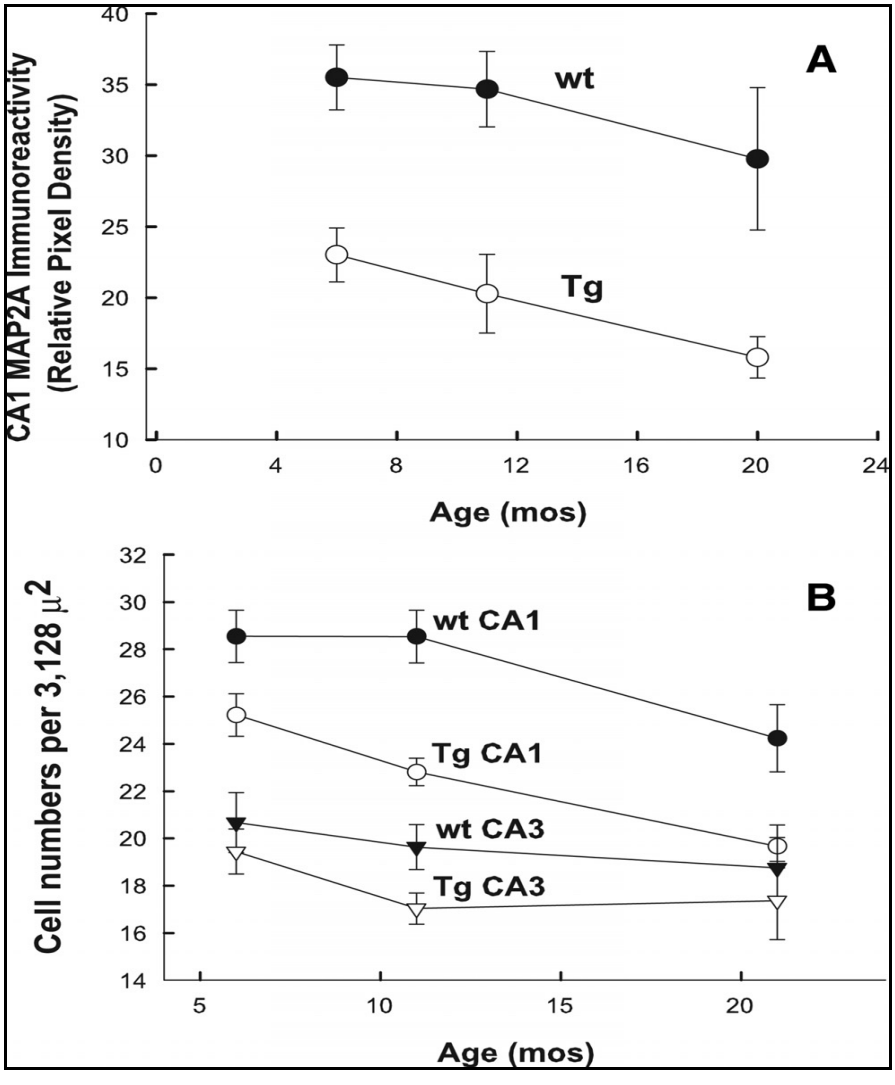

Figure 11 Age-associated changes in MAP2A labeling in dendrites and cell bodies of the CA1 of hippocampus of wt and Tg mice. A MAP2A labeling in SR dendrites of the CA1 measured across age for wt and Glud1 mice. The data shown are means (+-SEM) of pixel density measurements from equal areas from 6-14 pairs of wt and Tg mice of the indicated ages. B, Cell counts of neurons obtained from a 3128 um2 area of SP in CA1 and CA3 of wt and Tg hippocampus. Cell bodies labeled with anti-MAP2A antibodies were counted. Bao et al. 2009

Conclusion

The Glud1 Tg mouse model generated in our laboratory demonstrated significantly increased GLUD1 levels, GLUD activity, extracellular glutamate, and increased glutamate release after stimulus as compared to wt. There were also many significant morphological changes observed in the Tg mice including cell layer thinning in the hippocampus, cortex, and striatum, accompanied by synaptic, neuronal, and dendritic losses. It was noted that the morphological changes observed were within specific brain regions, for example, the cerebellum showed no changes despite the fact that *Glud1* was over-expressed in all neuronal cells. In addition, the morphological changes in the various brain regions of the Tg mice were further exacerbated by advancing age. The observation that not all of the neurons underwent the same morphological changes gives support to the idea that not all neurons suffer equally through age or as a result of extracellular glutamate. These findings support previous work which has shown that there is region-specific neuronal vulnerability to damaging agents, such as those that induce oxidative stress (Wang, Pal et al. 2007) (Wang, Pal et al. 2005).

Selective neuronal vulnerability has also been observed in many neurodegenerative diseases and it is seen in the cerebral cortex, hippocampus, and amygdala of those with Alzheimer's disease. Therefore, the Glud1 Tg mice may be used to probe the molecular and cellular pathways involved in selective neuronal vulnerability as it may relate to excess extracellular glutamate. There is not much information on this topic and several pathways have been suggested, including mitochondrial dysfunction, to account for differential vulnerability of

certain neurons. Mitochondrial dysfunction as a factor involved in glutamate-mediated toxicity has been proposed by other investigators and reduced energy levels in AD due to dysfunctional mitochondria have been described (Francis, Sims et al. 1993) (Beal 1998).

4. MITOCHONDRIAL DYSFUNCTION AS A RESULT OF EXCESS GLUTAMATE

Mitochondrion Overview

Mitochondria were first described in 1895 by Richard Altmann, but it was not until 1912 that B.F. Kingsbury linked mitochondria to cell respiration. Thereafter, the function of mitochondria began to be elucidated and in the 1950s the phrase “powerhouses” of cells was used to coin them (Siekevitz 1957; Ernster and Schatz 1981). Mitochondria are organelles found in eukaryotic cells and they vary in number and location according to the cell type. Human cells contain numerous mitochondria, about 1000-2000 per cell.

The main function of mitochondria is to provide cells with energy in the form of ATP through the process of cellular respiration. Since the number of mitochondria varies in different cell types, different amounts of ATP are produced in different cell types. When the demand for ATP is high, for example in muscle cells, the volume of mitochondria per cell is high. Mitochondria are also involved in a variety of other processes including cell death, cell differentiation, cell signaling, Ca^{2+} buffering, and control of cell cycle and cell growth (Schon and

Przedborski 2011). Overall, mitochondria have very critical roles in eukaryotic cells (Campbell, Williamson et al. 2006) (McBride, Neuspiel et al. 2006).

Function

The process of glycolysis yields the product pyruvate which is oxidized and combined with Coenzyme A to form carbon dioxide, NADH, and acetyl CoA. by mitochondrial pyruvate dehydrogenase. Acetyl CoA is the primary substrate which feeds into the TCA cycle. All of the enzymes of the citric acid cycle are localized in the mitochondrial matrix and the cycle consists of a series of ten chemical reactions. The overall function of this cycle is to produce energy by the catabolism of fats, proteins, and sugars and the oxidation of acetyl CoA. An important and key regulatory step in the cycle is the oxidative decarboxylation of α-ketoglutarate to form succinyl-CoA which is an intermediate in the cycle. This process is required in order to complete Alpha-ketoglutarate may also enter the directly into the TCA cycle following deamination of glutamate in the mitochodnria by glutamate dehydrogenase. Therefore, glutamate dehydrogenase is key for generating an intermediate of the citric acid cycle. This reaction also generates nicotinamide adenine dinucleotide (NADH) which is the primary substrate that feeds into the electron transport chain to generate ATP. Therefore, glutamate dehydrogenase can contribute to the TCA cycle by supplying the primary substrate for the electron transport chain activities, or ATP generation.

Electron transport system

The products of the citric acid cycle, NADH and flavin adenine dinucleotide ($FADH_2$) function as substrate, to fuel the activities of the electron transport chain. Once inside the mitochondria NADH and $FADH_2$ are oxidized by enzymes of the electron transport chain, respectively NADH:ubiquinone reductase (Complex I) and succinate dehydrogenase

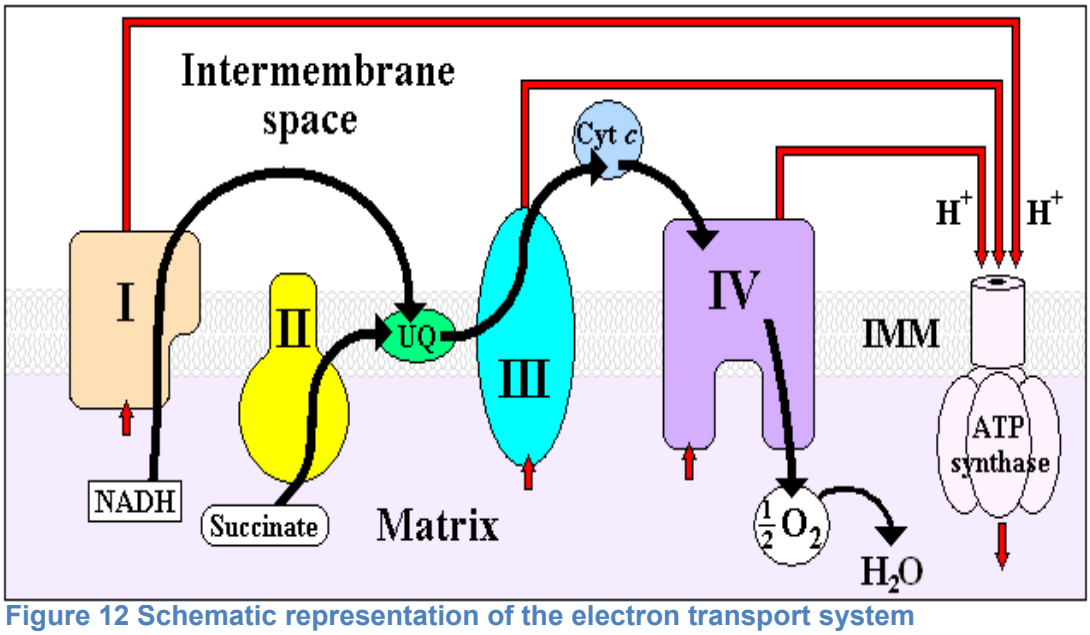

Figure 12 Schematic representation of the electron transport system

(Complex II). Through a series of oxidation-reduction reactions the electrons from the substrates are transferred to molecular oxygen which is ultimately broken down to water. As electrons are transferred through the chain, energy is obtained and used to pump hydrogen protons from the matrix into the inner membrane space (Fig. 12). The generation of this electrochemical proton

gradient is the overall purpose of the electron transport chain enzyme activities. The energy from the electrochemical proton gradient drives ATP synthase to generate adenosine triphosphate (ATP) from adenosine diphosphate (ADP) and inorganic phosphate.

Effects of altered electron transport system activities

The main output of the electron transport system (ETS) is the generation of a membrane potential (Ψ_m) and production of ATP; therefore, any changes in ETS activities can alter ATP output. Studies have documented that inhibition of complexes of the ETS, i.e. NADH: cytochrome c oxireductase (Complex I+CoA+complex III) and cytochrome c oxidase (COX) (complex IV) result in decreased ATP levels (Brusque, Borba et al. 2002). In addition, increased ETS activities have been demonstrated to be followed by an increase in ROS generation (Raha, Myint et al. 2002) (Maj, Raha et al. 2004). Major sites in the ETS which are contributors to the ROS generation are the ubiquinone of complex III and complex I (Liu, Fiskum et al. 2002) (Turrens and Boveris 1980) (Turrens, Alexandre et al. 1985) (Cadenas and Davies 2000). Studies have demonstrated that calcium is also a key player involved in altering ETS activities (McCormack and Denton 1993).

Calcium effects on the mitochondrion

Ca2+ has been demonstrated to activate key dehydrogenases of glycolysis and the TCA cycle including pyruvate dehydrogenase, α-ketoglutarate dehydrogenase, isocitrate dehydrogenase, Ca^{2+} can also stimulate ATP synthase, α-glycerophosphate dehydrogenase, and the adenine nucleotide translocase (ANT) (McCormack and Denton 1993) (Das and Harris 1990) (Wernette, Ochs et al. 1981) (Mildaziene, Baumann et al. 1995). The end result is an up-regulation of oxidative phosphorylation (electron transport system activities) leading to an increase of ATP synthesis. Ca^{2+} uptake into mitochondria is driven by the mitochondrial membrane potential (Ψ_m) (Brookes, Yoon et al. 2004) and the net movement of Ca^{2+} ions consumes the Ψ_m.

Despite the beneficial effects of Ca^{2+}, excess levels of calcium have been demonstrated to exert several negative effects on mitochondrial function including ROS generation, cytochrome c release, and apoptosis (Aarts, Wei et al. 2003) (Loeffler and Kroemer 2000) (Di Giorgi, Lartigue et al. 2002) (Green and Reed 1998) (Grijalaba, Vercesi et al. 1999). The generation of ROS through a Ca2+ driven pathway can arise from multiple processes. Ca2+ uptake is driven by the Ψ_m and studies have demonstrated that chemical uncouplers (i.e. 2,4-dinitrophenol) decrease ROS generation in whole cells; therefore, ROS generation is exponentially dependent on the Ψ_m (Starkovv and Fiskum 2003) (Okuda, Lee et al. 1992). An increase in mitochondrial calcium levels has been demonstrated to trigger PT pore opening (Halestrap and Brennerb 2003) and this is linked to cytochrome C release (Loeffler and Kroemer 2000). Cytochrome c

release has been demonstrated to be accompanied by an immediate increase in ROS (Green and Reed 1998) (Grijalaba, Vercesi et al. 1999).

ROS effects on mitochondrion

Calcium, the mitochondrial membrane potential, and ETS activities are involved in the generation of mitochondrial ROS. Once produced, excess levels of ROS can exert negative effects on mitochondria. ROS can damage mtDNA which encodes for essential components of the ETS proteins, i.e. complex I. As stated earlier, an inhibition of complex I activity would decrease ATP generation. In addition, Nianyu et al., demonstrated that mitochondrial ROS production was induced by mitochondrial complex I inhibitors and this inhibition also induced mitochondrial permeability transition, increased the potential difference across the mitochondrial membrane, cytochrome c release, caspase 3 activation, and DNA fragmentation in cells; therefore, linking mitochondrial bioenergetics, ROS generation, and apoptosis (Nianyu 2002).

Of particular interest is the observation that neurons express differential vulnerability to oxidative stress brought about by ROS. In the brain the hippocampus is divided into four regions, CA1 through CA4, and these regions respond to oxidative stress differently. When exposed to oxidative stress cells in the CA1 region have low survival rates, while cells in the CA3 region are resistant (Wilde, Pringle et al. 1997) (Wang, Pal et al. 2005) (Sarnoska 2002). Also agents that induce oxidative damage also cause massive cell death of neurons in

the cerebellar granule cell layer, but not in the cerebral cortex area (Wang, Zaidi et al. 2009).

5. OVERALL CONCLUSIONS

Glutamate has been shown to lead to neurotoxicity and subsequent neurodegeneration (Lucas and Newhouse 1957) (Camacho and Massieu 2006) through changes in synaptic function, loss of glutamatergic neurons, synapses, and dendrites. All of these characteristics are also observed during aging or in age-associated neurodegenerative diseases (Segovia, Porras et al. 2001) .

In the *Glud1* Tg mice, we detected region-specific differences between wt and Tg mice in the loss of neurons and synapses and these differences became more pronounced with advancing age. A question that we probed was what were the molecular and cellular determinants involved in the glutamate-induced region specific neuronal damage. Our laboratory has published data that has begun to shed some light in these two issues. Integrated bioinformatic analyses of gene expression has identified pathways and gene networks underlying neuronal responses in the Tg mice (Wang, Bao et al. 2010). Based on the results of these studies, enhanced gene expression associated with oxidative stress, inflammation, neuronal growth and synaptic transmission were all up-regulated in the hippocampus of the Tg mice as compared with that from the wt mice. These results could be interpreted as showing that the Tg mice undergo compensatory responses to the chronic exposure to excess glutamate by up-regulating genes involved in protection against stress while enhancing growth of

neuronal processes and re-establishing synapses. It is important to note, however; that gene expression does not always correlate with protein expression so it will be important not only to identify the factors involved, but the pathways. My work has focused on investigating the role of mitochondria in inducing region specific neuronal degeneration under the conditions of the combined effects of aging and excess glutamate activity in the central nervous system.

Rationale

A change in the production of intermediates and products of the TCA cycle would change the amount of substrate feeding into the electron transport chain and alter ETS activities. Specifically, changes in glutamate dehydrogenase levels and activities would change the levels of α-ketoglutarate and levels of NADH produced in the citric acid cycle which would alter electron transport chain activities due to the change in substrate availability. As stated earlier an alteration of ETS activities would affect the generation of ATP, generation of ROS, mitochondrial membrane potential, and mitochondrial calcium homeostasis. Take together a change in any of these has been shown to be involved in cell damage and apoptosis. As mentioned earlier, changes in α-ketoglutarate would led to increased extracellular glutamate levels which has also been shown to led to neuronal damage and death.

The Glud1 Tg mouse model generated in our laboratory has been demonstrated to exhibit increased levels of glutamate dehydrogenase activity, increased levels of extracellular glutamate, increased depolarization induced

glutamate release, and to undergo region specific neuronal and synaptic damage as compared to wt mice (Bao, Pal et al. 2009). Therefore, to identify the molecular and cellular pathways involved in the glutamate-induced region specific damage has been my goal. The focus of my work as examined the effect(s) of excess extracellular glutamate on mitochondrial function. Specifically, I have focused on whether there are changes in mitochondrial bioenergetics (Chapter 2), mitochondrial Ca^{2+} regulation (Chapter 3), and mitochondrial reactive oxygen species generation (Chapter 4) during the aging process in different brain regions in wild type and *Glud1* Tg mice. Figure 13 illustrates a schematic representation of the hypothesized effects over-expression of the Glud1 would exert on mitochondrion.

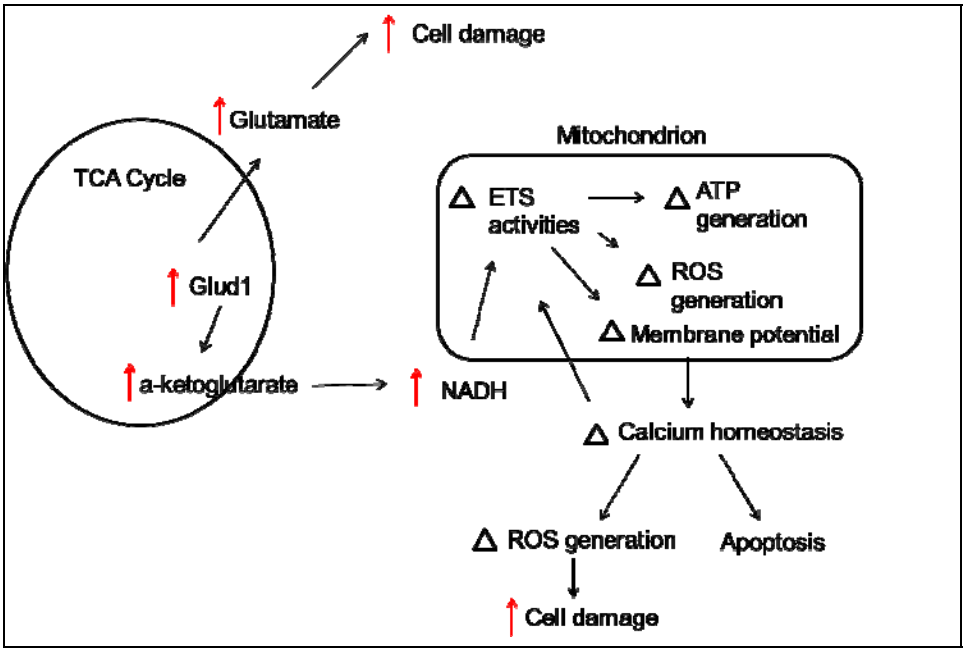

Figure 13 Hypothesized effects of over-expression of glutamate dehydrogenase (Glud1) on mitochondrion and cells.

Objective

To identify the molecular and cellular pathways underlying glutamate induced region specific vulnerability.

Hypothesis

The region specific and age-associated morphological and functional changes observed in the *Glud1* Tg mice may occur as an adaptive or compensatory consequence of mitochondria dysfunction. The Tg mice might exhibit adaptive or compensatory changes in mitochondria function and the key measures affected might be mitochondrial bioenergetics, calcium homeostasis, membrane potential, and the generation of ROS.

Citations

Aarts, M., W. Wei, et al. (2003). "A key role for TRPM7 channels in anoxic neuronal death." Cell **115**: 863-877.

Ashpole, N., W. Song, et al. (2012). "Calcium/calmodulin-dependent protein kinase II (CaMKII) inhibition induces neurotoxicity via dysregulation of glutamate/calcium signaling and hyperexcitability." J Biol Chem **287**: 8495-8506.

Bao, X., R. Pal, et al. (2009). "Transgenic Expression of *Glud1* (Glutamate Dehydrogenase 1) in Neurons: *In vivo* model of enhanced glutamate release, altered synaptic plasticity, and selective neuronal vulnerability." Journal of Neuroscience **29**: 13929-13944.

Bao, X., R. Pal, et al. (2009). "Transgenic expression of Glud1 (glutamate dehydrogenase 1) in neurons: in vivo model of enhanced glutamate release, altered synaptic plasticity, and selective neuronal vulnerability." J Neurosci **29**(44): 13929-13944.

Barnes, C. (1979). "Memory deficits associated with senescence: an neurophysiological and behavioral study in rat." J Comp Physiol **93**: 74-104.

Beal, M. (1998). "Mitochondrial dysfunction in neurodegenerative diseases." Biochim Biophys Acta **1366**: 211-223.

Brookes, P., Y. Yoon, et al. (2004). "Calcium, ATP, and ROS: a mitochondrial love-hate triangle." Am J Physiol Cell Physiol **287**: C817-C833.

Brusque, M., R. Borba, et al. (2002). "Inhibition of the mitochondrial respiratory chain complex activites in rat cerebral cortex by methylmalonic aci." Neurochem Int **40**: 593-601.

Cadenas, E. and K. Davies (2000). "Mitochondrial free radical generation, oxidative stress, and aging." free RAdical Biology and Medicine **29**: 222-230.

Camacho, A. and L. Massieu (2006). "Role of glutamate transporters in the clearance and release of glutamate during ischemia and its relation to neuronal death." Archives of medical research **37**: 11-18.

Campbell, N., B. Williamson, et al. (2006). "Biology: Exploring Life ".

Choi, D. (1992). "Bench to bedside: the glutamate connection." Science **258**: 241-243.

Clark, A., K. Magnusson, et al. (1997). "In vitro autoradiography of hippocampal excitatory amino acid binding in aged Fisher 344 rats: relationship to performance in the morris water maze." Behav Neurosci **106**: 324-335.

Cooper, A. (2012). "The role of glutamine synthetase and glutamate dehydrogenase in cerebral ammonia homeostasis." Neurochemical research.

Cotman, W. C. and T. D. Monaghan (1988). "Excitatory Amino Acid Neurotransmission: NMDA Receptors and Hebb-Type Synaptic Plasticity." Ann. Rev. Neurosci. **11**: 61-80.

Das, A. and D. Harris (1990). "Control of mitochondrial ATP synthase in heart cells: inactive to active transitions caused by beating or positive inotropic agents." Cardiovasc Res **24**: 411-417.

Debanne, D., G. Daoudal, et al. (2003). "Brain plasticity and ion channels." J Physiol Paris **97**: 4-6.

Del Bigio, M. (2000). "Calcium-mediated proteolytic damange in white matter of hydrocephalic rats?" J Neuropath Exp Neurol **59**: 946-954.

Di Giorgi, F., L. Lartigue, et al. (2002). "The permeability transition pore signals apoptosis by directing Bax translocation and multimerization." FASEB J **16**: 607-609.

Donzanti, B., J. Hite, et al. (1993). "Extracellular glutamate levels increase with age in the lateral striatum: potential involvement of presynaptic D-2 receptors." Synapse **13**: 376-382.

Ernster, L. and G. Schatz (1981). "Mitochondria: A historical review." Journal of Cell Biology **91**: 227s-255s.

Francis, P., N. Sims, et al. (1993). "Cortical pyramidal neurone loss may cause glutamatergic hypoactivity and cognititve impairment in Alzheimer's disease: Investigative and therapeutic perspectives." J Neurochem **60**: 1589-1604.

Francis, T. P. (2003). "Glutamatergic systems in Alzheimer's disease." International Journal of Geriatric Psychiatry **18**: S15-S21.

Francis, T. P., N. Sims, et al. (1993). "Cortical pyramidal neurone loss may cause glutamatergic hypoactivity and cognitive impairment in Alzheimer's disease: investigative and therapeutic perspectives." Journal Neurol Neurosurg Psychiatry **66**: 137-147.

Freeman, G. and G. Gibson (1987). "Selective alteration of mouse brain neurotransmitter release with age." Neurobiol Aging **8**: 147-152.

Green, D. and J. Reed (1998). "Mitochondria and apoptosis." Science **281**: 1309-1311.

Grijalaba, M., A. Vercesi, et al. (1999). "Ca2+-induced increased lipid packing and domain formation in submitochondrial particles. A possible early step in the mechanism of Ca2+-stimulated generation of reactive oxygen species by the respiratory chain." Biochemistry **38**: 13279-13287.

Halestrap, A. and C. Brennerb (2003). "The adenine nucleotide translocase: a central component of the mitochondrial permeability transition pore and key player in cell death." Curr Med Chem **10**: 1507-1525.

Hedden, T. and J. Gabrieli (2004). "Insights into the ageing mind: a view from cognitive neuroscience." Nat Rev Neurosci **5**: 87-96.

Kaiser, L., N. Schuff, et al. (2005). "Age-related glutamate and glutamine concentration changes in normal human brain: 1H MR spectroscopy study at 4 T." Neurobiol Aging **26**: 665-672.

Laube, B., H. Hirai, et al. (1997). "Molecular determinants of antagonists discrimination by NMDA receptor subunits: Analysis of the glutamate binding site on the NR2B subunit." Neuron **18**: 493-503.

Levy, W. and O. Steward (1979). "Synapses as associative memory elements in the hippocampal formation." Brain Res **175**: 233-245.

Liu, Y., G. Fiskum, et al. (2002). "Generation of reactive oxygen species by the mitochondrial electron transport chain." Journal of Neurochemistry **80**: 780-787.

Loeffler, M. and G. Kroemer (2000). "The mitochondrion in cell death control: certainties and incognita." Exp Cell Res **256**: 19-26.

Lucas, D. and J. Newhouse (1957). "The toxic effect of sodium L-glutamate on the inner layers of the retina." A.M.A Archives of ophthalmology **58**: 193-201.

Maj, M., S. Raha, et al. (2004). "Regulation of NADH/CoQ oxidoreductase: Do phosphorylation events affect activity?" The Protein Journal **23**: 25-32.

Matsugami, T., K. Tanemura, et al. (2006). "From the Cover: Indispensability of the glutamate transporters GLAST and GLT1 to brain development." Proc Natl Acad Sci **103**: 12161-12166.

McBride, H., M. Neuspiel, et al. (2006). "Mitochondria: More that just a powerhouse." Curr Biol **16**: R551-560.

McCormack, J. and R. Denton (1993). "Mitochondrial calcium transport and the role of mitochondrial calcium in the regulation of energy metabolism." Dev Neurosci **15**: 165-173.

Mildaziene, V., M. Baumann, et al. (1995). "Calcium indirectly increases the control exterted by the adenine nucleotide translocator over 2-oxoglutarate oxidation in rat heart mitochondria." J Bioenerg Biomembr **324**: 231-238.

Nianyu, L. (2002). "The role of mitochondrial reactive oxygen species in apoptosis." Purdue Dissertation.

Okuda, M., H. Lee, et al. (1992). "Comparison of the effect of a mitochondrial uncoupler, 2,4-dinitrophenol and adrenaline on oxygen radical production in the isolate perfused rat liver." Acta Physiol Scand **145**: 159-168.

Otmakhov, N., J. Tao-Cheng, et al. (2004). "Persistent accumulation of calcium/calmodulin-dependent protein kinase II in dendritic spines after induction of NMDA receptor-dependent chemical long-term potentiation." J Neurosci **24**: 9324-9331.

Palaiologos, G., L. Hertz, et al. (1989). "Role of aspartate aminotransferase and mitochondrial dicarboxylate transport for release of endogenously supplied neurotransmitter in glutamatergic neurons." Neurochem Res **14**: 359-366.

Peters, A., C. Sethares, et al. (2008). "Synapses are lost during aging in the primate prefrontal cortex." Neuroscience **152**: 970-981.

Potier, B., J. Billard, et al. (2010). "Reduction in glutamate uptake is associated with extrasynaptic NMDA and metabotropic glutamate receptor activation at the hippocampal CA1 synpase of aged rats." Aging Cell **9**: 722-735.

Procter, A., A. Palmer, et al. (1988). "Evidence of glutamatergic denervation and possible abnormal metabolism in Alzheimer's disease." J Neurochem **50**: 790-802.

Pull, I., H. McIlwain, et al. (1970). "Glutamate, calcium ion-chelating agents and the sodium and potassium ion contents of tissues from the brain." Biochem J **116**: 181-187.

Raha, S., A. Myint, et al. (2002). "Control of oxygen free radical formation from mitochondrial complex I: roles for protein kinase A and pyruvate dehydrogenase kinase." Free Radic. Biol. Med **32**: 421-430.

Rothstein, J., H. Dykes, et al. (1996). "Knockout of glutamate transporters reveals a major role for astroglial transport in excitotoxicity and clearance of glutamate." Neuron **16**: 675-686.

Sanhueza, M., G. Fernandez-Villalobos, et al. (2011). "Role of the CaMKII/NMDA receptor complex in the maintenance of synaptic strength." J Neurosci **31**: 9170-9178.

Saransaari, P. and S. Oja (1995). "Age-related changes in the uptake and release of glutamate and aspartate in the mouse brain." Mech. Ageing. Dev. **81**: 61-71.

Sarnoska, A. (2002). "Application of organotypic hippocampal culture for study of selective neuronal death." Neuropathol **40**: 101.

Schon, A. E. and S. Przedborski (2011). "Mitochondrial: The Next (Neurode)Generation." Neuron **70**.

Segovia, G., A. Porras, et al. (2001). "Glutamatergic neurotransmission in aging: a critical perspective." Mechanisms of Ageing and Development **122**: 1-29.

Siekevitz, P. (1957). "Powerhouse of the cell." Scientific Americana **1**: 131-140.

Starkovv, A. and G. Fiskum (2003). "Regulation of brain mitochondrial H2O2 production by membrane potential and NAD(P)H redox state." J Neurochem **86**: 1101-1107.

Turrens, J., A. Alexandre, et al. (1985). "Ubisemiquinone is the electron transport donor for superoxide formation by complex III of heart mitochondria." Arch Biochem Biophys **237**: 408-414.

Turrens, J. and A. Boveris (1980). "Generation of superoxide anion by the NADH dehdyrogenase of bovine heart mitochondria." Biochem. J. **191**: 421-427.

Wang, X., X. Bao, et al. (2010). "Transcriptomic responses in mouse brain exposed to chronic excess of the neurotramsitter glutamate." BMC Genomics **11**: 1471-2164.

Wang, X., R. Pal, et al. (2007). "Genome-wide transcriptome profiling of region-specific vulnerability to oxidative stress in the hippocampus." Genomics **90**: 201-212.

Wang, X., R. Pal, et al. (2005). "High intrinsic oxidative stress may underlie selectie vulnerability of the hippocampal CA1 region." Brain Res. **140**: 120-126.

Wang, X., R. Pal, et al. (2005). "High intrinsic oxidative stress may underlie selective vulnerability of the hippocampal CA1 region." Molecular Brain Research **140**: 120-126.

Wang, X., A. Zaidi, et al. (2009). "Genomic and biochemical approaches in the discovery of mechanisms for selective neuronal vulnerability to oxidative stress." BMC Neurosci. **10**: 12.

Wenk, G. and C. Barnes (2000). "Regional changes in the hippocampal density of AMPA and NMDA receptors across the lifespan of the rat." Brain Res **885**: 1-5.

Wernette, M., R. Ochs, et al. (1981). "Ca2+ stimulation of rat live mitochondrial glycerophosphate dehydrogenase." J Biol Chem **256**: 12767-12771.

Wilde, G., A. Pringle, et al. (1997). "Inflammation as a causative factor in the aetiology of Parksinon's disease." Br. J. Pharmacol. **150**: 963-976.

Zeng, L., Y. Ouyang, et al. (2007). "Abnormal glutamate homeostasis and impaired synaptic plasticity and learning in a mouse model of tuberous sclerosis complex." Neurobiol Dis **28**: 184-196.

Chapter Two: Effects of the Over-Expression of Neuronal Glutamate Dehydrogenase (GLUD1) on Brain Mitochondrial Electron Transport Chain Activities

6. INTRODUCTION

The effects on neuronal function and structure(s) caused by acute treatments with glutamate have been extensively studied and described (Aarts, Wei et al. 2003). However, these studies have been difficult due to the decreased lifespan and severe brain damage the acute treatments and exposures inflict on cells and mouse models (Tanaka, Watase et al. 1997) (Rothstein, Dykes-Hoberg et al. 1996). In addition, these models undergo exposure to glutamate that is not localized and are therefore they would not be ideal for investigating glutamate induced damage at nerve terminals.

Rationale for Glud1 Tg mouse model

The Glud1 Tg mouse model generated in our laboratory has already been demonstrated to contain increased levels of glutamate dehydrogenase activity, increased levels of chronic extracellular glutamate, increased depolarization induced glutamate release, and to undergo region specific neuronal and synaptic damage as compared to wt mice. Therefore, this model provides a means for studying the effects of chronic, localized excess levels of extracellular glutamate on neuronal function over the lifespan of an organism. In addition, it also serves

as a model for identifying the molecular and cellular pathways involved in the glutamate-induced damage that is region specific.

Rationale for the studies described

The Glud1 Tg mouse model was generated with a neuronal specific promoter, enolase, and was shown to be over-expressed in only neuronal cells (Bao, Pal et al. 2009). Despite the over-expression of Glud1 in all neuronal cells, only specific brain regions were damaged i.e., cerebellum was resistant while hippocampus was vulnerable (Bao, Pal et al. 2009). This raised the possibility that another pathway was involved in the region specific damage besides that of increased glutamate induced damage.

Mitochondrial effects of glutamate dehydrogenase

Changes in glutamate dehydrogenase levels and activities are expected to change the levels of α-ketoglutarate, levels of NADH produced in the TCA cycle, and can alter electron transport chain activities due to the change in substrate availability. Changes in ETS activities can affect the generation of ATP, generation of ROS, mitochondrial membrane potential, mitochondrial calcium homeostasis and generation of ROS (Chapter 1). Taken together a change in any of these has been shown to be involved in cell damage and apoptosis (Brookes, Yisang et al. 2004) (Gunter, Yule et al. 2004) (Gunter, Buntinas et al. 2000) (Muller, Roberts et al. 2003). The studies described below were designed

to determine if mitochondrion bioenergetics is altered in the Glud1 T mouse model.

Experimental Design

In previous work from our laboratory it was noted that cerebellar granule (CbG) and hippocampal CA1 neurons are more sensitive to paraquat insults (a form of oxidative stress) than cerebral cortical and hippocampal CA3 neurons (Wang, Zaidi et al. 2009). Preliminary studies conducted in our laboratory have begun to shed light into the molecular pathways and genes that may be involved in the differential neuronal response to oxidative stress (Wang, Pal et al. 2005) (Wang, Pal et al. 2007); however, there is still much information lacking. The goals of the studies described below were to probe mitochondrial function across different brain regions in order to determine whether, under conditions of increased glutamate activity in brain, there are differential responses in mitochondria isolated from different regions. The overall plan was to select three different brain regions, cerebellum, frontal cortex, and hippocampus, for the studies on mitochondrial metabolism and integrity. The initial studies were focused on the activity of electron transport complexes as they represent the pathway of oxidative phosphorylation and a major source of ROS in cells (Liu, Fiskum et al. 2002) .

2. MATERIALS

All materials were purchase from Sigma-Aldrich unless otherwise noted. Protease inhibitor cocktail was purchased from Calbiochem, Catalog #539134. Bicinchoninic Acid Protein Assay Kit was purchased from Thermo Scientific # 23225. Complex I subunit NDUFB8 monoclonal antibody was purchased from Invitrogen Catalog #459210.

3. METHODS

Generation of Tg Glud1 mice

The GLUD1 transgenic mice were generated as published in Bao, X et al., 2009. Briefly "Tg mice were generated by microinjecting fertilized oocytes from super-ovulating C57BL6/SJL hybrid mice with linearized DNA containing the cDNA of mouse *Glud1*. The cDNA was placed under the control of the *Nse* promoter. This promoter was excised from pNSE-LacZ vector by digesting the SV40 polyA tail (BamHI and EcoRI), blunting and cloning it into pGEM-7Z between SmaI and BamHI. Then the *Nse* promoter was excised from pNSE-LacZ (BamHI and SphI digestion) and cloned into the modified pGEM-7Z. A linker containing multiple restriction sites (Bg1II/EcoRV/Hink1II/MluI/XbaI/KpnI; sense sequence, 5'-AGATCTGATATCAAGCTTACGCGTCTAGAGGTAC-3') was cloned between SphI (blunted) and KpnI of pGEM-7Z, which contained the *Nse* promoter and SV40 polyA tail (pNSE-GEM-7Z). The open reading frame (ORF) of *Glud1* cDNA was excised from pUC19 [by SacI 5'-untranslated region (UTR)/HpaI 3'-UTR] and subcloned into the Eco721 site of a reconstructed

pSindRep5 Sindbis virus vector, into which a polylinker (Bc1I/XhoI/SacI/NotI/PvuI) was introduced. The orientation of the *Glud1* ORF insert was confirmed by sequencing; the insert was digested (XbaI/XhoI) and cloned into pNSE-GEM-7Z to create the pNSE-GLUD1 vector. This vector was digested with EcoRI, and the DNA was microinjected into the pronuclei of 215 fertilized mouse oocytes and transferred to the oviducts of pseudopregnant mice. Forty-eight pups were born after transfer of oocytes microinjected with the pNSE-GLUD1 construct. Of these pups, four had the transgene for *Glud1*. Genotyping was performed on genomic DNA extracted from tail biopsies obtained from 3- to 4-week-old pups. The DNA was subjected to Southern blot and PCR analysis. For the identification of the *Glud1* transgene by PCR, the primers used were as follows: F_1, 5'-GATATCGGGTGCATCTGAG-3'; and R_1, 5-GGTTTATGAGGACACAGAGG-3' (900 bp product). PCR amplification was performed using *pfu* polymerase and either 100 ng of genomic DNA or 1 ng of DNA from the pNSE-GLUD1 vector (reaction conditions: 32 cycles of 95C for 30 s, 53C for 30 s, 72C for 1 min). Southern blot analyses were used to confirm the PCR results. pNSE-GLUD1 and genomic DNA from tail clippings were digested with EcoRV. A 790 bp fragment from the *Glud1* ORF was used as a proble for hydridization with genomic DNA"- (Bao, Pal et al. 2009).

Surgical procedure

Mice from the three different ages, 9 months, 15 months, and 22 months were sacrificed under CO_2 anesthesia and decapitated by a guillotine. The brain was quickly removed and the cerebellum, frontal cortex, and hippocampus were dissected. The hippocampus was removed using the technique of Navarro, Ana et al., 2007. To reveal the hippocampus, a linear incision in both cortical sides was made extending from the posterotemporal pole of one hemisphere to the anterior pole of the frontal lobe at a 30^{o} angle, with the incision depth adjusted to cut only the cortex and subjacent corpus callosum. The excised brain regions were washed and immersed in homogenization buffer which contained (in mM): 230 mannitol, 70 sucrose, 1 EGTA, 10 HEPES, 0.1 benzamide, 0.1 benzamidine.HCl, 50 sodium fluoride, 1 sodium orthovanadate, 10 sodium pyrophosphate decahydrate, 10 β-glycerophosphate, plus 20 μl of protease inhibitor cocktail III.

Mitochondrial Preparations

Homogenization of the cerebellum, frontal cortex, and hippocampus was carried out using a glass Dounce homogenizer (20-30 strokes) (1 gram of tissue / 9 ml homogenization buffer). The homogenate was centrifuged at 1,000 xg for 5 min at 4 ^{o}C to remove cell debris and nuclei. After centrifugation, the pellet was discarded and the supernatant (S1) was transferred to a clean microcentrifuge tube. The S1 was centrifuged at 10,000 xg for 10 min at 4 ^{o}C to obtain the mitochondrial pellet (P2). The supernatant (S2) was also harvested and immediately frozen at -80 ^{o}C for later analysis. The P2 fraction was re-

suspended in a small volume of homogenization buffer, 350 μl for the hippocampus and 450 μl for the cerebellum and frontal cortex homogenates and the re-suspeneded pellets divided into 25 μl aliquots, snap frozen in liquid nitrogen, and stored at -80 ^{o}C.

Citrate Synthase Assay

A citrate synthase assay kit was used to determine total citrate activity and percent of leakiness of mitochondria in the isolated P2 pellets. The P2 pellets described previously, were suspended in bicine buffer (buffer containing no detergent) using 200 μl per gram of tissue. The suspension was split into two tubes and centrifuged at 11,000 xg for 10 min. The supernatant in the first tube was removed and the pellet was re-suspended in CelLytic M buffer (a buffer containing detergent) and the pellet in the second tube was re-suspended with bicine buffer using 200 μl per gram of tissue. The samples in the bicine and CelLytic M buffer were assayed for protein content using a colorimetric Bicinchoninic Acid Protein Assay Kit at 37 ^{o}C. The total citrate synthase activity was measured spectrophotometrically at 412 nm with a kinetic program of no lag time, 1.5 minute read with 10 second interval readings. The assay was performed in 96-well plates. All solutions were warmed before starting the reactions. Three different reaction samples were prepared. One reaction sample contained 5 μl of CelLytic M mito-pellet, 186 μl 1x Assay buffer, 2 μl 30 mM Acetyl CoA solution, and 2 μl 10 mM 5,5'-Dithiobis-(2-nitrobenzoic acid) (DTNB). The second sample contained all of the above but differed in the fact

that it contained 5 μl of the mito-pellet in bicine buffer. The third reaction contained everything that was in the first reaction except the sample was not the CelLytic M mito-pellet, but in this reaction we added 2 μl of citrate synthase diluted solution (positive control). All sample reactions were mixed well by gentle vortexing. The absorbance of the reaction mixtures was followed for 1.5 minutes to measure the baseline reaction. This was done in order to determine the endogenous levels of thiol or deacetylase activity. After baseline measurements, 10 μl of oxaloacetic acid (OAA) was added to each well to start the reaction. A multichannel pipette was used in order to start the reaction in all the wells simultaneously. While adding the OAA, the wells were mixed with the pipette and the plates were shaken for 5 seconds before reading the absorbance. The absorbance of the reaction mixture was followed for 1.5 minutes to measure the total citrate synthase activity. Three brain region samples from four mice from each genotype were used and all reactions were run in triplicate.

Complex I to IV Assays

The activities of the ETC complexes were assayed at 37 ^{o}C spectrophotometrically. Enzyme activites for coupled complexes I-III, II-III and for individual complexes I, II, and IV were determined using the mito-pellets from the different brain regions and from different ages. Prior to running the assays the mito-pellets were thawed at room temperature and ruptured (Janssen, Trijbels et al. 2007) as technique stated in Navarro et al. 2007. Briefly, samples were passed through a syringe with a hypodermic needle then placed on dry ice for 5

minutes. This process was repeated 3 times. The BCA protein assay was run to determine the protein concentration of each sample after mitochondrial rupturing. For the coupled reactions for complexes I-III and II-III, ruptured mito-pellets were suspended in a medium that contained 0.1 M potassium phosphate buffer (pH 7.4), 10 μg mitochondrial protein, 20 mM KCN, and 0.5 mM cytochrome C oxidized. For complex I-III assays 100 μm of NADH was added immediately prior to reading the reaction. For complex II-III assays 50 mM of succinate was added immediately prior and all assays were measured at an absorbance of 550 nM. All reactions were carried out in 96-well microplates and the rate of the reaction was monitor by measuring changes in absorbances on Biotek-Synergy HT plate reader. Temperature of 30 ^{o}C was maintained and samples were shaken and absorbance measurements initiated 6 sec after mixing and continued for 10 min at 15 sec intervals. Blanks contained all of the reagents and mitochondria, but did not contain either NADH or succinate. Blank absorbances were subtracted from reaction values.

For the measurement of complex IV, reaction samples contained 0.1 M potassium phosphate buffer (pH 7.4), 10 μg mitochondrial sample, and 692 μM reduced cytochrome C. Blanks contained no protein sample and these values were subtracted from the reaction values. Cytochrome C was reduced by placing 2 mM oxidized cytochrome c in a brown colored microcentrifuge tube, adding five drops of sodium borohydride, mixing well, and incubating at 51 ^{o}C for one hour with periodic mixing (every 15 minutes). At the end of the incubation period, four drops of 0.1 N HCl were added to remove excess sodium borohydride. The solution was neutralized by adding four drops of 0.1 n NaOH.

The final concentration of reduced cytochrome c was adjusted to 692 μm with distilled water using an absorbance measurement. An aliquot of this reaction was scanned and a spectrum was obtained to ensure cytochrome c was reduced as observed by a shift in the absorbance maximum at 550 nM. Reduced cytochrome c was kept at -20 ^{o}C until use.

Complex I (NADH:ubiquinone oxido-reductase) activity was assayed following Janssen et al. 2007 (Janssen, Trijbels et al. 2007) . Mito-pellets were ruptured as described above and the ruptured mitochondria (3 mg/ml) were incubated at 37 ^{o}C in a medium that contained 25 mM potassium phosphate (pH 7.4), 3.5 mg/mL BSA, 60 μM 2,6-dichlorophenol-indophenol (DCIP), 70 μM decylubiquinone, and 1.0 μM antimycine-A. Following 3 min of incubation, 20 μL of 10 mM NADH were added and the absorbance was measured spectrophotometrically at 600 nm for 4 minutes at 30 second intervals. At the end of 4 min, 1.0 μL of 2 μM rotenone was added and the absorbance was measured again at 30 second intervals for 4 min.

Complex II (succinate dehydrogenase) activity was assayed following the methods as described in Janssen et al. 2007. Ruptured mitochondria (3 mg/mgl) were incubated in a medium that contained 80 mM potassium phosphate (pH 7.4), 1 mg/mL BSA, 1 mM EDTA, 80 μM DCIP, 50 μmM decylubiquinone, 1 μM antimycin-A, and 3 μM rotenone, pH 7.8. The reaction mixture was incubated at 37 ^{o}C for 10 min then 0.3 mM KCN and 10 mM succinate were added to start the reaction. Absorbance was measured at 600 nm for 5 min at 30 second-intervals. For assay blanks, 5 mM malonate was used in place of succinate and

absorbance values for the blanks were subtracted from sample values. All measurements were from mitochondria from 3 brain regions obtained from mice at each age and all reactions were run in triplicate. Three-way ANOVA analyses were used to determine statistical significance.

ELISA estimation of NADH: ubiquinone oxido-reductase protein levels

An enzyme-linked immunosorbant assay (ELISA) was used to quantify the levels of mitochondrial complex I (NADH:ubiquinone oxido-reductase). Complex I subunit NDUFB8 monoclonal antibody was used. ELISA microplates were used for the assay. One hundred microliters of poly-D-lysine (10μg/ml in PBS) were added to the microplate, covered with saran wrap and incubated at room temperature for 30 min. This was followed by the addition of 100 μl of mito-pellet added to the respective wells (dilutions in PBS) (0.5 mg per well) and further incubation for 1h at 23 ^{o}C. The proteins were attached to the well by adding 100 μl of 0.5% glutaraldehyde in PBS. Each well was washed 3 times for 20 sec with 200 μl of PBS-0.05% Tween 20. Following the washes, 200 μl of 100 mM Glycine-2% gelatin in PBS was added to each well and incubated at 37 ^{o}C for 30 min. After this incubation the wells were washed again 2x with 200 μl of PBS-0.05% Tween 20 and 100 μl of anti-NDUFB8 primary antibody (1:1000 dilution) were added. To the control wells, 100 μl of PBS-Tween was added. The microplates were incubated for 2 h at 23 ^{o}C, with gentle shaking and washed 3 times with 200 μl of PBS-0.05% Tween 20, before the addition of 100 μl anti-mouse antibody conjugated to alkaline phosphate (1:1000 dilution). After

incubation for 1 h at 23 ^{o}C, the wells were washed 15 times with 200 μl PBS-0.05% Tween 20 and to each well was added 150 μl of p-nitrophenyl phosphate (PNPP) + buffer tablets and the plate developed in the dark for 30 min, the absorbance measured at 405 nm and the reaction was stopped with 50 μl of 3M NaOH.

Data analysis

Determination of Citrate Synthase Activity

The absorbance was plotted against time for each reaction. The change in absorbance at 412 nm per min was measured in the linear range of the endogenous activity. The net citrate synthase activity was calculated by subtracting the ΔA_{412} in/min of the activity in the absence of substrate from the (ΔA_{412})/minute of the activity in the presence of substrate. The net absorbance change was then used to calculate the citrate synthase activity using the equation:

Units (μmole/ml/min)=(ΔA_{412})/min) x vol(ml) x (dil)/Ext. coeff x L (cm) x vol_{enz} (ml)

where dil is the dilution factor of the original sample, vol (ml) is the reaction volume (0.2 mL); vol_{enz} (ml) is the volume of the enzyme sample in ml, Ext. coeff. is the extinction coefficient of TNB at 412 nm, which is 13.6 mM^{-1} cm^{-1}, and L (cm) is the pathlength for the absorbance measurements.

Estimation of mitochondrial membrane integrity.

The ΔA_{412}/minute in the linear range of the activity of citrate synthase performed in the CelLytic M buffer and that in the bicine buffer were calculated. The ratio between the calculated citrate synthase activity in bicine buffer versus that in CelLytic M buffer gave the percentage of leaky or ruptured mitochondria:

(% ruptured mitochondria=activity in bicine buffer x 100 / activity in CelLytic M).

Determination of V_{max} and "K_M" values for the combined activity of complexes I-III.

A derivative of the Michaelis-Menten kinetics equation was used to determine time-dependent kinetics of product formed for all enzyme activity assays. The equation used was: (V-(K_M * ln([So]/[So]-[P])t=[P]/t where V=a; K_M=b; ln([So]/[So]-[P])/t=x; and [P]/t= y. Thus the equation became a-bx=y, a linear equation in which I estimated a, the velocity and b, the K_M. The first calculation determined the starting concentration of substrate [S_o] and concentration of product [P] formed. The concentration was determined for each time period. The second calculation was ln([So]/[So]-[P]). This calculation was done for all time periods. The third calculation was [P]/t where [P] was the concentration of product formed and t was the time of the reaction. The calculation was done for all time periods (Fig.1). All above calculations were carried out in Excel 09. SigmaPlot 11.0 was used to plot: [P]/t vs ln([So]/[So]-[P])/t. The plot below is an example of the plots analyzed.

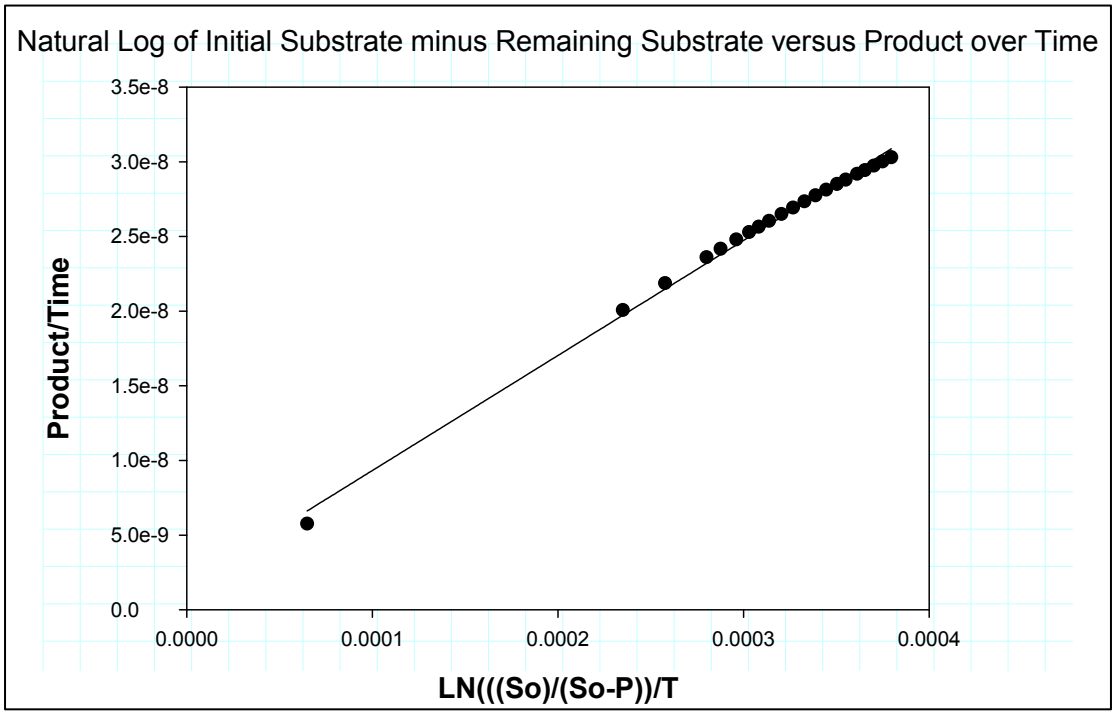

Figure 8 Time dependent kinetic plot

Final V_{max} values were determined by multiplying Y_o (slope) by the time (60 mins), the volume of the reaction, and dividing by the amount of protein, and are reported as nmoles/mg protein/minute.

Statistical analyses

A combination of student's t-test, three-way ANOVA analysis and post-hoc Bonferroni analyses were used to determine statistical significance on SigmaPlot 11.0.

4. RESULTS

Citrate synthase activity in wt and Glud1 Tg mice

Citrate synthase is the first enzyme of the tricarboxylic acid (TCA) cycle and is located within the mitochondrial matrix. This enzyme catalyzes the conversion of acetyl coenzyme A (acetyl CoA) and oxaloacetic acid (OAA) to form citric acid. Since this enzyme is located within the mitochondrial matrix its activity can only be measured in intact mitochondria. Therefore, the activity of this enzyme is a marker of the integrity of the mitochondria

In order to determine whether the sustained over-expression and over-activity of GLUD1 in mitochondria had any effect on the first enzymatic step of the TCA cycle, the citrate synthase activity was measured in permeabilized mitochondria (total enzyme activity). In addition, the activity of citrate synthase in non-permeabilized mitochondria was estimated in order to assess the leakiness of the mitochondrial preparations obtained from Tg and wt mice. This was necessary in order to ensure that any enzymatic changes detected were not due to differentially leaky mitochondria. The brain mitochondria used in these and all subsequent studies were obtained from cerebellu, frontal cortex, and hippocampus, of Tg and wt mice at three ages, 9, 15, and 22 mo-old mice (see Methods section). A total of 4 mice were used for the studies representing each genotype, age, and brain region. The total citrate synthase activity was not significantly different between wt and Tg mice and there were no significant differences across the different brain regions or across the 3 ages (Fig 2A-C). In

addition, the percent of “leaky” mitochondria was not significantly different regardless of the mouse brain, the age of the mice or the site of origin of the mitochondria. Also, the brain regions or the age of the mice did not have an effect on the integrity of the isolated mitochondria (Fig. 3A-C). We conclude from these findings that the total citrate synthase activity is similar in both genotypes and that both genotypes are similarly intact as determined by the percent of leaky mitochondria data.

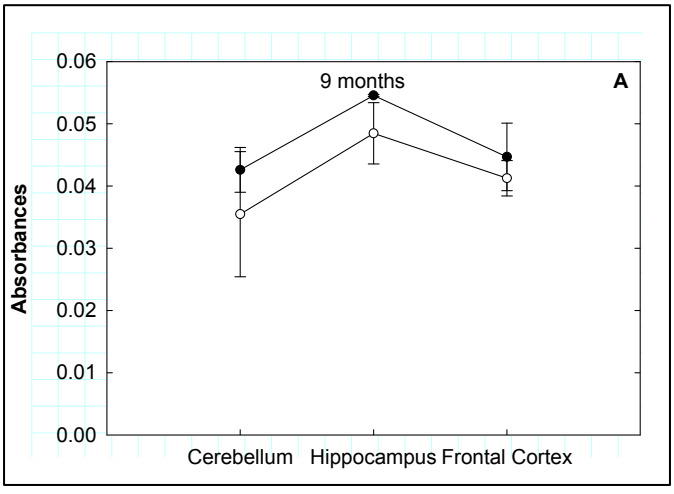

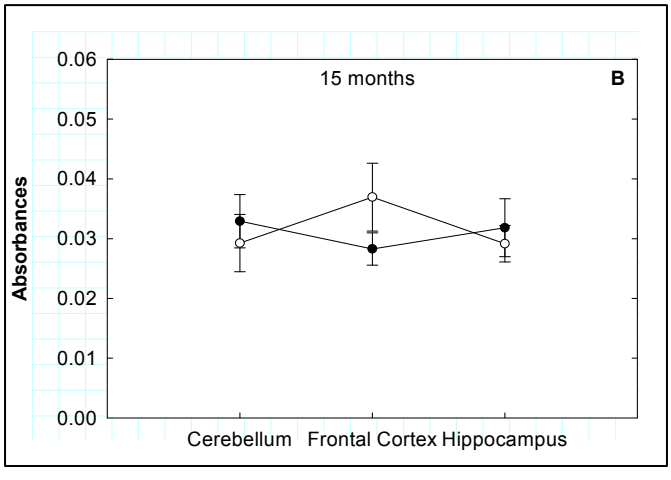

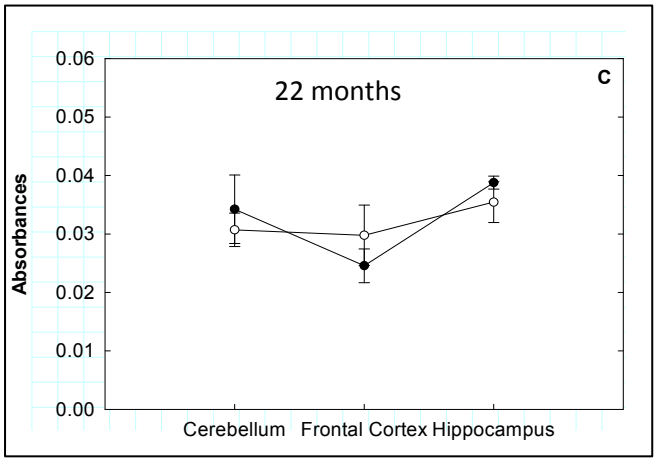

Figure 9 Total citrate synthase activity of Tg and wt mice at A) 9 months B) 15 months and C) 22 months. Mitochondria were isolated from Cerebellum, Frontal Cortex, and Hippocampus. All experiments were performed using n=4 of each genotype. Open circle indicate Tg and dark circles wt mouse mitochondria.

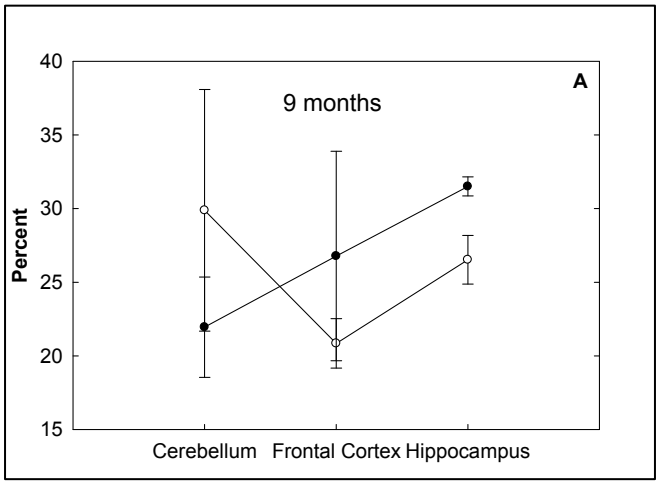

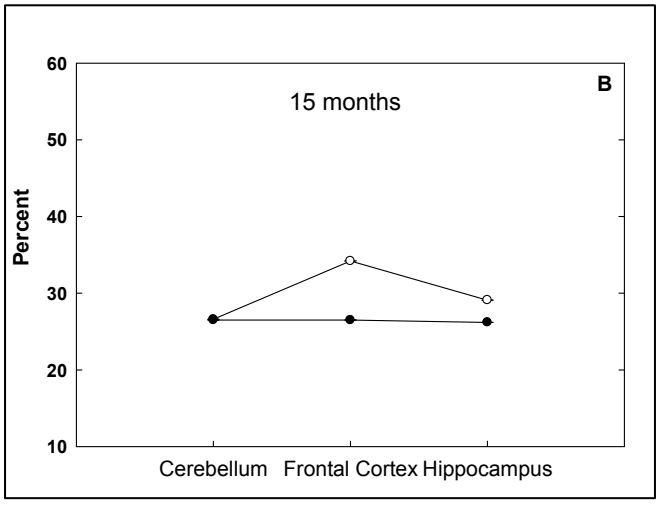

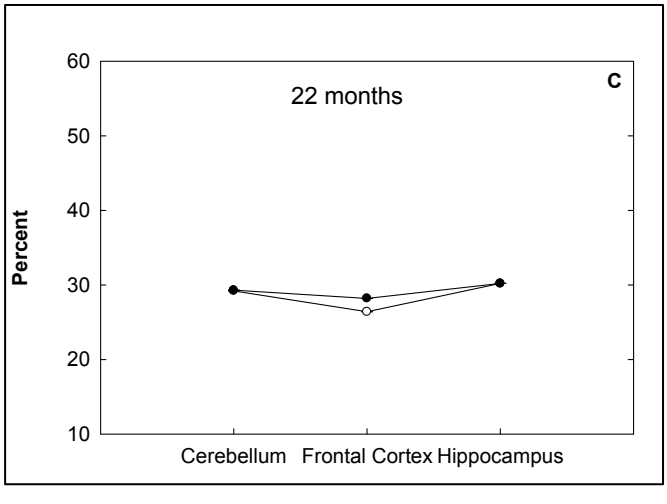

Figure 3 Percent of leaky mitochondria of Tg and wt mice at A) 9 months B) 15 months and C) 22 months. Mitochondria were isolated from Cerebellum, Frontal Cortex, and Hippocampus. All experiments were performed using n=4 of each genotype. Open circle indicate Tg and dark circles wt mouse mitochondria.

Complex I-III activity of mitochondria from different brain regions and across age of wt and Tg mice

In aging and in age-associated neurodegenerative diseases, deficits in mitochondrial electron transport chain activities have been demonstrated (Curti, Giangare et al. 1990) (Sohal 1993) (Freddari-Bertoni, Fattoretti et al. 2004) (Paradies, Ruggiero et al. 1997) (Brown-Borg, Johnson et al. 2012). In our study, we looked at the coupled reactions of complex I-III to determine if there are differences in these two enzymatic steps of the electron transport chain between wild type and Tg mice. We observed that in mitochondria from the cerebellum and hippocampus, the V_{max} values for the activity of Complex I-III decreased with advancing age, whereas this pattern was not observed for the mitochondria from the frontal cortex. At the age of 9 months, there were significant differences in Complex I-III V_{max} values between the two genotypes with the Tg brain mitochondria exhibiting lower activity in the cerebellum and higher activity in the cortex (Fig. 4) ($p=0.02$). These differences in complex I-III V_{max} between genotypes were only seen at 9 months of age.

The estimates of K_M values were representative of the combined enzymatic activity of two complexes, I and III and therefore, they did not represent either enzyme. Nevertheless, the estimated K_M for the combined enzymatic activities showed no significant differences between wt and Tg mitochondria, from any region and any of the ages tested.

When the V_{max} data for the mitochondria from all the brain regions, across all ages, and the two genotypes (shown in figure 5) were analyzed by three-way

ANOVA (with *post-hoc* analysis using the Bonferroni test) a significant effect of age ($p=0.002$) and a significant set of interactions between genotype and brain region ($p=0.011$) as well as age and brain region ($p=0.017$) were noted. These analyses confirmed the trend toward decreases in complex I-III V_{max} during the aging process and the fact that mitochondria from different brain regions, such as the frontal cortex, differ from those from other regions, such as cerebellum or hippocampus, in both the age effect and the genotype differences. As noted above, cortical mitochondria from Tg mice had higher estimated V_{max} for complex I-III than mitochondria from the wt mice.

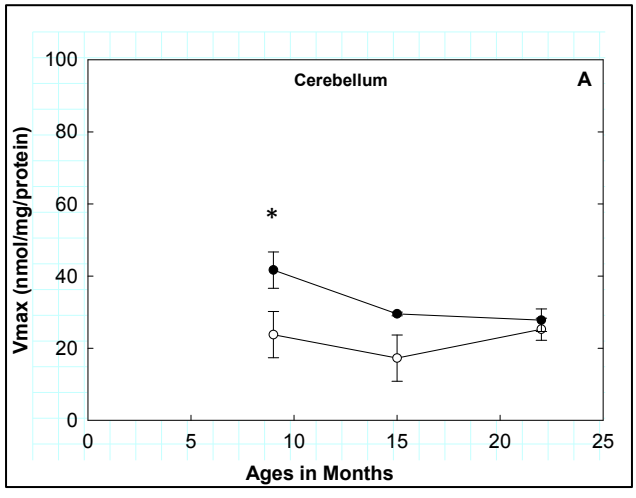

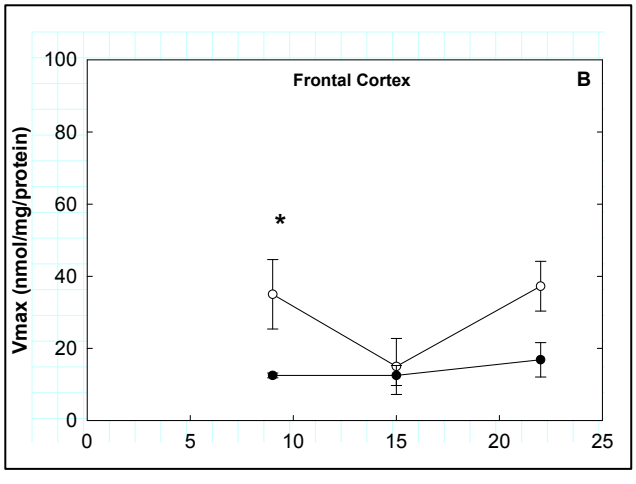

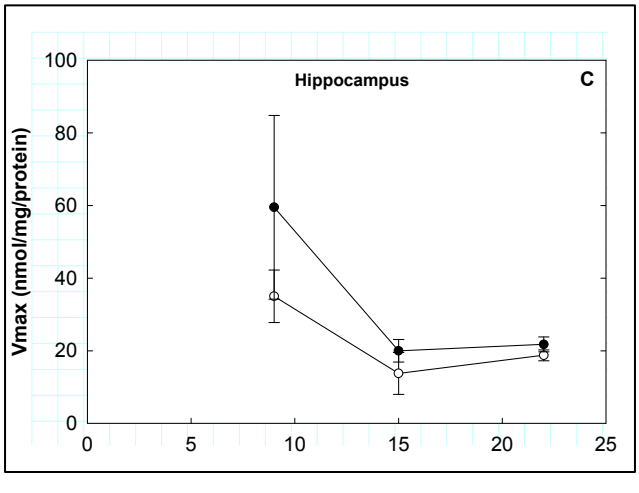

Figure 4: Complex I-III V_{max} values across age of Tg and wt mice Mitochondria were isolated from A) Cerebellum B) Frontal Cortex and C) Hippocampus. All experiments were performed using n=4 mice of each genotype. Open circles indicate Tg and dark circles wt mouse mitochondria. Student's t-test *=p<0.05.

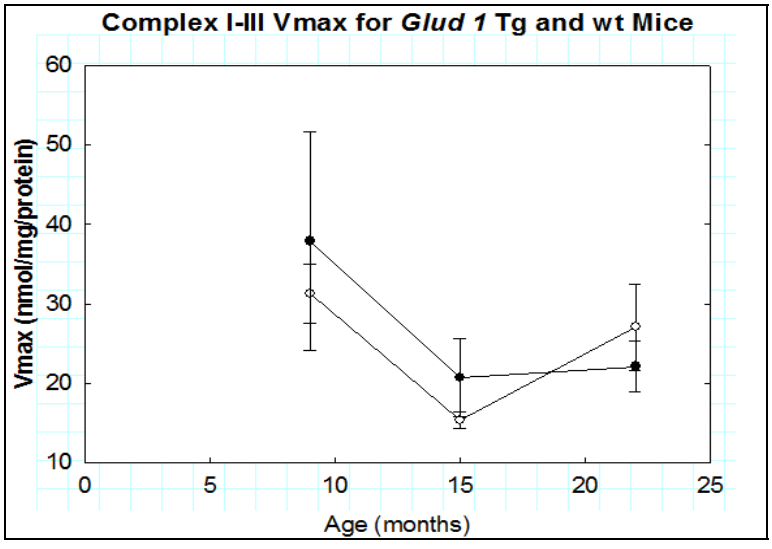

Figure 5: Combined data of V_{max} values across age of Tg and wt mice. Mitochondria were isolated from cerebellum, frontal cortex, and hippocampus. All experiments were performed using n=4 of each genotype. Open marks indicate Tg and dark circles wt mouse mitochondria.

Complex II-III activity of mitochondria in different brain regions across age of Tg and wt mice

Complex II is an entry point for $FADH_2$ and like Complex I it is also involved in the transfer of reducing equivalents to the acceptor ubiquinone. Succinate, the substrate of complex II, is a product of the TCA cycle generated by the metabolic conversion of α-ketogluturate to succinyl Co-A, the immediate precursor of succinate. Thus, we hypothesized that complex II activity might be increased in the mouse brains that over-expressed GLUD1 and probably over-produced α-ketoglutarate. In order to assess whether over-expression of GLUD1 had an effect on Complex II-III activities we measured the activity and estimated the V_{max} of the coupled Complex II-III reactions in mitochondria from cerebellum, frontal cortex, and hippocampus of wt and Tg mice. The data shown in figure 6 were indicative of a progressively increasing V_{max} for the activity of complex II-III with advancing age, especially in cerebellum and frontal cortex mitochondria, and for both wt and Tg mice. There were no significant differences between wt and Tg mice, except for the mitochondrial Complex II-III activities in the frontal cortex ($p=0.038$) and hippocampus ($p=0.027$) at 9 months of age (the V_{max} for the Tg mice is higher as compared with wt) (Fig. 6A-C).

When the V_{max} data for the mitochondria from all the brain regions, across all ages, and the two genotypes (figure 7) were analyzed by three-way ANOVA (with *post-hoc* analysis using the Bonferroni test) a significant genotype effect ($p=0.005$), a significant age effect ($p\leq0.001$), and a significant brain region effect

($p \leq 0.001$) were noted. There was also a significant interaction of age x region ($p \leq 0.001$). These analyses confirmed the trend of increasing complex II-III activity in the three brain regions of both wt and Tg mice, with the increases in the Tg mice being higher than those in the wt mice, thus supporting the possibility that Complex II-III may have higher activity in Tg mice in order to accommodate increases in succinate formation.

The estimates of K_M values were representative of the combined enzymatic activity of two complexes, I and III, therefore, they did not represent either enzyme. Nevertheless, the estimated K_M for the combined enzymatic activities showed no significant differences between wt and Tg mitochondria, from any region and any of the ages tested.

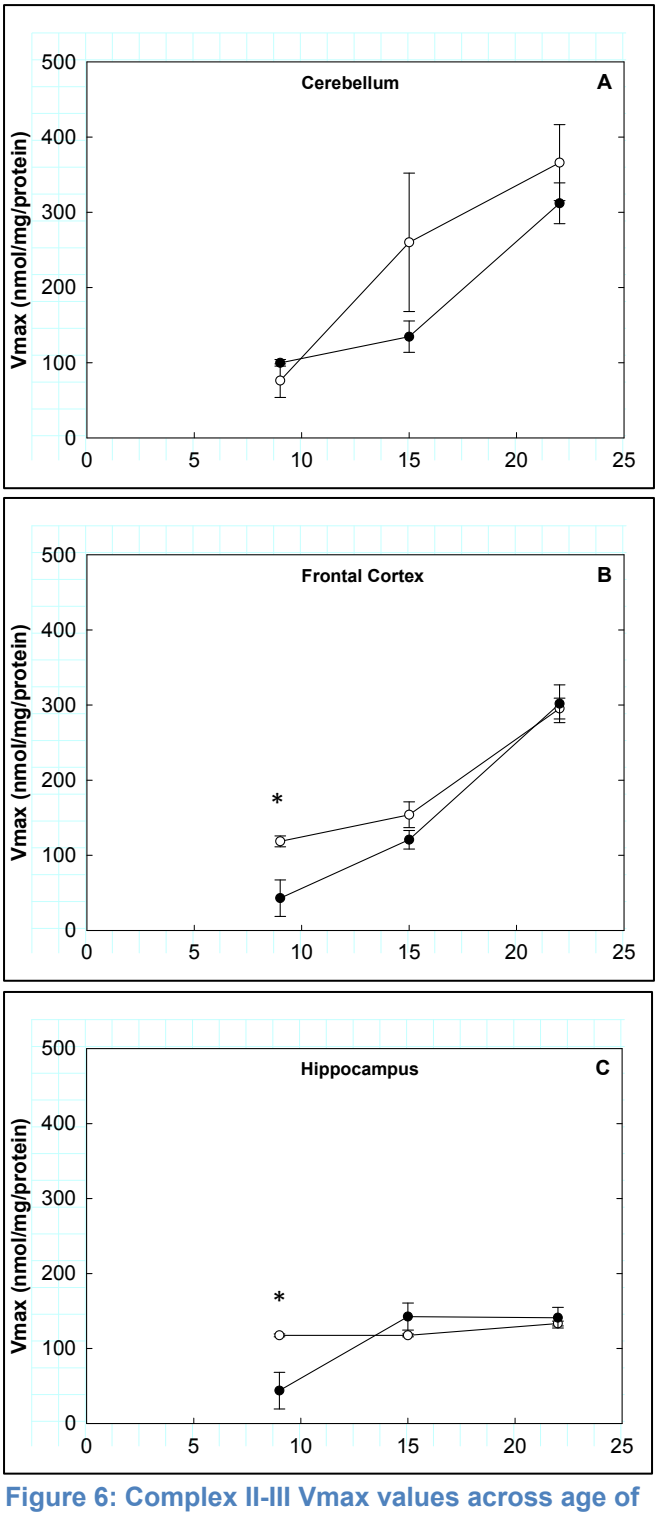

Figure 6: Complex II-III Vmax values across age of Tg and wt mice. Mitochondria were isolated from A) Cerebellum B) Frontal Cortex and C) Hippocampus. All experiments were performed using n=4 of each genotype. Open marks indicate Tg and dark circles wt mouse mitochondria. Student's t-test *p=<0.05.

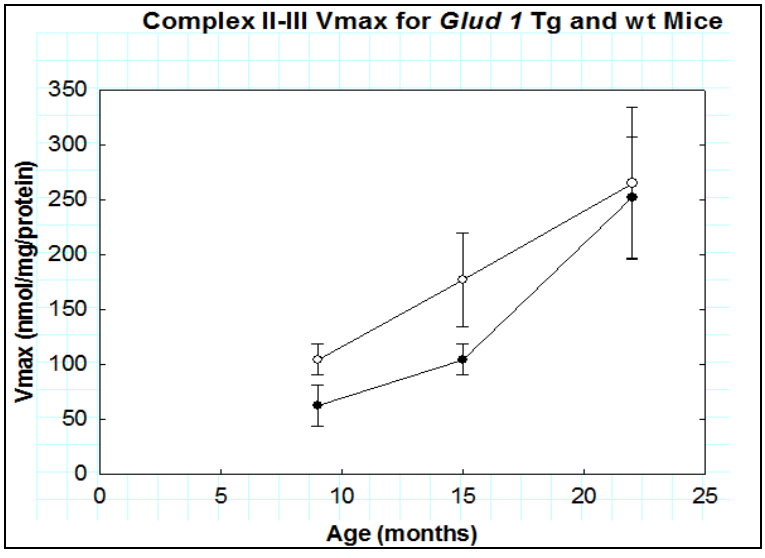

Figure 7: Vmax values for Complex I-III A) and II-III B) across 9, 15, and 22 months. Mitochondria were isolated from Cerebellum, frontal cortex, and hippocampus and combined as one sample. All experiments were performed using n=4 of each genotype. Open marks indicate Tg and dark circles wt mouse mitochondria.

Contribution of mitochondrial Complex I and Complex II to the estimates of Complex I-III and Complex II-III activities

Having observed differential genotype effects on complex I-III and complex II-III V_{max} values in different brain regions, we explored the likelihood that these differences were due to differential complex I or complex II activities. In these studies, complex I and complex II activities were measured independently using established assay procedures (Janssen, Trijbels et al. 2007). As shown in figure 8A, the estimated V_{max} values for Complex I were significantly lower in the mitochondria isolated from the cerebellum from Tg mice as compared with those from wt mice ($p=0.029$). These results fit with the observed significantly lower Complex I-III activities in cerebellar mitochondria (Fig. 4).

On the other hand, the V_{max} for Complex II activity in cerebellar and cortical mitochondria from Tg mice did not differ significantly from those of wt (Fig. 8B, C). These results also fit the observed lack of significant differences between cerebellar mitochondria from Tg and those from wt mice with respect to the V_{max} of Complex II-III (Fig. 6). Thus, the V_{max} values of the individual enzymes for Complex I and Complex II appeared to reflect the differences observed in the coupled reactions of Complex I-III and Complex II-III.

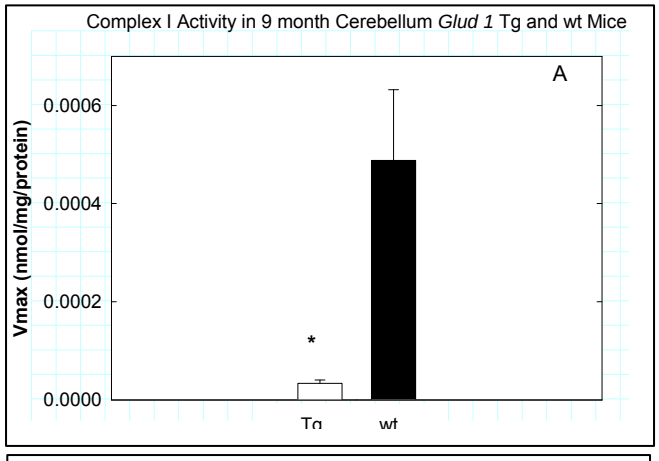

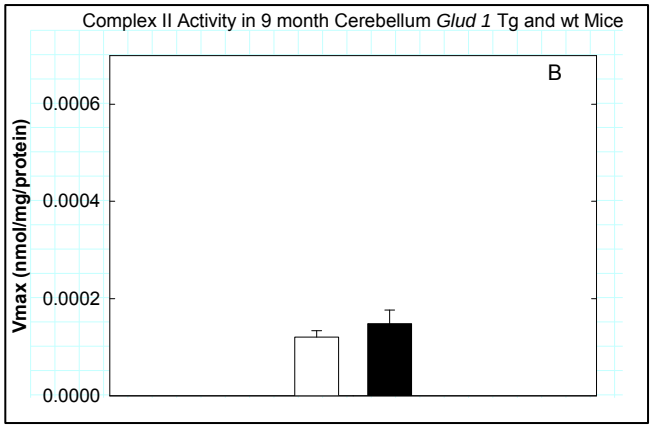

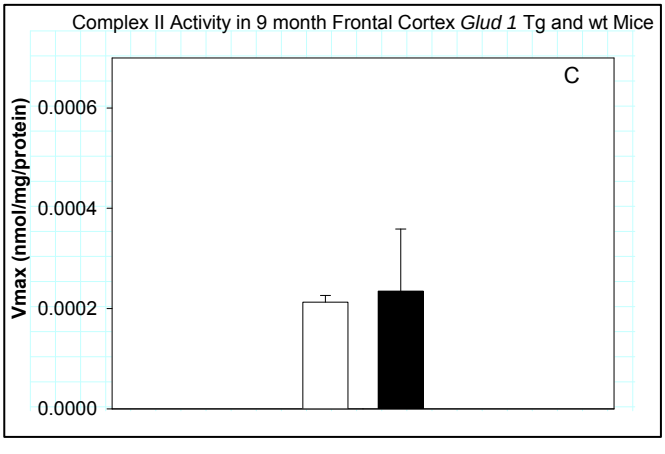

Figure 8: Complex I (A) and Complex II (B, C) Vmax values in 9 month cerebellum (A, B) and frontal cortex (C) from Tg and wt mice. All experiments were performed using n=4 of each genotype. Open bars indicate Tg and dark circles wt mouse mitochondria. Student's t-test p=0.029.

Estimation of complex I protein levels in mitochondria from wt and Glud1 mice

Having observed a significant genotype difference in Complex I activity, especially at 9 months in mitochondria from the cerebellum, the question that needed to be addressed was whether this difference could be attributed to differential protein levels for Complex I. Previous studies that have examined protein levels for Complex I reported contradictory results. Some studies have demonstrated that Complex I protein levels increase with age (Brown-Borg, Johnson et al. 2012) while others have shown that Complex I protein levels significantly decrease with age (Gomez, Monette et al. 2009). We subjected the mitochondrial proteins from the 3 brain regions and across the 3 age groups to ELISA immunochemical analyses in order to quantify the levels of a subunit of Complex I (NDUFB8) as an index of possible changes in the expression of the proteins in this Complex. Based on the ELISA assay results (Fig. 9), there were no significant differences in protein levels for NDUFB8 between genotypes and different brain regions, but three-way ANOVA analysis indicated a significant age effect for both genotypes (age $p<0.001$). Across all there brain regions and in both genotypes the levels of the subunit NDUFB8 significantly decreased across advancing age. Assuming that the subunit NDUFB8 was representative of the levels of all subunits of Complex I, the differences in V_{max} for Complex I at 9 months described in preceding sections are not likely the result of differences in Complex I protein levels. At 9 months there was a significant genotype effect, the Tg Vmax for Complex I was significantly lower than wt, yet Complex I protein

levels for both genotypes are very similar. The Vmax for Complex I-III significantly decreases across age in both genotypes in the Cerebellum and frontal cortex and this significant age effect may partially be due to decreased Complex I protein levels. The likelihood of this being the only cause for the decreased Complex I-III activity across age is very small as Complex I protein levels significantly decreases across age in all three brain regions, while Complex I-III activity significantly decreases only in the hippocampus and cerebellum.

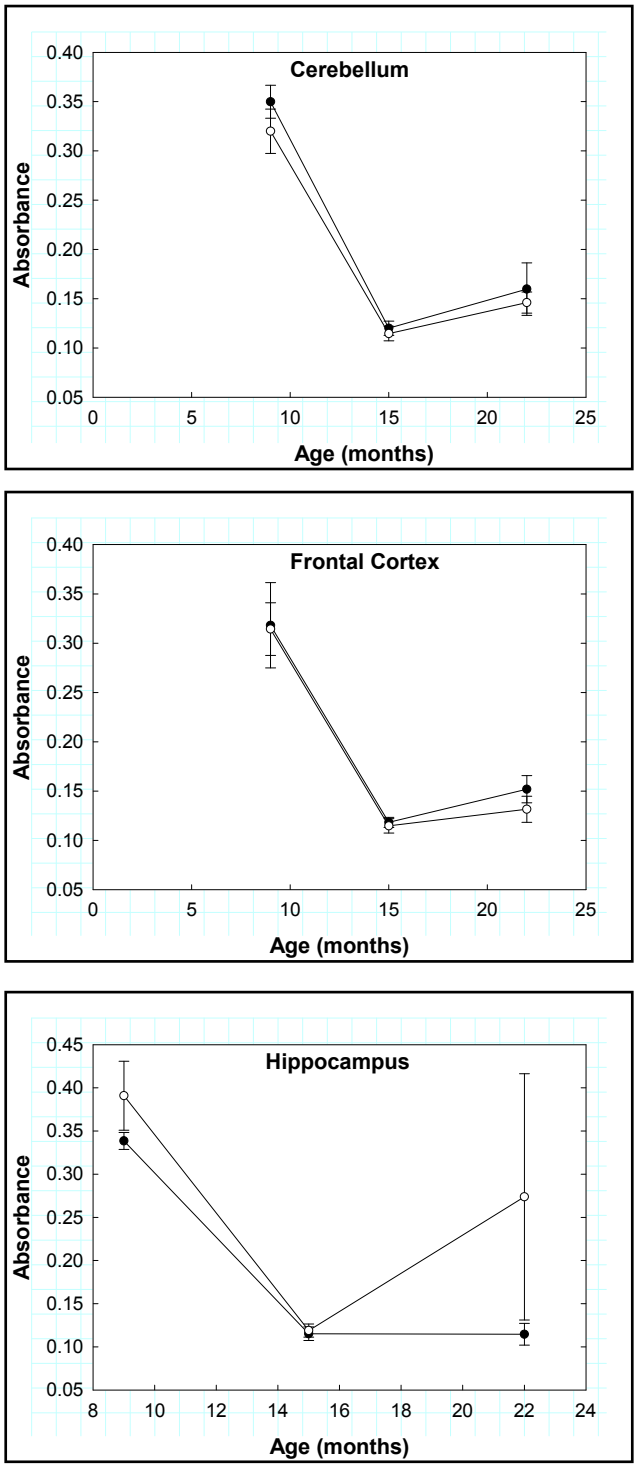

Figure 9: Absorbance values for NDUFB8 of complex I in A) Cerebellum B) Frontal Cortex and C) Hippocampus across age. Mitochondria were isolated from cerebellum, frontal cortex, and hippocampus. All experiments were performed using n=4 of each genotype. Open marks indicate Tg and dark circles wt mouse mitochondria.

Complex IV activity in mitochondria from different brain regions of Tg and wt mice across age

The fourth enzymatic step in the electron transport system is that of cytochrome C oxidase (Complex IV). It is well established that there are decreases in cytochrome c oxidase activity (complex IV) with advancing age, and some investigators have observed a differential level of decline in specific brain regions (Curti and Giangare 1990) (Sohal 1993) (Freddari-Bertoni and Fattoretti 2004) (Paradies and Ruggiero 1997). Cytochrome c oxidase activity was measured in the present studies in the three different brain regions and across the three ages of Tg and wt mice as those for Complexes I-III. The results shown in Fig. 10A-C represent the means (±SE) of Complex IV activity in mitochondria from 4 Tg and 4 wt mice at each age shown. As is obvious, there was a marked decline in enzyme activity with advancing age of the mice. Three-way ANOVA analysis indicated that there were no significant region or genotype differences, but there was a significant age effect ($p<0.001$). The same results were observed when the enzyme activity values for mitochondria from the cerebellum, frontal cortex, and hippocampus were averaged together (Fig. 11). There was a significant age effect ($p=0.001$), but no significant region or genotype effect as determined by three-way ANOVA analysis.

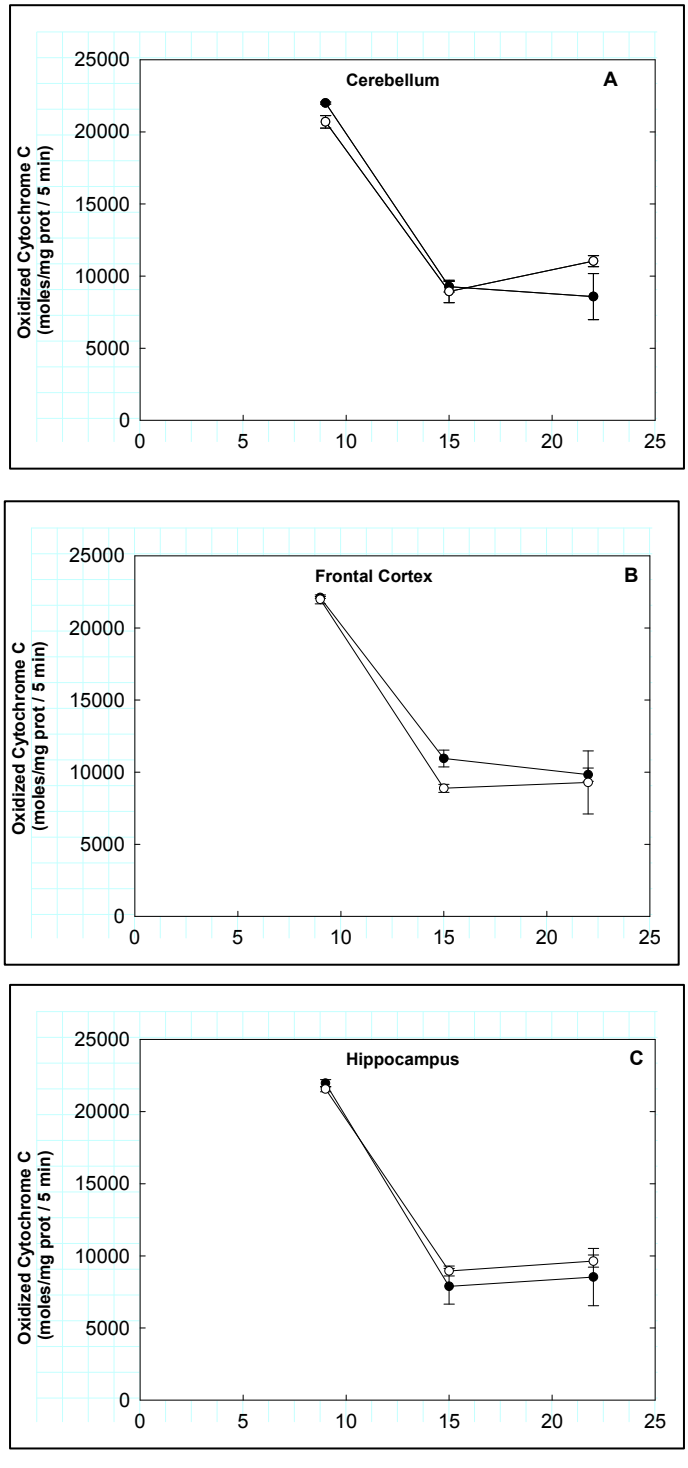

Figure 10 Complex IV Vmax values across age of Tg and wt mice. Mitochondria were isolated from A) Cerebellum B) Frontal Cortex and C) Hippocampus. All experiments were performed using n=4 of each genotype. Open marks indicate Tg and dark circles wt mouse mitochondria. Three-way ANOVA analysis indicated significant age effect p=<0.001.

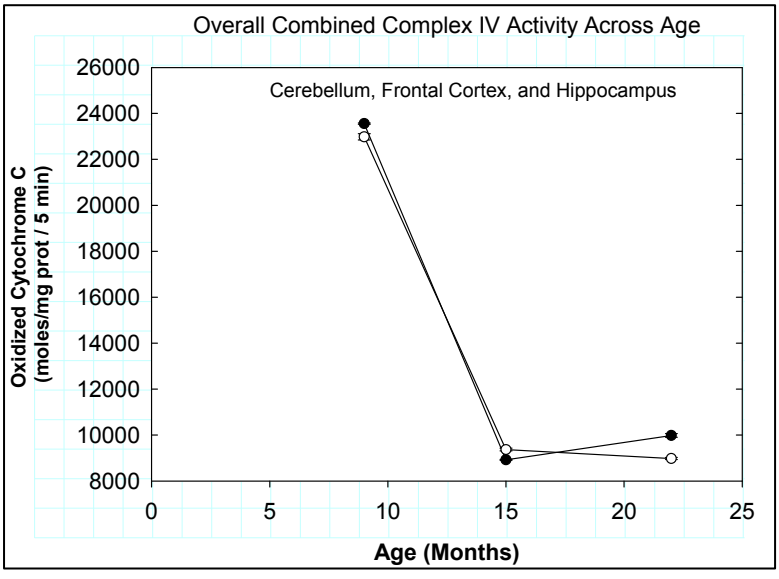

Figure 11 Complex IV Vmax values across age in Tg and wt mice mitochondria. Mitochondria were isolated from Cerebellum, Frontal Cortex, and Hippocampus and combined as one sample. All experiments were performed using n-4 of each genotype. Open circles indicate Tg and dark circles wt mouse mitochondria. Three-way ANOVA analysis indicated significant age effect p=<0.001.

5. DISCUSSION.

The data presented in this chapter demonstrate the following:

Complex I-III and Complex I V_{max} values are lower in the Tg mitochondria at 9 months. Both Tg and wt mouse mitochondria exhibited decreases in Complex I-III V_{max} across age. There were no differences in Complex I protein levels between Tg and wt or across regions or age.
Complex II-III V_{max} values are equal or higher in Tg mitochondria at 9 months vs. wt. Both Tg and wt mouse mitochondria exhibited increases in Complex II-III V_{max} across age.
Complex IV V_{max} values are the same in Tg and wt mitochondria. Both Tg and wt mouse mitochondria exhibited decreases in Complex IV V_{max} across age.
No differences in mitochondrial integrity or citrate synthase activity.

Overall, the only significant genotype effects were exhibited at an early age, 9 months. At 9 months there were significant genotype effects in Complex I-III, Complex I, and Complex II-III Vmax values with variances on which genotype had higher Vmax activity. By 15 and 22 months no genotypes differences were observed in any of the ETS activities. These results indicate that whatever differences in ETS activities exist as direct result of over-expression of GLUD1, occur only early in age and with advancing age the Tg mice undergo some type(s) of adaptive change(s) to become similar in ETS activities to the wt mice. This would explain why by 15 and 22 months there are no significant genotype effects.

Apart from the significant genotype effects at 9 months both genotypes exhibited similar trends in ETS activities across advancing age. Complex I-III activity significantly decreased across advancing age while Complex II-III activity increased. Even though these trends were similar, they were region specific and the values were significantly different in the three regions. Complex I-III activity decreased in both genotypes across age only in the cerebellum and hippocampus while remaining stable in the frontal cortex. Complex II-III activity increased in both genotypes across age only in the cerebellum and frontal cortex while remaining stable in the hippocampus. These results would indicate that there are region specific differences in ETS activities and these differences are likely not the result of over-expression of GLUD1, but the result of an adaptive or compensatory mechanism. The cause for the adaptive or compensatory mechanism is either the result of changes across age or differences in the three brain regions. The significant region effects may be due to differences in

mitochondrial calcium concentrations and mitochondrial calcium uptake in the brain regions, which would directly affect the ETS activities and these are key measure which we plan to explore in chapter three.

Overall, studies measuring electron transport chain activities have demonstrated that with advancing age coupled Complex I-III activity decreases in different tissues (Brown-Borg, Johnson et al. 2012). We also observed the same decrease in activity with advancing age and this was observed for both genotypes. In wt mice the decreases in activity with age have been attributed by some to be the results of decreases in the protein complexes of the electron transport chain (Gomez, Monette et al. 2009). Our bioenergetic data is not likely the result of differences in Complex I protein levels as our ELISA assay demonstrated that there are no significant genotype effects. In addition, the significant age effect indicated by three-way ANOVA results in decreases in Complex I protein levels across age in all three brain regions, yet the Complex I-III Vmax significant decreases was only for specific regions. These results indicate that Complex I protein levels are not directly contributing to the Vmax data.

Results obtained in wt mice are in agreement with what others have reported as an overall decrease with age in Vmax values of Complex I-III; however, our values are slightly lower than others have reported. Others have reported Vmax values of Complex I-III activity of anywhere from 80-400 nmol/min x mg and our values are below 100 (Gomez, Monette et al. 2009). One reason for this discrepancy could be the type of mitochondria isolation technique we used. It could be argued that we damaged our mitochondria in our isolation

technique; however, our citrate synthase data argue against this idea. In support of our data isolated mitochondria samples are better for understanding mechanisms and many methods and protocols have been well established.

The mitochondria isolated from the Tg mice also demonstrated an age-dependent decrease in Complex I-III activity. These results were surprising in that we might have expected the opposite, an increase in activity with advancing age. The rationale for this expectation is that since the Tg mice over-express the glutamate dehydrogenase gene this would increase production of NADH due to glutamate deamination. Since NADH is the primary substrate which feeds into Complex I of the respiratory chain increased glutamate-dehydrogenase protein and activity should lead to increased levels of NADH and to increased complex I activity. A decrease in the Vmax values for complex I activity could be the result of several factors. Even though we increased the protein levels and activity of glutamate dehydrogenase we do not know if the levels of α-ketoglutarate were also increased. Studies have demonstrated that GLUD1 favors the production of α-ketoglutarate and measuring the levels of this protein in the Tg mouse model would eliminate the possibility that it did not.

An additional possibility for the decreased Complex I-III activity is not due to substrate limitation, but to a regulatory attempt to decrease the heightened activity due to increased substrate availability. In support of this idea Complex I activity is regulated by phosphorylation of specific subunits by protein kinase A (PKA), which increases complex I activity on the other hand, phosphorylation by pyruvate dehydrogenase kinase (PDK) which decreases complex I activity (Maj, Raha et al. 2004) (Raha, Myint et al. 2002). The regulation of these kinases

would function as a compensatory mechanism and would explain why we demonstrated significant genotype effects in Vmax values for Complex I-III at 9 months which decreased with advancing age. The Tg mouse is exposed to over-expression of GLUD1 and excess extracellular glutamate since birth, resulting in a change in NADH levels. If increased substrate availability increases Complex I activity developmentally then by 9 months the cells may have up-regulated compensatory mechanisms in an attempt to decrease the complex I activity. Throughout the aging process this regulation would have resulted in Complex I Vmax values in the Tg mice to be closer to the Vmax values in the wt mice at the older ages, i.e. 15 and 22 months. Our data demonstrate that with advancing age the Complex I Vmax values for the Tg and wt mice are closer in range. This idea is supported by studies that have shown that pyruvate dehydrogenase activity (PDK) is stimulated by the presence of increased NADH (Maj, Raha et al. 2004).

The observation that at a specific age there were region specific differences in complex I activity could be due to several factors. Complex I is a large protein made up of 45 subunits, seven of which are encoded by mtDNA. Several studies have shown that there is a differential expression of many of the subunits across different brain regions (Wirtz and Schuelke 2011). This differential expression is thought to be due to region specific dependence of complex I, i.e. higher levels of the subunits in cerebellar Purkinje cells resulting in increased complex I activity needed for higher brain order functions. In addition, this same group also showed increased levels of the subunits in hippocampal CA1/CA3 regions which correlates with our data in which we demonstrated

increased Complex I-III activity in the cerebellum and hippocampus as compared to the frontal cortex at 9 months (Wirtz and Schuelke 2011).

In addition to a differential expression of Complex I subunits leading to altered activity, mutations in the subunits of Complex I could also lead to altered activity. If a specific brain region is more susceptible to oxidative damage or accumulates reactive oxygen species faster or in higher amounts, these radicals could lead to increased oxidation of the subunits, thereby decreasing complex I activity. It would be interesting to look at whether different brain regions in the wt and Tg mice have different or similar levels of reactive oxygen species and what happens to those levels with advancing age (chapter 4).

The Tg mice did not show the regional differences observed in the wt mice did leading us to believe that there were other mechanisms, in addition to or apart from complex I, leading to the neurodegeneration observed in the Tg mice; possibly the altered activity of other complexes along the respiratory chain.

With regard to Complex II-III activity, we observed that there was an overall increase in Vmax values with advancing age in three different brain regions and when the regions were combined. These results are very interesting in that most studies have demonstrated decreases in complex II activity with advancing age (Choksi, Nuss et al. 2011). The difference in the trend could be a compensatory mechanism in an attempt to make up for the decreased complex I-III activity with age. If there is a decrease in overall ATP output due to decreased complex I-III activity, the cell might be attempting to make up for this bioenergetic deficit by increasing Complex II-III activity. If this is the case, then an increase in the substrate which feeds into this complex would be necessary. Succinate is

the main substrate which feeds into Complex II and in the Tg mice succinate levels might be increased due to the increased α-ketoglutarate intermediate which should result in an overall up-regulation of the TCA cycle. If this is the case there would be increased levels of succinate available and with advancing age these levels would increase leading to increased levels of complex II-III activity. This same idea; however, may not be as likely since we saw the increase in activity in both genotypes. Therefore the increase in activity in complex II-III cannot be entirely due to the over-expression of the glutamate dehydrogenase gene, but an overall compensatory mechanism utilized by all cells.

There were no differences between Tg and wt mouse mitochondria in terms of complex IV (cytochrome c oxidase) activity. The only significant effect demonstrated was an age effect, with advancing age there was a significant decrease in complex IV activity. These data are in agreement with data by many others that have shown a decrease in activity with advancing age (Paradies, Ruggiero et al. 1997) (Sohal 1993) (Curti, Giangare et al. 1990). Complex IV activity followed the same pattern as Complex I-III activity. Complex I-III activity may have "diluted out" the Complex II-III activity simply because Complex I is the main entry point for the chain and under normal physiological settings the electron flow into the chain operates at a 4:1 NADH:succinate ratio (Gnaiger 2009).

We observed a lower Vmax for Complex I activity in the Tg as compared to wt mice. This result was not expected as a higher availability of NADH due to over-expression of GLUD1, should result in higher Complex I activity. A possible

explanation could be a down regulation of complex I activity as an adaptive response to the increased substrate. Complex I-III activity decreased across age while Complex II-III activity increased across age. This might be the result of a compensatory response in order make up for the decreased I-III activity and/or might be the result of increased succinate due to the over-expression of GLUD1.

Overall, we demonstrated changes in electron transport activities that were genotype, region, and complex specific. Additionally, we observed different patterns in the activities of these complexes with advancing age. A consequence of changes in electron transport system activities is altered generation of a proton gradient in the inner mitochondrial membrane. Such a gradient is necessary to drive calcium uptake into mitochondria. Altered calcium homeostasis because of changes in mitochondrial function is a frequently invoked pathway leading to neurodegeneration. In addition, the increase in glutamate levels in Tg mice would lead to increased glutamate receptor activation and therefore increases in calcium in the postsynaptic cell. This led to the next series of studies to examine whether the mitochondria from Tg mice had higher concentrations of calcium due to the increases in glutamate and whether calcium uptake into mitochondria was altered in the different ages and regions, possibly as a result of any changes in mitochondrial membrane potential.

Citations

Aarts, M., W. Wei, et al. (2003). "A key role for TRPM7 channels in anoxic neuronal death." Cell **115**: 863-877.

Bao, X., R. Pal, et al. (2009). "Transgenic Expression of *Glud1* (Glutamate Dehydrogenase 1) in Neurons: *In vivo* model of enhanced glutamate release, altered synaptic plasticity, and selective neuronal vulnerability." Journal of Neuroscience **29**: 13929-13944.

Brookes, P., Y. Yisang, et al. (2004). "Calcium, ATP, and ROS: a mitochondrial love-hate triangle." Am J Physiol Cell Physiol **287**.

Brown-Borg, H., T. Johnson, et al. (2012). "Expression of oxidative phosphorylation components in mitochondria of long-living Ames dwarf mice." AGE **34**: 43-57.

Choksi, K., J. Nuss, et al. (2011). "Mitochondrial electron transport chain functions in long-lived Ames dward mice." Aging **3**: 1-14.

Curti, D. and M. Giangare (1990). "Age-related modifications of cytochrome c oxidase activity in discrete brain regions." Mechanims of Ageing and Development **55**: 17-180.

Curti, D., M. Giangare, et al. (1990). "Age-related modificaitons of cytochrome c oxidase activity in discrete brain regions." Mechanisms of Ageing and Development **55**: 171-180.

Freddari-Bertoni, C. and P. Fattoretti (2004). "Cytochrome oxidase activity in hippocampal synaptic mitochondria during aging: a quantitative cytochemical investigation." Ann. N.Y. Acad. Sci **1019**: 33-36.

Freddari-Bertoni, C., P. Fattoretti, et al. (2004). "Cytochrome Oxidase Activity in Hippocampal Synaptic Mitochondria during Aging: A Quantitative Cytochemical Investigation." Ann. N.Y. Acad. Sci. **1019**: 33-36.

Gnaiger, E. (2009). "Mitochondrial Pathways through Complexes I + II: Convergent electron transport at the Q-junction and additive effect of substrate combinations." Mitochondrial pathways and respiratory control: 21-33.

Gomez, L., J. Monette, et al. (2009). "Supercomplexes of the mitochondrial electron transport chain decline in the aging rat heart." Arch Biochem Biophys **1**: 30-35.

Gunter, T., L. Buntinas, et al. (2000). "Mitochondrial calcium transport: mechanisms and functions." Cell caclium **28**: 285-296.

Gunter, T., D. Yule, et al. (2004). "Calcium and mitochondria." FEBS Lett **567**: 96-102.

Janssen, A., F. Trijbels, et al. (2007). "Spectrophotometric Assay for Complex I of the Respiratory Chain in Tissue Samples and Cultured Fibroblasts." Endocrinology and Metabolism **53**: 729-734.

Janssen, A., F. Trijbels, et al. (2007). "Spectrophotometric Assay for Complex I of the

Respiratory Chain in Tissue Samples and

Cultured Fibroblasts." Clinical Chemistry **53**: 729-734.

Liu, Y., G. Fiskum, et al. (2002). "Generation of reactive oxygen species by the mitochondrial electron transport chain." Journal of Neurochemistry **80**: 780-787.

Maj, M., S. Raha, et al. (2004). "Regulation of NADH/CoQ Oxidoreductase: Do phosphorylation events affect activity?" The Protein Journal **23**: 25-32.

Maj, M., S. Raha, et al. (2004). "Regulation of NADH/CoQ oxidoreductase: do phosphorylation events affect activity?" Protein J **23**: 25-32.

Muller, F., A. Roberts, et al. (2003). "Architecture of the Qo site of the cytochrome bc1 complex probed by superoxide production." Biochemistry **42**: 6493–6499.

Paradies, G., F. Ruggiero, et al. (1997). "Age-dependent decline in the cytochrome c oxidase activity in rat heart mitochondria: role of cardiolipin." FEBS Lett **406**: 136-138.

Paradies, G. and R. Ruggiero (1997). "Age-dependent decline in the cytochrome c oxidase activity in rat heart mitochondria: role of cardiolipin." FEBS Lett **406**: 970-981.

Raha, S., A. Myint, et al. (2002). "Control of oxygen free radical formation from mitochondrial complex I: roles for protein kinase A and pyruvate dehydrogenase kinase." Free Radic. Biol. Med **32**: 421-430.

Rothstein, D. J., M. Dykes-Hoberg, et al. (1996). "Knockout of Glutamate Transporters Reveals a Major Role for Astroglial Transport in Excitotoxicity and Clearance of Glutamate." Neuron **16**: 675-686.

Sohal, R. (1993). "Aging, cytochrome oxidase activity, and hydrogen peroxide release by mitochondria." Free Radical Biology and Medicine **14**: 583-588.

Sohal, R. (1993). "Aging, cytochrome oxidase activity, and hydrogen peroxode release by mitochondria." Free radical biology and medicine **14**: 583-588.

Tanaka, K., K. Watase, et al. (1997). "Epilepsy and exacerbation of brain injury in mice lacking the glutamate transporter GLT-1." Science **276**: 1699-1702.

Wang, X., R. Pal, et al. (2007). "Genome-wide transcriptome profiling of region-specific vulnerability to oxidative stress in the hippocampus. ." Genomics **90**: 201-212.

Wang, X., R. C. Pal, XW, et al. (2005). "High intrinsic oxidative stress may underlie selective vulnerability of the hippocampal CA1 region. ." Brain Res Mol Brain Res **140**: 120-126.

Wang, X., A. Zaidi, et al. (2009). "Genomic and biochemical approaches in the discovery of mechanisms for selective neuronal vulnerability to oxidative stress." BMC Neuroscience **10**: 1-20.

Wirtz, S. and M. Schuelke (2011). "Region-specific expression of mitochondrial complex I during murine brain development." PLoS ONE.

Chapter Three: Effects of the Over-Expression of Neuronal Glutamate Dehydrogenase (GLUD1) on Brain Mitochondrial Calcium Homeostasis

7. INTRODUCTION

Eukaryotic cells produce ~95% of their energy in the form of ATP; the major source of the ATP generated is the mitochondria through the process of oxidative phosphorylation. In addition to being the source of the majority of the cell's energy, mitochondria also play a pivotal role in calcium (Ca^{2+}) regulation within the cell. Calcium uptake into mitochondria was first described in the early 1960s and since then many laboratories have described the mechanisms involved in mitochondrial Ca^{2+} uptake and the overall significance of mitochondrial regulation of Ca^{2+} homeostasis (DeLuca and Engstrom 1961). Mitochondrial Ca^{2+} transport is crucial in regulating cytoplasmic free calcium concentrations [Ca^{2+}], i.e., Ca^{2+} buffering. Mitochondria serve as a calcium reservoir and protect cells from any Ca^{2+}-induced cell stress. Mitochondria also function as a source of releasable Ca^{2+} back into the cytosol as needed.

Mitochondrial Ca^{2+} levels also control the activation of three important dehydrogenases within mitochondria and links mitochondrial Ca^{2+} to oxidative phosphorylation. Specifically, a component of the glycolytic pathway that links that pathway to the TCA cycle, the enzyme pyruvate dehydrogenase, two TCA cycle enzymes, α-ketoglutarate and isocitrate dehydrogenase, and an enzyme of

the electron transport chain, ATP synthase, are all controlled by intra-mitochondrial free Ca^{2+} concentrations ($[Ca^{2+}]_m$) (Das and Harris 1990) (Mailer 1990) (Balaban 2002) (Das and Harris 1990) (Hansford and Zorov 1998) (McCormack and Denton 1993). Because of the multiple regulatory steps in which mitochondrial Ca^{2+} is involved, Ca^{2+} dysregulation in mitochondria can have very damaging effects on cell metabolism and viability. For example, large increases in $[Ca^{2+}]_{m+}$ have been associated with pathophysiological conditions and cell death (Krieger and Duchen 2002). The mechanism through which Ca^{2+} leads to cell death (apoptosis) is by opening the mitochondrial PT pore and causing cytochrome c release, a critical event in initiating caspase activation and apoptosis (Loeffler and Kroemer 2000).

In chapter two, the effects of the over-expression of GLUD1 on mitochondrial bioenergetics were examined. In this chapter, the effects of increased expression of GLUD1 in mitochondria on $\Delta\Psi_m$ and Ca^{2+} homeostasis were explored. The change in mitochondrial bioenergetics would alter chemiosmosis which would change the $\Delta\Psi_m$. As a consequence of this change in $\Delta\Psi_m$, Ca^{2+} homeostasis would be changed since $\Delta\Psi_m$ drives Ca^{2+} uptake into mitochondria (Brookes, Yoon et al. 2004) (Hill and Kats 2007) (Rottenberg and Scarpa 1974). Our hypothesis was that $\Delta\Psi_m$ and Ca^{2+}homeostasis would be altered due to changes in both the TCA and ETS enzyme activities.

8. MATERIALS

All chemicals used were purchased from Sigma-Aldrich unless otherwise noted. Fluo-3 Acetoxymethyl ester (Fluo-3/AM) was from Invitrogen (Catalog #F-1241).

9. METHODS

Isolation of mitochondrial pellets

Mitochondrial samples from three different brain regions cerebellum, frontal cortex, and hippocampus were isolated as described in chapter two materials and methods section.

Determination of Ca^{2+} steady state levels and kinetics

To determine the calcium steady state levels and mitochondrial Ca^{2+} kinetics we followed the method described in Saavedra-Molina et al (Saavedra-Molina, Uribe et al. 1990). Brain mitochondria (0.5 mg/ml) were incubated for 20 min at 25 ^{o}C with shaking in a medium containing (in mM): 220 mannitol, 70 sucrose, 2 MOPS (pH 7.4), 2 phosphate-tris, 2 $MgCl_2$, and in (μM): 10 Fluo-3/AM, 600 EGTA, plus 0.003% pluronic acid. The extra-mitochondrial Ca^{2+} concentration in the medium was maintained at different levels between 100 nM and 1 μM by using an EGTA (600 μM) Ca^{2+} buffering medium. The program MAXCHELATOR (http://maxchelator.stanford.edu/) was used to determine the concentration of

EGTA and Ca^{2+} that was needed to maintain a specific free Ca^{2+} concentration $[Ca^{2+}]_f$. The fluorescence of mitochondrial suspensions was monitored in a BioTek Synergy HT spectrophotometer with an excitation wavelength set at 506 nm and emission at 526 nm. The kinetic measurements were obtained over a period of 25 min and at 30-sec intervals. All measurements were done in triplicate on a 96-well plate. The mitochondrial samples were isolated from three brain regions and from four mice of each genotype and at each age.

Measurement of free intramitochondrial calcium concentrations ($[Ca^{2+}]_m$)

Isolated brain mitochondrial samples (0.125 mg/ml) were incubated for 20 min at 25 ^oC with shaking in a buffer containing (in mM): 210 mannitol, 70 sucrose, 10 MOPS, plus 0.5% bovine serum albumin, 10 μM Fluo-3/AM, and 0.003% pluronic acid,. After incubation in the above described medium, the mitochondria were centrifuged, resuspended and re-precipitated twice, (Eppendorf microfuge) for 2 min and finally re-suspended in the above described medium. Fluorescence was measured as described above. In each assay, a minimum and a maximum fluorescence for Ca^{2+} (F_{min}/F_{max}) were obtained by treating the mitochondrial samples at the end of each assay with a combination of EGTA and deoxycholate (0.6 mM and 0.05% w/v, respectively) in order to obtain the value for F_{min}, and with 8 mM Ca^{2+} final concentration in order to measure F_{max}. The Ca^{2+} concentration was calculated by using the formula described under data analysis. All measurements were done in triplicate on a 96-well plate.

Measurement of mitochondrial Ca^{2+} due to uptake

Mitochondrial Ca^{2+} uptake was determined according to the methods described above except for the addition in the incubation solutions of extra-mitochondrial Ca^{2+} at either 100 nM Ca^{2+} or 1μM. All samples included 2.5 μM thapsigargin (Tg) in order to block Ca^{2+} uptake into the ER. In some samples, substrates were added in order to energize the mitochondria, metabolic inhibitors, either rotenone or antimycin, or an inhibitor of the uniporter and of the Ca^{2+}/H^{+} exchanger, RU-360, were added. The two substrates used to energize mitochondria were 5 mM glutamate/5 mM malate or 5 mM succinate. When the combination of 5 mM glutamate/5 mM malate was used as the substrate, two different assays were carried out: one in which Ca^{2+} transport was measured in the presence of 2 μM rotenone and the other in its absence. The rotenone-inhibited Ca^{2+} levels were determined by subtracting the $[Ca^{2+}]_m$ after rotenone addition from the estimated $[Ca^{2+}]_m$ in its absence. These values represented the rotenone-sensitive and glutamate/malate-activated Ca^{2+} uptake into the mitochondrial matrix. When 5 mM succinate was used as the substrate, 2 μM antimycin was used as an inhibitor. The contribution of the Ca^{2+} uniporter and of the Ca^{2+}/H^{+} exchange carriers to overall Ca^{2+} uptake measured under the conditions described above was determined by performing the Ca^{2+} uptake assays in the presence or absence of ruthenium red Ru-360, 10μM.

Determination of $\Delta\Psi_m$ using tetramethylrhodamine

Isolated brain mitochondrial samples (0.5 mg/ml) were incubated for 30 min at 37 ^{o}C in a buffer containing (in mM): 135 KCl, 20 MOPS, 5 K_2HPO_4, 5 $MgCl_2$, and 2.5 tetramethylrhodamine methyl ester dye (TMRM). The TMRM dye was dissolved in methanol. Resting state (no substrate) measurements were obtained for a period of 3 min and at 15-sec intervals. Following the resting state measurements, the mitochondria were energized with a substrate either, 10 mM glutamate/10 mM malate or 10 mM succinate, and fluorescence readings were obtained for a period of 3 min and at 15-sec intervals. These measurements were followed by the addition of a substrate and inhibitor, either 2 μM rotenone when 10 mM glutamate/10 mM malate was the substrate or 2 μM antimycin when 10 mM succinate was the substrate, fluorescence was monitored for another 3 min taking measurements at 15-sec intervals. At the conclusion of the assay, the membrane potential un-coupler carbonylcyanide-*p*-trifluoromethoxyphenylhydrazone (FCCP; 1 μM) was added. The $\Delta\Psi_m$ was determined by the changes in TMR fluorescence in response to respiratory substrates. All assays were run on four mitochondrial samples from each brain region of Tg and wt mice at each of the three ages described above.

Data analysis

Determination of $[Ca^{2+}]_m$

The $[Ca^{2+}]_m$ was determined by measuring the F_{min} and F_{max} in each assay as described above. The $[Ca^{2+}]_m$ was estimated using the following equation:

$$[Ca^{2+}]F_m = K_d\ (F-F_{min})\ /\ (F_{max}-F)$$

where F is the fluorescence of the sample, K_d is the dissociation constant for Ca^{2+} binding to Fluo-3, estimated previously to be equal to 0.40 μM (Saavedra-Molina, Uribe et al. 1990). All samples were run in triplicates on a 96-well plate.

3. RESULTS.

$\Delta\Psi_m$ in mitochondria from wt and Tg mice

Based on our studies of differential Complex II-III activities in Tg *vs*. wt mitochondria (chapter 2), we hypothesized that there would be differences between Tg and wt also in H^+ concentration in the intermembrane space and in $\Delta\Psi_m$. Using intra-mitochondrial TMR fluorescence as the measure of $\Delta\Psi_m$, assays were performed under resting state and energized conditions. The measurements obtained clearly indicated that both the wt and Tg mouse mitochondria from the cerebellum, frontal cortex, and hippocampus exhibited increases in the $\Delta\Psi_m$ following activation of the ETS by glutamate/malate (Fig. 1A-C). This observation was similar to what was documented previously

(Calderon-Cortex and Cortes-Rojo 2008). A major difference between mitochondria from wt and Tg mice was the high $\Delta\Psi_m$ of the Tg mitochondria in the resting state as compared with the $\Delta\Psi_m$ of wt mitochondria. The addition of the Complex I inhibitor rotenone, markedly suppressed the mitochondrial $\Delta\Psi_m$ to levels equal to or slightly below those observed in the resting state (Fig. 1A-C). The addition of the protonophore FCCP led to the complete collapse of the $\Delta\Psi_m$, as expected (Fig.1A-C).

Having established the apparent validity of the $\Delta\Psi_m$ measurements using TRM fluorescence as the measure of $\Delta\Psi_m$, in the remaining assays only the treatments with the addition of a substrate were carried out. In these measurements of $\Delta\Psi_m$, a mean value for the baseline measurements was obtained and this value was subtracted from each data point following the addition of a Complex I or II substrate. Mitochondria obtained from the three different brain regions and across the three ages of Tg mice, had an almost 2-fold higher $\Delta\Psi_m$ in the resting state as compared with that of the wt mouse mitochondria (Fig 2A-C). Student's t-test revealed a highly significant genotype difference ($p \leq 0.001$) between Tg and wt mice across all ages and regions (Fig. 2A-C). The measurements of $\Delta\Psi_m$ of the combined brain regions cerebellum, frontal cortex, and hippocampus revealed significant age ($p=0.001$) and genotype ($p=<0.001$) effects as determined by three-way ANOVA analysis (Fig. 3).

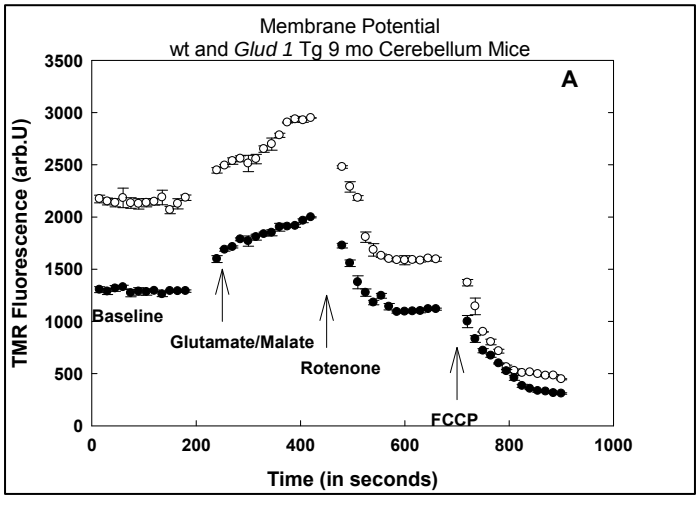

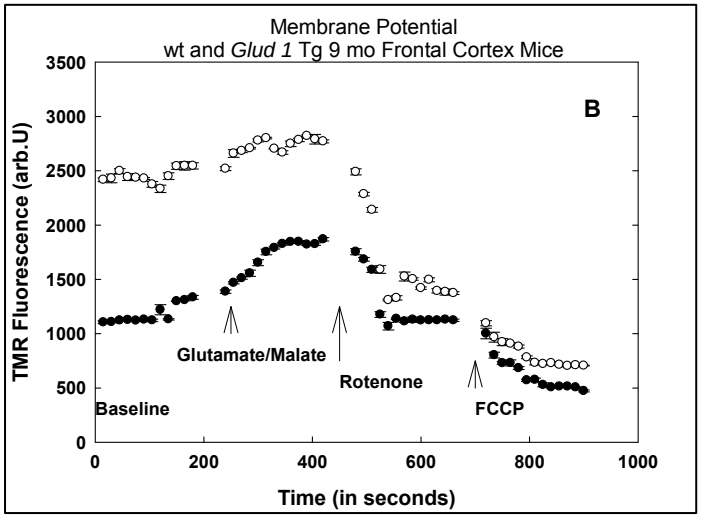

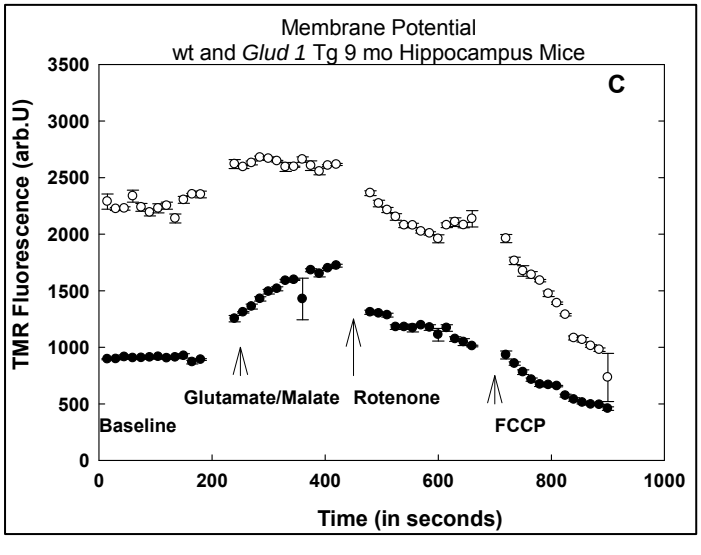

Figure 1: Membrane potential as measured by TMR fluorescence of Tg and wt mice mitochondria from 9 month A) Cerebellum B) Frontal cortex and C) Hippocampus. The data represent the average (+-S.E.) from 4 mitochondrial preparations. All measurements of fluorescence were obtained every 15 sec. Each treatment was 3 mins long. Open circles denote Tg and dark circles wt samples.

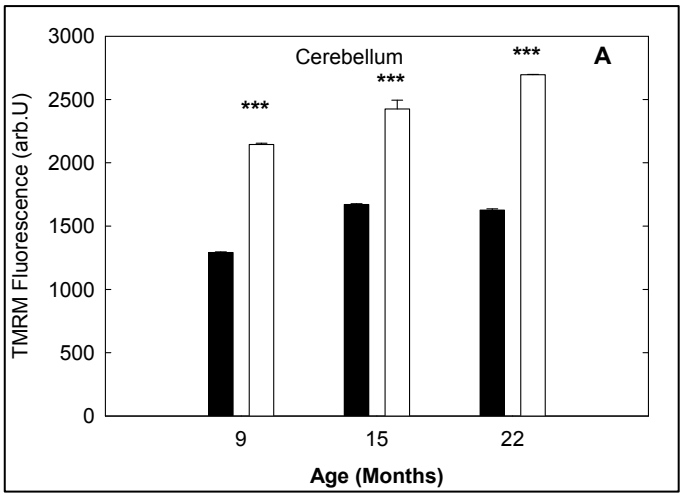

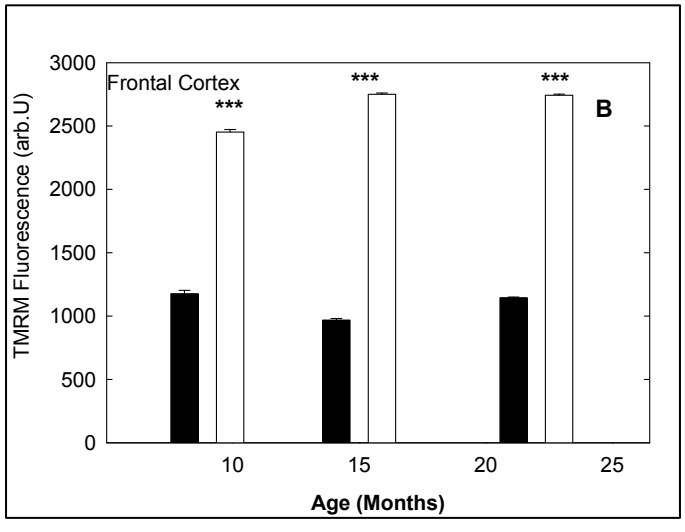

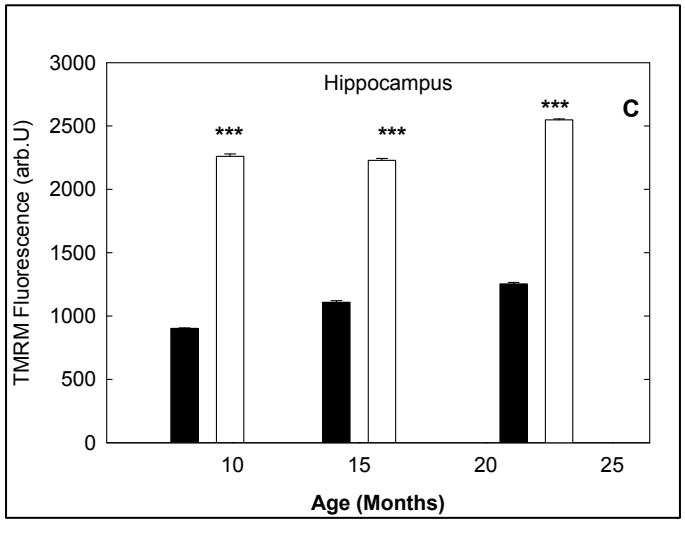

Figure 2: Membrane potential across age of Tg and wt mice. Mitochondria were isolated from A) Cerebellum B) Frontal Cortex and C) Hippocampus. All experiments were performed using n=4 mice of each genotype. Open bars indicate Tg and dark bars wt mouse mitochondria. ***=p≤0.001 (Student's t-test).

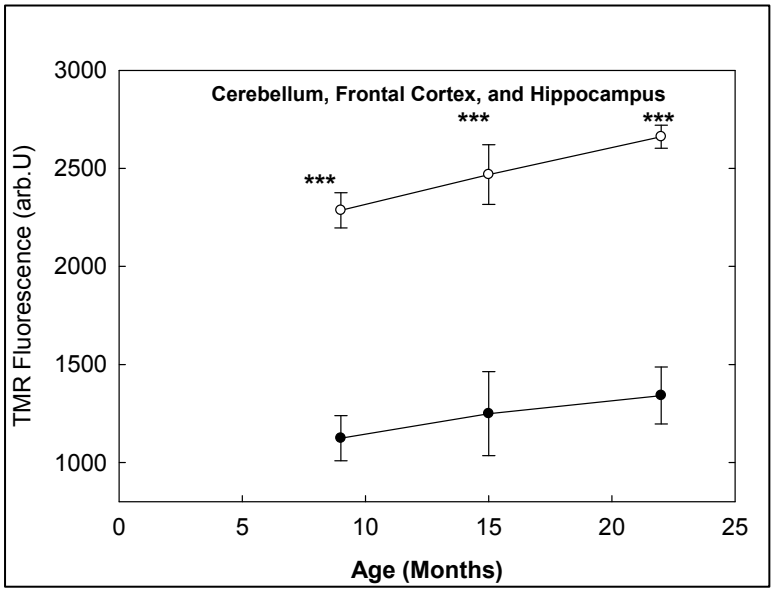

Figure 3: Membrane potential average across age. Mitochondria were isolated from cerebellum, frontal cortex, and hippocampus and were combined as one sample. All experiments were performed using n=4 mice f each genotype. Open circles indicate Tg and dark circles wt mitochondria. Student's t-test ***=p≤0.001.

$\Delta\Psi_m$ in energized Tg and wt mitochondria across age, brain region, and in response to different substrates

The mitochondrial $\Delta\Psi_m$ was measured following the addition of substrates, either 10 mM each of glutamate/malate or succinate. To determine the net change in membrane potential following substrate addition, the average value of baseline TMR fluorescence in the absence of substrate was subtracted from the values in the presence of the different substrates. Once the baseline values were subtracted, the plots of fluorescence vs. time following the addition of substrate were essentially linear increases in fluorescence across time (Fig. 4).

The slopes of the lines were estimated and the values for each brain region at each age of Tg and wt mice were analyzed using three-way ANOVA.

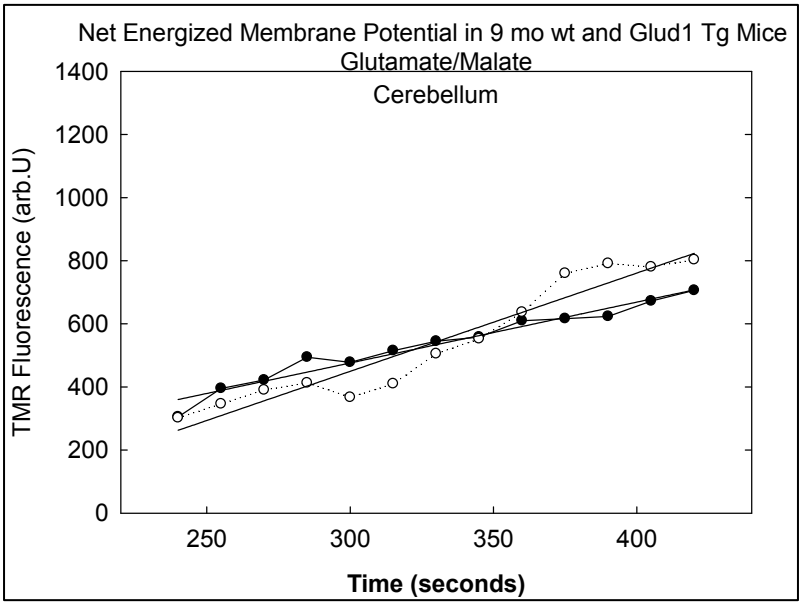

Figure 4: Energized membrane potential in 9 month cerebellum wt (dark circles) and Tg (open circles) samples. In the presence of 5mM glutamate/malate. Three min reading with 15 sec intervals.

Approach for estimating steady state concentrations and kinetics of $[Ca^{2+}]_m$

In figure 5B, an extra-mitochondrial Ca^{2+} concentration of 400 nM was maintained using an EGTA buffer system. After ~7 min of fluorescence measurements, $[Ca^{2+}]_m$ reached a steady state. The addition of an extra amount of EGTA in the extramitochondrial medium (600 μM EGTA) caused a rapid decrease in Fluo-3 reaching a steady state within 100 sec. This drop was expected as EGTA functions as a Ca^{2+} chelator and would bind free Ca^{2+} thus causing re-equilibration of $[Ca^{2+}]_m$ and a drop in fluorescence. The addition of ionomycin caused a further decrease in fluorescence, as expected, because ionomycin functions as an ionophore that would lead to calcium efflux from the mitochondria and its chelation by EGTA. The subsequent addition of deoxycholate (DOC) had a similar effect as ionomycin, and was again expected as DOC is a mild detergent that would permeabilize the mitochondrial membrane and lead to the release of calcium from the mitochondrial matrix. In figure 5A there was zero extra mitochondrial Ca^{2+} in the beginning of the assay and the fluorescence values were very low and similar to those values in 5B when EGTA was used in the medium to chelate Ca^{2+}. After addition of 400 nM of extra mitochondrial Ca^{2+} the fluorescence values reached levels similar to that in 5A when the assay contained 400 nM of extra mitochondrial Ca^{2+} in the medium at the beginning of the measurements. With the addition of 400 nM of Ca^{2+} the values remain steady after a few seconds. The addition of EGTA together with DOC caused a marked decrease in fluorescence, as would be expected as a result of loss of intramitochondrial Ca^{2+} and its chelation in the extramitochondrial

medium by the chelator EGTA. These results indicate that the steady state levels and kinetics of mitochondrial calcium can be determined.

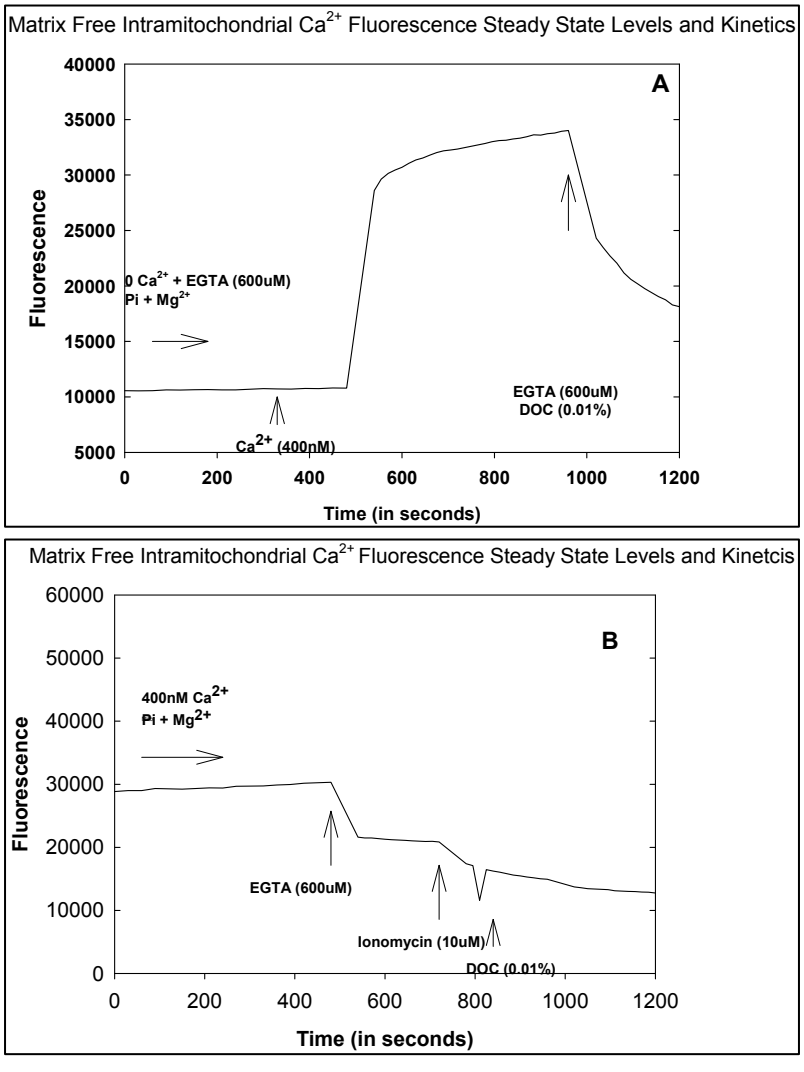

Figure 5: Determination of mitochondrial free calcium in mouse brain cerebellum. Mitochondria (0.5mg/ml) were loaded with fluo-3 with A) zero calcium or B) 400 nM calcium with 2mM phosphate-tris and 2mM MgCl2. Additions of other reagents were made where indicated by the arrows.

Resting $[Ca^{2+}]_m$ across age and brain regions of wt and Tg mice

Initially we wanted to determine if there were differences in the levels of $[Ca^{2+}]_m$ in the Tg vs. the wt mice. Our hypothesis was that there would be differences in the levels due to the observed significant differences in $\Delta\Psi_m$ between the wt and Tg mice. It has been shown previously that Ca^{2+} homeostasis and Ca^{2+} uptake is driven by the $\Delta\Psi_m$ (Gunter, Buntinas et al. 2000) (Gunter, Yule et al. 2004) (Rottenberg and Scarpa 1974) (Brookes, Yisang et al. 2004; Santo-Domingo and Demaurex 2010). The levels of $[Ca^{2+}]_m$ were measured as described above in mitochondria isolated from three brain regions of Tg and wt mice of three different ages.

Other investigators have shown that $[Ca^{2+}]_m$ levels increase with age (Peterson and Gibson 1983) (Xiong, Verkhratsky et al. 2002). This accumulation is thought to occur as a result of decreased ATP generation which is required by the plasma membrane and ER calcium-ATPases to pump calcium out of the cell or sequester Ca^{2+} into the ER. With advancing age, the mitochondrial electron transport chain activities decrease, especially Complex IV as we (Chapter 2) and others have shown before, thus leading to an overall decrease in ATP generation (Kann and Kovacs 2006). Therefore, it was important to determine whether there were differences in the levels of free $[Ca^{2+}]_m$ in the brain mitochondria of wt and Tg mice across the ages of 9, 15, and 22 mos of age.

Across the three brain regions examined, there were similar levels of $[Ca^{2+}]_m$, even during the aging process. The $[Ca^{2+}]_m$ in wt mice varied little across the three age groups, while in the Tg mice, there appeared to be some

increase in $[Ca^{2+}]_m$ in the oldest set of mice, especially in the cerebellum (Fig 6A). Overall, there were no significant differences in the levels of $[Ca^{2+}]_m$, except at 22 months in the cerebellum, Tg levels were higher as compared to wt (Fig. 6A) ($p=0.038$). However, when the data were combined and analyzed by three-way ANOVA, a significant genotype effect ($p=0.002$) was observed with the Tg mouse mitochondria exhibiting higher levels of $[Ca^{2+}]_m$ across regions and ages.

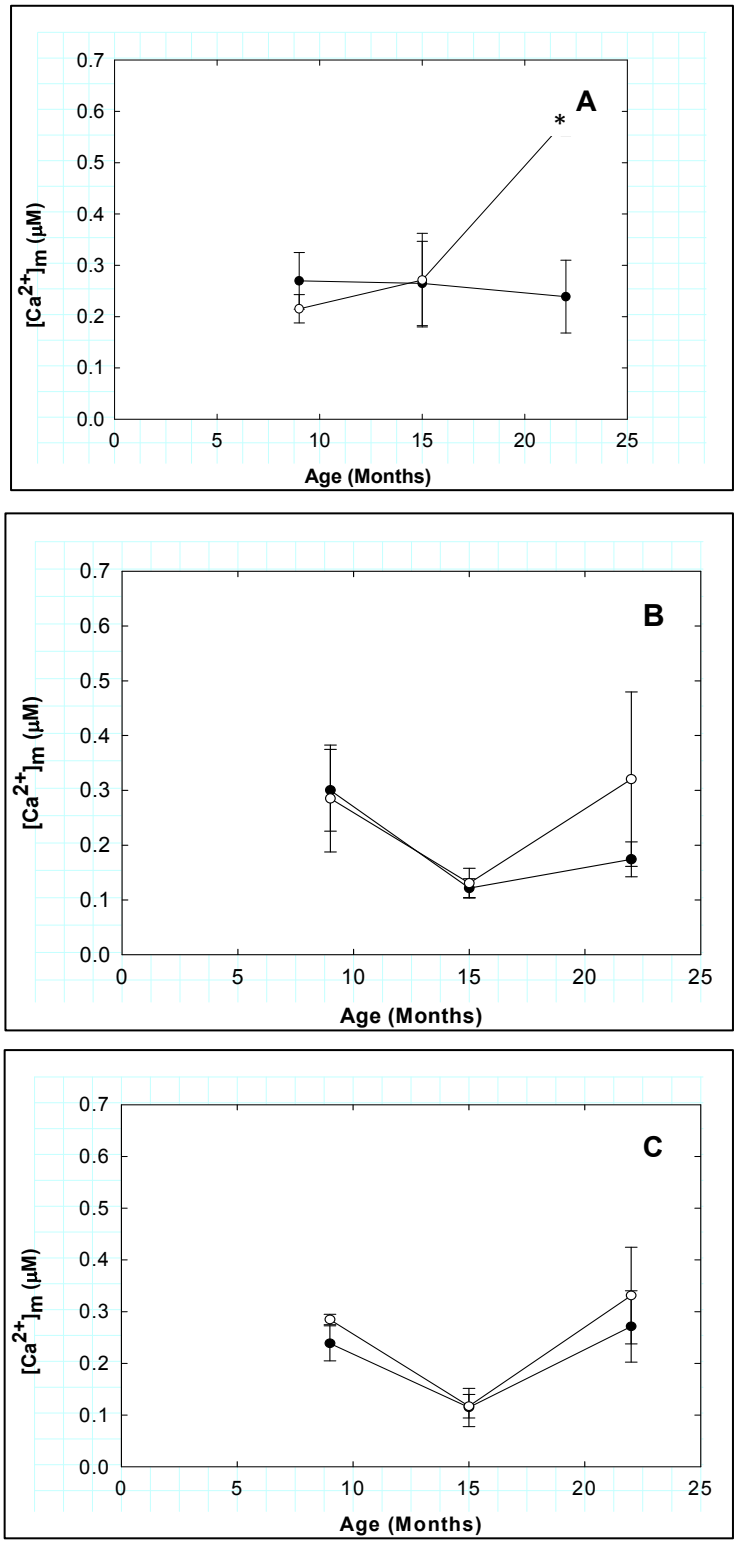

Figure 6: Free Intramitochondrial calcium levels across age of Tg and wt mice. Mitochondria were isolated from A) Cerebellum B) Frontal Cortex and C) Hipocampus. All experiments were performed using n=4 mice of each genotype. Open circles indicate Tg and dark circles wt mice mitochondria. The results shown represent the average (±SE) from an n=4 mice, each sample measure in triplicates. Student's t-test *p=0.038.

Ca^{2+} concentration due to uptake into brain mitochondria obtained from Tg and wt mice

The generation of ATP by mitochondria is regulated by Ca^{2+} through its activation of key mitochondrial matrix dehydrogenases (McCormack, Halestrap et al. 1990). Thus, periodic increases in cytoplasmic $Ca^{2+,}$ also known as calcium oscillations, cause increases in mitochondrial NADH levels (Pralong, Spat et al. 1994) thereby providing a mechanism by which Ca^{2+} concentrations regulate mitochondrial bioenergetics. If Ca^{2+} plays such an important regulatory role in mitochondrial bioenergetics, and if the $\Delta\Psi_m$ is the result of H^+ release into the intermembrane space following increased respiratory activity, then Ca^{2+} uptake into mitochondrial might also differ in the Tg as compared with wt mice. A question being addressed by the following studies was whether the lifelong exposure to glutamate might lead to gradual increases in $[Ca^{2+}]_m$ as a buffering response or to a down-regulation of Ca^{2+} uptake as a compensatory response that would prevent excessive increases in $[Ca^{2+}]_m$ and possible mitochondrial and cell damage.

The differences we observed in Ca^{2+} levels under resting conditions could be a result of several processes, such as changes in the concentration of bound vs. free intra-mitochondrial calcium levels. In order to determine whether any such differences in $[Ca^{2+}]_m$ were the direct result of altered Ca^{2+} uptake, we measured $[Ca^{2+}]_m$ following the addition of exogenous Ca^{2+}, i.e., the transport activity of mitochondria. Our rationale for using two exogenous Ca^{2+} concentrations, a high (1 μM) and low (100 nM) extra-mitochondrial Ca^{2+}

concentration, was based on studies which have shown that the uptake of Ca^{2+} by mitochondria is regulated by cytoplasmic Ca^{2+} levels. Specifically, the majority of Ca^{2+} uptake occurs through the Ca^{2+} uniporter and this channel has been shown to be activated by external Ca^{2+} and deactivated by removal of extra-mitochondrial Ca^{2+} (Kroner 1986) (Kirichok, Krapivinsky et al. 2004) (Baughman, Perocchi et al. 2011; De Stefani, Raffaello et al. 2011). We chose the concentration of 100 nM as our low concentration because this is approximately equal to the concentration of calcium in the cytosol under normal physiological conditions.

Calcium uptake occurs in respiring mitochondria, so we used two different substrates to increase the membrane potential by increasing ΔpH across the inner mitochondrial membrane; the two substrates used were glutamate/malate (NADH-generating) and succinate ($FADH_2$-generation). The effects of advancing age on Ca^{2+} uptake into mitochondria from different brain regions were also examined. Because it has been shown that high local Ca^{2+} concentrations can cause Ca^{2+} release from the ER and transfer of such Ca^{2+} to mitochondria (Rizzuto and Pozzan 2006), we measured Ca^{2+} uptake into mitochondria in the presence of thapsigargin, an inhibitor of ER Ca^{2+} ATPase and of Ca^{2+} uptake into the ER. This was done in order to ensure that the calcium uptake we were measuring was due only to mitochondrial calcium uptake and not uptake into the ER that may remain attached to mitochondria as the so-called mitochondrial associated membranes.

The parameter that affected Ca^{2+} uptake most significantly was the concentration of exogenous Ca^{2+} added to the assay. When low Ca^{2+}

concentrations were present (100 nM) the uptake of Ca^{2+} in the presence of glutamate/malate decreased in both wt and Tg mouse mitochondria with advancing age of the mice and across all regions (Fig. 7A-C).This decrease reached significant levels for mitochondria isolated from the cerebellum and hippocampus (Fig.7A and C, p=0.008) as determined by three-way ANOVA. When Ca^{2+} uptake was measured in the presence of succinate as the substrate and of 100 nM extramitochondrial Ca^{2+}, there were no significant differences as determine by three-way ANOVA analysis (Fig. 9A-C). A trend of decreasing Ca^{2+} uptake with advancing age was observed, once again, when mitochondrial metabolism was activated by succinate, especially in mitochondria from the frontal cortex and hippocampus, although the effect was not as pronounced as it was when glutamate/malate was used as the substrate.

Significant genotype, region, age, and substrate-specific effects were seen in the Tg mice, but not the wt mice, when Ca^{2+} uptake was measured in the presence of high extramitochondrial Ca^{2+} concentration (1 μM) and glutamate/malate as the substrate. Under these conditions, the brain mitochondria from wt mice maintained stable Ca^{2+} uptake activity across different brain regions and with advancing age while the mitochondria from Tg mice exhibited significantly decreased Ca^{2+} uptake with advancing age ($p \leq 0.001$) as shown in Fig. 8 A-C. The estimated Ca^{2+} uptake in mitochondria isolated from the cerebellum and cortex of Tg mice was significantly higher compared with that in mitochondrial from the same two regions of the brain of wt mice (p=0.011, three-way ANOVA). When succinate was used as the substrate and in the presence of 1 μM extramitochondrial Ca^{2+}, the levels of Ca^{2+} uptake were very

low as compared to when glutamate/malate was used the substrate (Fig.10 A-C). There were no significant region, age, or genotype effects detected in mitochondrial uptake measured under these conditions as indicated by three-way ANOVA analysis.

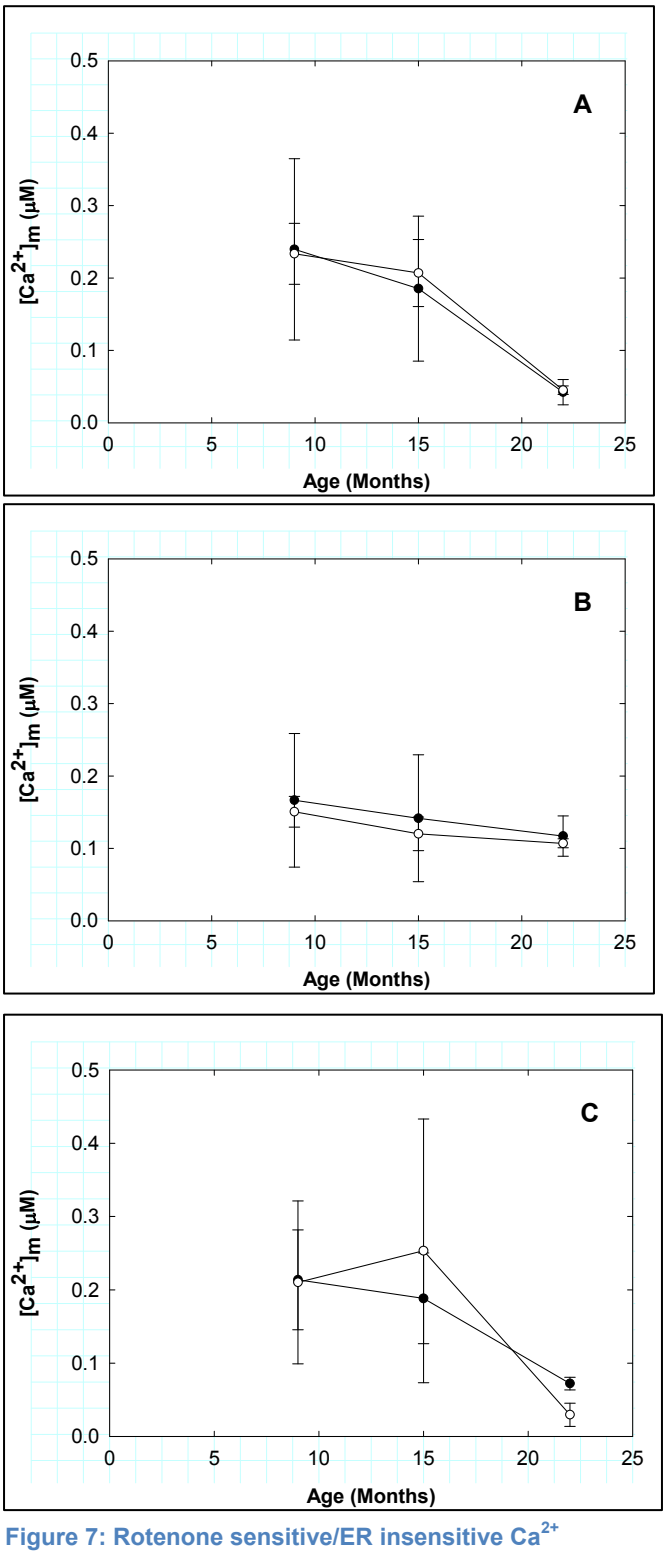

Figure 7: Rotenone sensitive/ER insensitive Ca^{2+} concentration due to uptake, across age of Tg and wt mice. Mitchondria were isolated from A) Cerebellum B) Frontal cortex and C) Hippocampus. All experiments were performed using n=4 mice of each genotype. Open circles indicate Tg and dark circles wt mouse mitochondria. 100nM calcium was added in the presence of 5 mM glutamate/malate. Three-way ANOVA analysis indicated a significant age effect in mitochondria from wt and Tg cerebellum and hippocampus p=0.008.

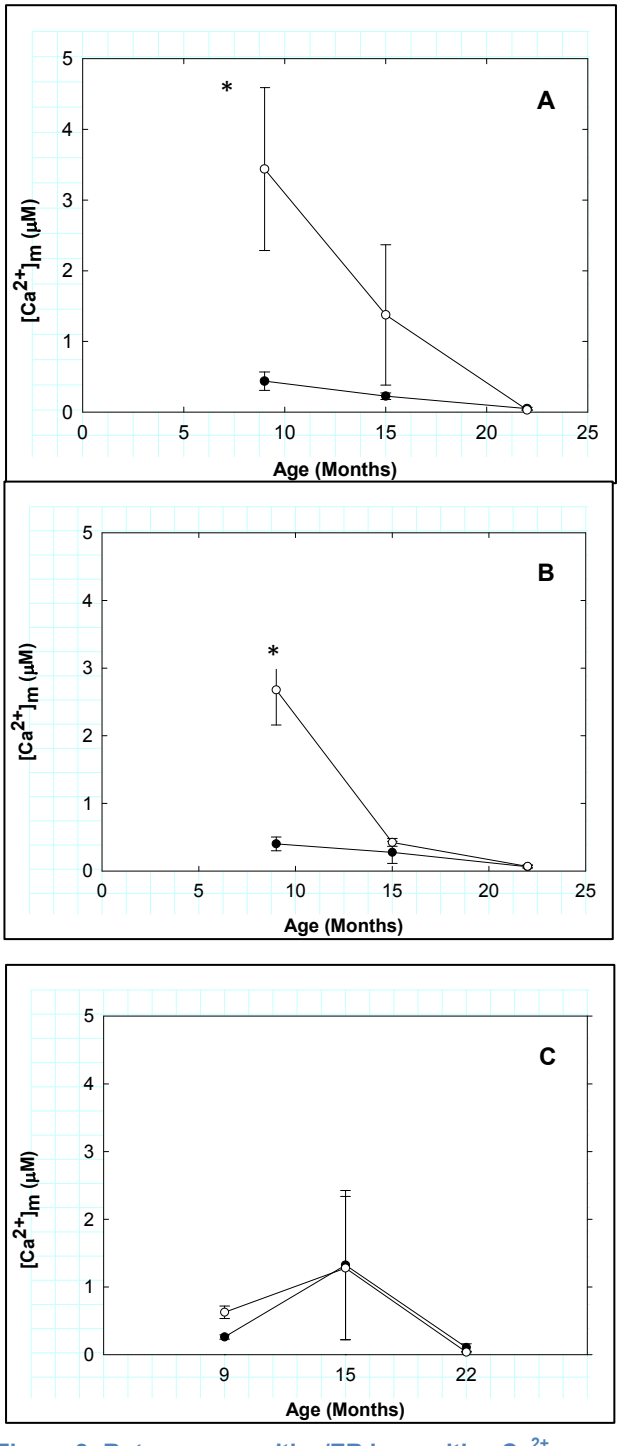

Figure 8: Rotenone sensitive/ER insensitive Ca^{2+} concentration due to uptake across age of Tg and wt mice. Mitchondria were isolated from A) Cerebellum B) Frontal cortex and C) Hippocampus. All experiments were performed using n=4 mice of each genotype. Open circles indicate Tg and dark circles wt mouse mitochondria. 1 μM calcium was added in the presence of 5 mM glutamate/malate. Three-way ANOVA analysis indicated a significant age effect in mitochondria from Tg cerebellum and frontal cortex p=0.011 and age effect in mitochondria from Tg mice p≤0.001

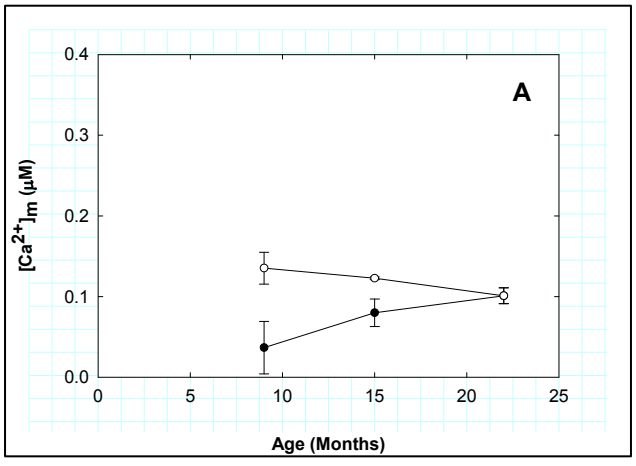

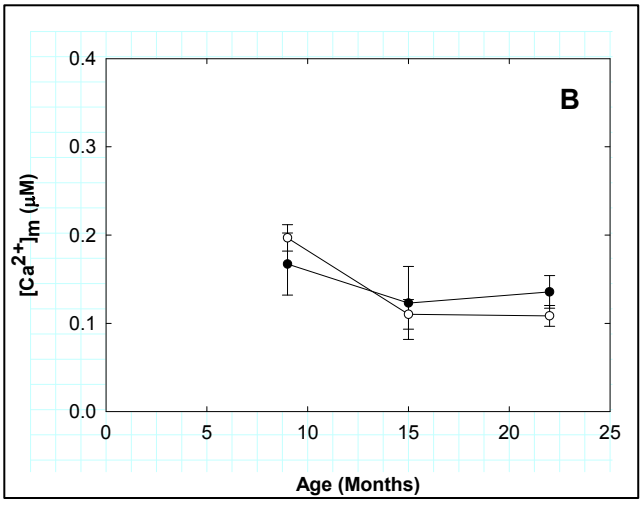

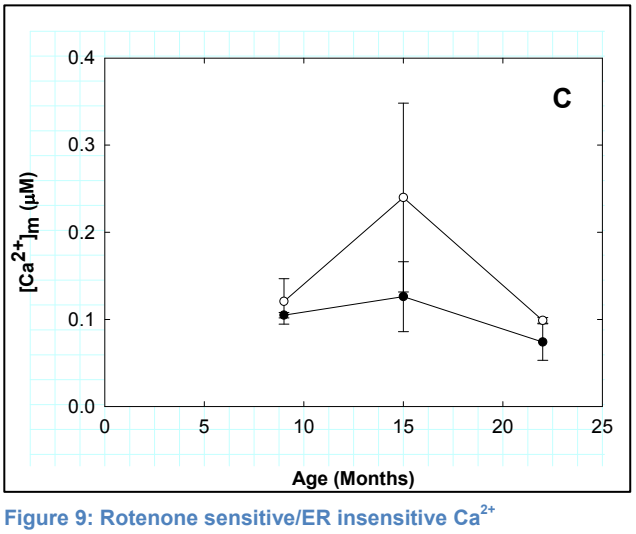

Figure 9: Rotenone sensitive/ER insensitive Ca^{2+} concentrations due to uptake across age of Tg and wt mice. Mitchondria were isolated from A) Cerebellum B) Frontal cortex and C) Hippocampus. All experiments were performed using n=4 mice of each genotype. Open circles indicate Tg and dark circles wt mouse mitochondria. 100nM calcium was added in the presence of 5 mM succinate.

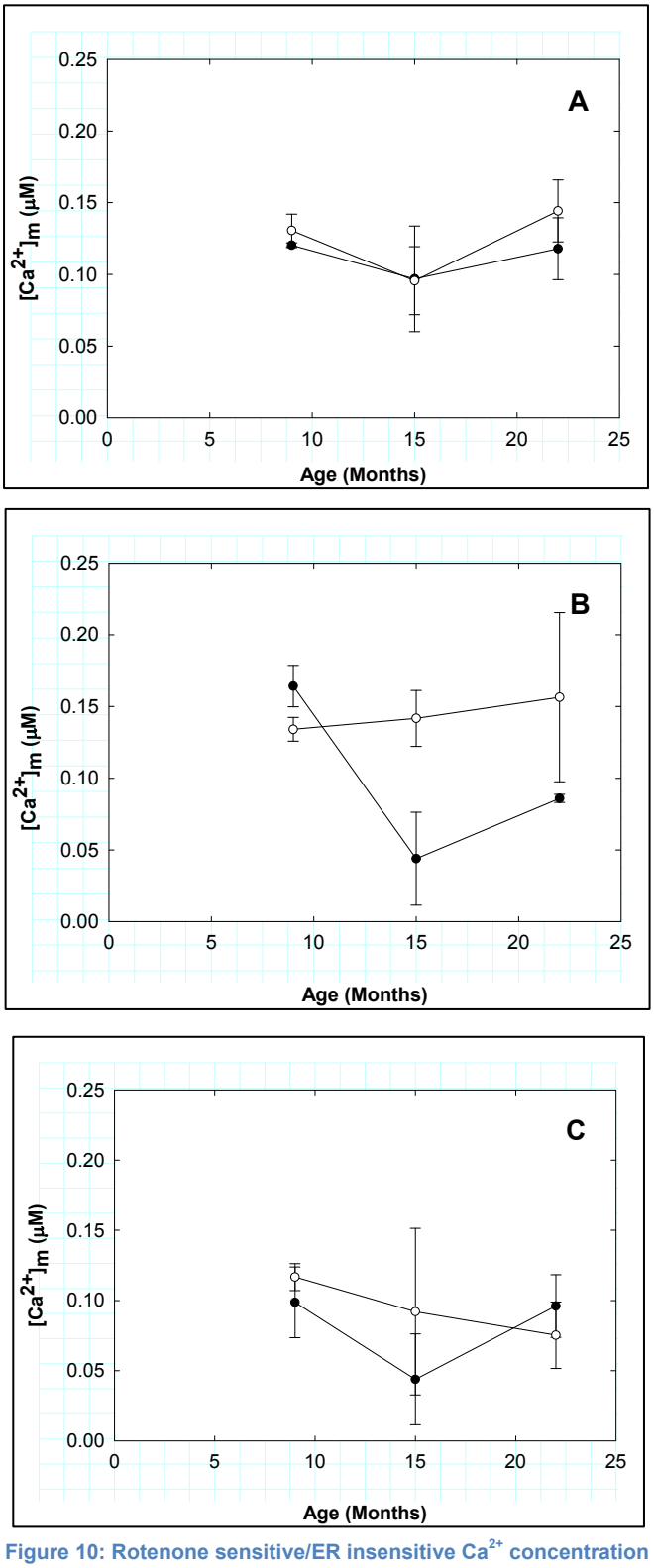

Figure 10: Rotenone sensitive/ER insensitive Ca^{2+} concentration due to uptake across age of Tg and wt mice. Mitchondria were isolated from A) Cerebellum B) Frontal cortex and C) Hippocampus. All experiments were performed using n=4 mice of each genotype. Open circles indicate Tg and dark circles wt mouse mitochondria. 1 μM calcium was added in the presence of 5 mM succinate.

Mitochondrial calcium uptake is blocked by the calcium inhibitor ruthenium red

Ca^{2+} uptake occurs through several pathways including "rapid-mode" uptake, Ca^{2+} uptake via the ryanodine receptor isoform (RyR)1, and through the mitochondrial Ca^{2+} uniporter (MCU) (Brookes, Yoon et al. 2004) (Santo-Domingo and Demaurex 2010) (Kirichok, Krapivinsky et al. 2004). The majority of calcium uptake into mitochondria has been shown to occur through the MCU (Santo-Domingo and Demaurex 2010). This channel allows for massive and fast entry of calcium ions into the mitochondria (Santo-Domingo and Demaurex 2010). An oxygen-bridged dinuclear ruthenium amine complex, RU-360, has been shown to be a potent and selective inhibitor of the mitochondrial calcium uniporter (DeLuca and Engstrom 1961) (Gunter and Gunter 1994) (De Stefani, Raffaello et al. 2011) and of the Ca^{2+}/H^{+} exchanger (Matlib, Zhou et al. 1998). To determine whether the uptake of Ca^{2+} was due to either the uniporter or the Ca^{2+}/H^{+} exchanger, Ca^{2+} uptake was measured in the presence of 1 μM extramitochondrial Ca^{2+} and in the presence or absence of 10 μM Ru-360. Thapsigargin-insensitive Ca^{2+} uptake by mitochondria energized by glutamate/malate was completely inhibited in the presence of Ru-360, thus demonstrating that the observed uptake of Ca^{2+} into mitochondria was dependent either on the Ca^{2+} uniporter or the Ca^{2+}/H^{+} exchanger, or both (Fig. 11).

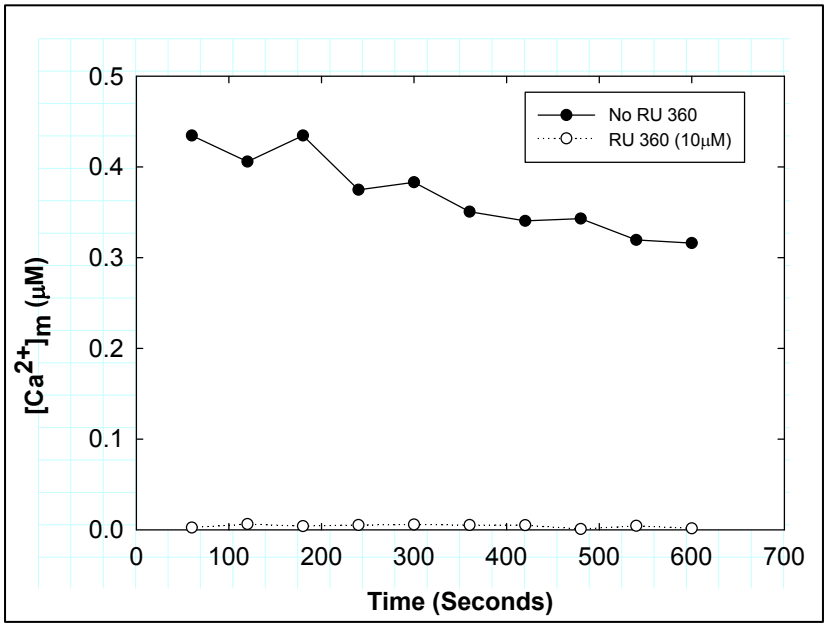

Figure 11: Mitochondrial calcium uptake in 9 month cerebellum mice across time. In the presence of 1μM calcium, 5mM glutamate/malate, and 2.5 μM thapsigarin. Dark circles indicate samples with no RU 360 and open circles in the presence of RU 360.

5. DISCUSSION

Significant genotype difference in baseline membrane potentials

Our measurements of TMR fluorescence demonstrate that there is a significant genotype effect ($p \leq 0.001$) across different brain regions and different ages, Tg mice being 2-fold higher than wt. The increase in TMR fluorescence reflects a $\Delta\Psi$ across the mitochondrial inner membrane. A high fluorescence signal demonstrates an increase in$\Delta\Psi_m$. This increase in $\Delta\Psi_m$ could be due to an increase in H^+ in the inner membrane space or an increase in negative ions in the mitochondrial matrix.

In the wt mouse mitochondria, we demonstrated that the resting state $\Delta\Psi_m$ is two-fold lower than that in Tg mouse mitochondria. Despite such large differences between Tg and wt in terms of $\Delta\Psi_m$, both genotypes had similar concentrations of $[Ca^{2+}]_m$, but the Tg mice displayed increased levels of Ca^{2+} uptake. The increase in Ca^{2+} uptake would therefore cause a collapse of the membrane potential due to the increase of positive ions in the matrix. However, a possibility could be that even though there is an increase of the Ca^{2+} uptake, the Ca^{2+} ions may not make it into the matrix, but get trapped in the inner membrane space, therefore increasing the potential difference instead of collapsing it. This would explain why we observed such a significant decrease in the membrane potential in the Tg mice compare to the wt. However, we would have only expected to see these significant differences in potential at an early age with a decrease in potential difference with advancing age. If Ca^{2+} uptake

was decreasing with age in the Tg mice then less Ca^{2+} would be plugging up the inner membrane space and contributing to the potential difference. In addition, only the cerebellum and frontal cortex exhibited these changes in Ca^{2+} uptake; however, in our membrane potential assays all three different brain regions exhibited significant genotypes differences. However, the Tg mice would have been exposed to increased levels of Ca^{2+} under normal conditions due to the GLUD1 protein as compared to the wt mice. This increased exposure could have already established a high concentration of Ca^{2+} ions being trapped in the mitochondrial inner membrane across all different brain regions and therefore resulting in a high potential difference regardless off the differential Ca^{2+} uptake across the different brain regions. And even though Ca^{2+} uptake decreased with age in the Tg mice, again the lifelong exposure to Ca^{2+} could have already established high baseline concentrations of Ca^{2+} ions being plugged in the mitochondrial inner membrane space that would contribute to a high potential difference in the Tg mice across all ages as compared to the wt mice.

No significant differences in net energized membrane potentials

An average value for the baseline kinetic values was determined and this value was subtracted from each time point after addition of either glutamate/malate or succinate to energize the mitochondria. An interesting finding was that after addition of a substrate and subtraction of the baseline mean measurement there was no longer a significant genotype effect. Membrane potential differences and trends were similar in both genotypes,

across different brain regions, and with advancing age. The time kinetic plots were fitted to a polynomial, linear equation and slopes (rate constants) were determined for the net energized $\Delta\Psi$. ANOVA 3-way analysis picked up no significant differences in the slopes with addition of either substrate, across different brain regions, or with advancing age. This finding was unexpected for two reasons. One is that addition of a substrate would energize mitochondria and contribute to the proton gradient, thus generating a larger potential difference in the inner membrane as compared to baseline and secondly we observed significant differences in Ca^{2+} uptake.

The addition of either glutamate/malate or succinate resulted in eliminating the $\Delta\Psi$ difference between the two genotypes. At baseline the Tg mice had a 2-fold higher potential difference as compared to wt; however, after addition of substrate the Tg potential difference was similar to that of wt. A reason for this could be that with addition of a substrate more hydrogen ions are being pumped into the inner membrane thereby increasing the potential difference in the wt mice to similar levels as the Tg mice.

Calcium uptake has been documented in many studies to be an energy driven process regulated by respiration and the proton electrochemical potential which is generated during respiration (Rottenberg and Scarpa 1794). Therefore Ca^{2+}uptake is driven by the potential difference across the mitochondrial inner membrane (Mitchell and Moyle 1967). Ultimately, Ca^{2+} enters the mitochondrial matrix through a process termed “down its electrochemical gradient”, or moving towards an area where there are fewer positive ions. Our studies showed that Ca^{2+} uptake in the Tg mice was highest at 9 months and decreased with

advancing age. Therefore, we would have expected to see a high potential difference at 9 months that also decreased with age.

Free intra-mitochondrial Ca^{2+}concentrations

Mitochondria normally contain between 5 and 20 nmol-Ca^{2+}/mg of protein and only ~0.01% of this total represents free or ionized intra-mitochondrial Ca^{2+} (Coll, Joseph et al. 1982). In our data the Ca^{2+}_{Fm} concentrations are in agreement with levels published in other studies (Coll, Joseph et al. 1982). In the wt mitochondria samples we observed no regional effect or age effect on the Ca^{2+}_{Fm} levels. Many studies have documented that Ca^{2+} uptake is altered during aging, specifically decreasing with age, and therefore cytoplasmic Ca^{2+}concentrations increase with age (Peterson and Gibson 1983). Due to the increase in cytosolic concentrations with advancing age we would have expected to see increases in Ca^{2+}_{Fm} as well. This idea is based on studies which have demonstrated that mitochondria function as a buffer when the cell cytosol experiences periods of high Ca^{2+} concentrations. Specifically, these studies demonstrated that when high insults of $Ca^{2+}$are applied, mitochondria increase Ca^{2+} uptake and therefore Ca^{2+}_{Fm} concentrations are increased (Coll, Joseph et al. 1982) (Aarts, Wei et al. 2003). A difference in our results could be that we measure Ca^{2+}_{Fm} concentrations where others have reported total levels of Ca^{2+}_{Fm}. In addition, mitochondria may also have developed a type of compensatory mechanism when the organelle itself experiences high levels of calcium. This would be important since Ca^{2+}_{Fm} plays such a pivotal role in bioenergetics and reactive oxygen species generation that developing regulatory

mechanisms within the mitochondria would be of critical importance. In our studies the wt mice may have had increased levels of Ca^{2+} uptake and therefore increased Ca^{2+}_{Fm} concentrations, but the Ca^{2+}ions may have been bound and therefore not measured in our assays. Specifically, studies have demonstrated increases in deposits of Ca^{2+} phosphate in mitochondria during periods of pathological stress, i.e., excess Ca^{2+}. These studies have shown that the role of phosphate in mitochondria is to buffer Ca^{2+} to maintain Ca^{2+}_{Fm} concentrations low (Chalmers and Nicholls 2003). Mitochondria therefore may have evolved this mechanism in an attempt to counteract the deleterious effects of excess Ca^{2+}. In addition, the observation that there were no regional differences in mitochondrial Ca^{2+} in the wt mice was also surprising. Studies have documented regional differences in cytosol Ca^{2+} levels and therefore would lead to differences in Ca^{2+}_{Fm} levels across regions (Haycock and Meligeni 1977). Many of these differences in cytosol Ca^{2+} levels are attributed to regional differences in neurotransmitter dynamics. A possible reason why there was no significant difference in mitochondrial Ca^{2+} levels across different brain regions in our studies could be due to the type of samples used. In many studies where they have measured Ca^{2+}_{Fm} and cytosol Ca^{2+} levels, investigators have carried out in vivo assays measuring levels in living cells using the calcium sensitive photoprotein aequorin that is specifically targeted to the mitochondria (Pinton, Rimessi et al. 2007) (Rizzuto, Brini et al. 1995). Neurotransmitter dynamics may play a stronger role in vivo because it allows for a physiological setting where all mitochondrial dynamics are interconnected. Specifically, studies have shown that mitochondria in an in vivo setting respond more efficiently and faster to

cytosol Ca^{2+} concentrations due to their increased capacity to sense the Ca^{2+} ions more efficiently in this type of setting (Rizzuto, Pinton et al. 1998) (Pinton, Wieckowski et al. 2004). After the addition of the substrate glutamate/malate we again demonstrated no significant differences in the wt samples across the different brain regions and with advancing age. A possible reason for this could be due to the fact that respiratory chain activities, specifically through Complex I, are not the only regulators of Ca^{2+}_{Fm} levels or again due to any of the reasons explained prior.

In the Tg mice, baseline Ca^{2+} concentrations and trends were similar to that of wt except in the cerebellum where there was a significant increase in Ca^{2+} concentrations with advancing age (genotype=p=0.002). Overall, in the Tg we would have expected dysregulation of Ca^{2+}homeostasis across all three different brain regions and with advancing age. The reason for this is due to the observations that glutamate has been documented in many studies to lead to a dysregulation of Ca^{2+} homeostasis (Budd and Nicholls 1996) (Khodorov 2003). Our laboratory has shown that over-expression of GLUD1 in neurons leads to increased levels of glutamate (Bao, Pal et al. 2009). The increase in glutamate levels would cause over-activation of glutamate receptors, primarily NMDA receptors, resulting in increased levels of Ca^{2+} flux into the post-synaptic cell. This would result in excess levels of cytoplasmic calcium and increased levels of intra-mitochondrial calcium. The observation that this was only seen in one tissue, cerebellum could be a structural difference in the tissues. Cerebellum contains granule cells which contain small cell bodies that are packed with mitochondria. The hippocampus and frontal cortex contain pyramidal cells which

have large cell bodies that may not contain as many mitochondria. The differences in the calcium levels across regions could be one of more mitochondria, therefore a significant difference in Ca^{2+}_{Fm} levels. After addition of glutamate/malate there was a significant age and genotype effect in the Tg samples, but only in the cerebellum and frontal cortex (genotype=p=<0.001 and age=p=<0.001). Possible reasons could again be because some other type of regulation of Ca^{2+} levels is in effect besides the respiratory chain activities or there could be morphological differences across the different brain regions which result in altered mitochondrial function, i.e. an imbalance of fission vs. fussion resulting in fragmented mitochondrion.

Mitochondrial Ca^{2+} concentration due to uptake-After substrate addition

In the Ca^{2+} uptake assays the most significant factor affecting mitochondrial Ca^{2+} uptake was the concentration of extra-mitochondrial Ca^{2+} added to the assay. More specifically the only time there was significant difference between genotypes, substrate, age, or regions was when a high extracellular Ca^{2+} concentration was added (1 μM). This finding was not surprising dince many studies have documented that the uniporter, which is the main pathway for Ca^{2+} entry into the mitochondria, is gated by extra-mitochondrial Ca^{2+} concentrations (Bragadin, Pozzan et al. 1979).

At a low extra-mitochondrial Ca^{2+} concentration (100 nM) there were no significant differences (as denoted by ANOVA 3-way analysis on SigmaPlot 11.0). At 100 nM Ca^{2+} concentration, using glutamate/malate as a substrate,

Ca^{2+} uptake concentrations were similar to those observed in the Ca^{2+}_{Fm} assay for both wt and Tg mice. In the wt mice Ca^{2+} uptake levels remained steady across different brain regions and with increasing age. Other studies have demonstrated that an increase in cytosolic Ca^{2+} concentrations mediates calcium release from depolarized mitochondria preloaded with Ca^{2+}. Leading to the hypothesis that mitochondrial Ca^{2+} entry is gated by cytosol Ca^{2+} concentrations and therefore resulting in cytosol Ca^{2+} needing to be higher than that of a conducting Ca^{2+} channel to see any significant differences in Ca^{2+}_{Fm} concentrations (Igbavboa and Pfeiffer 1988), In addition, the kinetic features of Ca^{2+} transport predict that Ca^{2+} uptake into mitochondria should not be significant under physiological conditions (100 nM is physiological extra-mitochondrial calcium concentration) due to the low affinity of the uniporter for Ca^{2+} (Pinton, Rimessi et al. 2007) (Rizzuto, Brini et al. 1995). These studies could explain why we did not see any significant differences in Ca^{2+} uptake concentrations with 100 nM Ca^{2+} added to the assay and why we did not see any significant differences in the Ca^{2+}_{Fm} concentrations. Regardless of the substrate used glutamate/malate or succinate, ANOVA 3-way analysis picked up no significant differences in the genotypes, with different substrates used, across the different brain regions, or with advancing age. In the wt mice we would have expected to see differences in difference brain regions and with advancing age, but again remained steady due to one of the reasons stated in the free intra-mitochondrial assays. These being in vitro and not in vivo studies may affect the mitochondrial Ca^{2+} transport assays and neurotransmitter dynamics. In support of this studies have documented that mitochondrial Ca^{2+} buffering in intact cells is different from that

of isolated mitochondrial samples. These differences are due to the concentration of extracellular Ca^{2+} and to the contribution of Ca^{2+} to the extracellular medium from other organelles such as the endoplasmic reticulum (Chalmers and Nicholls 2003).

When a high concentration, 1 μM, of Ca^{2+} is added the Tg samples display significant differences as compared to wt samples, across different brain regions, and with advancing age. In this assay the Ca^{2+} uptake concentrations are significantly higher at 9 months as compared to the wt and decrease with advancing age in the cerebellum and frontal cortex. This may seem perplexing since our Ca^{2+}_{Fm} assay showed low levels of Ca^{2+}_{Fm} (0.1-0.3 μM) that were similar in both genotypes across the different regions and with advancing age. First one must take into account that Ca^{2+} uptake is not proportional to a net increase in mitochondrial Ca^{2+} concentrations. In support of this studies have shown that Ca^{2+} addition to mitochondria results in formation of Ca^{2+} phosphate deposits and therefore does not result in increases in Ca^{2+}_{Fm} (Chalmers and Nicholls 2003). So even though there is a significant amount of Ca^{2+} uptake occurring at 9 months the Tg mitochondria may attempt to shut down the deleterious effects of high intra-mitochondrial Ca^{2+} by increasing binding to phosphate or by increasing mitochondrial Ca^{2+} efflux; therefore, resulting in low levels of Ca^{2+}_{Fm} as seen in our assays. In addition, the Tg mice might be very efficient at handling this type of stress, i.e. high amounts of Ca^{2+} due to the prolonged exposure of glutamate and subsequent excess Ca^{2+} flux into the cell. This would allow the Tg mitochondria to have undergone a type of “conditioning” that would allow them to efficiently handle when they are stressed by a bolus

application of extracellular Ca^{2+}. The decrease in Ca^{2+} uptake with advancing age is the opposite of what we demonstrated in terms of Ca^{2+}_{Fm} concentrations, which increased with age. This could simply be due to compensatory pathway in where the mitochondria are decreasing calcium uptake due to the rise in intra-mitochondrial calcium. If this is the case then the explanation for the rise in intra-mitochondrial Ca^{2+} concentrations is not due to increased Ca^{2+} uptake, but to a change in the bound versus free intra-mitochondrial Ca^{2+} concentrations. Specifically, if with advancing age there is an increase or decrease in phosphate this would affect the amount of free intra-mitochondrial Ca^{2+}.

The studies demonstrate that addition of succinate causes no significant differences in Ca^{2+} uptake between genotypes, across different brain regions, and with advancing age. With the addition of glutamate/malate significant differences were observed between genotypes, across different brain regions, and with advancing age. The observation that succinate induced no significant differences, with high or low extracellular Ca^{2+}, was not surprising. Mitochondrial Ca^{2+} uptake is controlled by a variety of processes one being respiration. The majority of respiration is driven by reducing equivalents feeding into complex I of the respiratory chain. Many studies have documented that Ca^{2+} regulates respiration directly. Specifically, these studies have demonstrated that Ca2+ regulates respiration by activating specific dehydrogenases which result in increased activity of the TCA cycle. This increase in activity leads to a rise in NADH levels which transfer electrons to complex I and results in an increase in mitochondrial metabolism (McCormack, Halestrap et al. 1990) (Hansford 1981). The increased metabolism leads to an increase in hydrogen pumping to the inner

membrane and the establishment of a potential difference which is also another driving force for Ca^{2+} uptake into mitochondria. Succinate contributes reducing equivalents to complex II, but Complex II does not pump hydrogen ions to the inner membrane causing no further increase and potential difference and therefore no significant increase in Ca^{2+} uptake.

Conclusions

The only significant genotype affect observed in Ca^{2+}_m concentrations was at 22 months in the mitochondria from cerebellum with the Tg mice having a higher concentration of Ca^{2+}_m as compared to wt. Across the different brain regions the concentrations of Ca^{2+}_m were similar and across advancing age the trends were also similar in both genotypes. These results indicate that the significant genotype effect observed is the result of over-expression of GLUD1 and that with advancing age the Tg mice are not able to either buffer (combine Ca^{2+} with phosphate in mitochondria to form calcium phosphate), or export Ca^{2+} out of the mitochondria as efficiently as wt mice, resulting in 2-fold higher levels of Ca^{2+}_m concentrations in the mitochondria from Tg mice as compared to wt. This significant genotype effect was only observed in the mitochondria from cerebellum regions and not from the frontal cortex or hippocampus. These results indicate that the mitochondria isolated from 22 month old Tg cerebellum regions contain higher concentrations of Ca^{2+} which may be the result of increased capacity of Ca^{2+} uptake which is neuronal cell type dependent, i.e. Purkinje neurons of the cerebellar cortex more efficient versus cortical and

hippocampal neurons. This might also be the reason why in our morphological studies the cerebellum neurons did not suffer cell death and/or damage as the other regions did. To determine if this was the case mitochondrial Ca^{2+} uptake assays were carried out.

The Ca^{2+} concentrations as a direct result of uptake varied dependent on the concentration of extra-mitochondrial Ca^{2+} added. When a low concentration of Ca^{2+} was added, 100 nM there were no significant genotype effects, all three brain regions had similar values of Ca^{2+}, while the cerebellum and hippocampus had similar trends and were different from the hippocampus. These results indicate that different brain regions exhibit different capacities in Ca^{2+} uptake. Across advancing age both genotypes demonstrated a significant age effect with uptake decreasing in the cerebellum and hippocampus and remaining stable in the frontal cortex. These results indicate that the differences in Ca^{2+} uptake are likely not the result of over-expression of GLUD1, but differences in Ca^{2+} uptake in the three brain regions and that with age these differences are further enhanced. When a large concentration of extra-mitochondrial Ca^{2+} is added, 1 μM there are significant genotype differences that are region and age specific. At 9 months the Tg mitochondria from cerebellum and frontal cortex have significantly higher Ca^{2+} uptake as compared to wt and with advancing age these differences diminish. These results indicate that the over-expression of GLUD1 caused differences which enhanced the Ca^{2+} uptake pathways in the Tg mitochondria from cerebellum and frontal cortex regions. A reason for this could be that the Tg mitochondria may have been pre-exposed and therefore "pre-conditioned" to handling excess levels of Ca^{2+} which should be the result of over-

expression of GLUD1 by over-activation of glutamate receptors and therefore increased Ca^{2+} concentrations in the cell. If this is the case then the Tg mitochondria may have developed enhanced Ca^{2+} uptake to decrease the Ca^{2+} concentrations in the cytoplasm and therefore prevent dell damage. In this scenario introduction of high levels of extra-mitochondrial Ca^{2+} (1 μM) would result in faster Ca^{2+} uptake and in the Tg mitochondria as compared to wt. In addition, only specific regions exhibited these genotype significant effects indicating that the adaptive changes in the Ca^{2+} uptake mechanisms were region specific. A possibility could be that only specific regions were pre-disposed to the high levels of calcium throughout the lifespan of the organism, i.e. differences in the levels of glutamate receptors in the brain regions which would result in only specific brain regions being "pre-conditioned" to high levels of Ca^{2+}. In support of this studies have demonstrated that there is region specific distribution of glutamate receptors (Martin, Blackstone et al. 1993) (Nusser 2000).

In our Tg mice at baseline there is a significant potential difference in all regions and across all ages. The establishment of such a high potential difference as compared to the wt mice could be that of the prolonged exposure of glutamate and thus lifelong exposure to excess Ca^{2+}. With time this excess Ca^{2+} could have entered the mitochondria, but remained "stuck" in the mitochondrial inner membrane thus generating a greater potential difference. A reason for the Ca^{2+} remaining in the inner membrane could simply be one of the mitochondria attempting to regulate matrix Ca^{2+} levels and thus regulate respiration. In this scenario even though there was an increase in Ca^{2+} uptake due to the large potential difference at 9 months, this would not have resulted in an increase in

free intra-mitochondrial Ca^{2+}, as was seen in our studies. The observation that the potential difference was significant in the Tg mice across all difference brain regions and with advancing age could again be because all neurons were over-expressing the *Glud1* gene, and therefore the inner membrane Ca^{2+} plugging would have occurred in all three brain regions. After energizing mitochondria with the substrate glutamate/malate region specific differences in the mitochondrial membrane potential were observed. Specifically, after substrate addition the mitochondria from wt samples in all of the brain regions increased steadily, while the mitochondria from Tg samples only increased in the cerebellum and remained steady in the hippocampus and frontal cortex. These results might indicate that the mitochondria from Tg samples in the frontal cortex and hippocampus have reached maximal potential difference and even upon substrate addition do not accumulate any further hydrogen protons, while the cerebellar mitochondria still continue to pump hydrogen protons and drive a potential difference across its mitochondrial inner membrane. The regional differences in membrane potential may in part explain the regions differences we observed in the Ca^{2+} uptake assays. The mitochondria from Tg cerebellum samples may continue to pump hydrogen protons and pump a greater potential difference in an effort to drive mitochondrial Ca^{2+} uptake. Studies have demonstrated that Ca^{2+} uptake is an energy dependent process and a greater potential difference would result in increased Ca^{2+} uptake. Increased Ca^{2+} uptake may be a response or adaptive mechanism by the cell to decrease cytosolic Ca^{2+} concentrations and avoid the harmful effects of excess Ca^{2+}.

Citations

Aarts, M., W. Wei, et al. (2003). "A key role for TRPM7 channels in anoxic neuronal death." Cell **115**: 863-877.

Balaban, R. (2002). "Cardiac energy metabolism homeostasis: role of cytosolic calcium." J Mol Cell Cardiol **34**: 1259-1271.

Baughman, J., F. Perocchi, et al. (2011). "Integrative genomics identifies MCU as an essential component of the mitochondrial calcium uniporter." Nature **476**: 341-345.

Bragadin, M., T. Pozzan, et al. (1979). "Kinetics of calcium carrier in rat liver mitochondria." Biochemistry **18**: 5972-5978.

Brookes, P., Y. Yisang, et al. (2004). "Calcium, ATP, and ROS: a mitochondrial love-hate triangle." Am J Physiol Cell Physiol **287**.

Brookes, P., Y. Yoon, et al. (2004). "Calcium, ATP, and ROS: a mitochondrial love-hate triangle." Cell Physiology **287**: C817-C833.

Calderon-Cortex, E. and C. Cortes-Rojo (2008). "Changes in mitochondrial functionality and calcium uptake in hypertensive rats as a function of age." Mitochondrion **8**: 262-272.

Chalmers, S. and D. Nicholls (2003). "The relationship between free and total calcium cocentrations in the matrix of liver and brain mitochondria." J Biol Chem **279**: 19062-19070.

Coll, K., S. Joseph, et al. (1982). "Determination of the matric free calcium concentration and kinetics of calcium efflux in liver and heart mitochondria." The Journal of Biological Chemistry **257**: 8696-8704.

Das, A. and D. Harris (1990). "Control of mitochondrial ATP synthase in heart cells: inactive to active transitions caused by beating or positive inotropic agents." Cardiovasc Res **24**: 411-417.

De Stefani, D., A. Raffaello, et al. (2011). "A forty-kilodalton protein of the inner membrane is the mitochondrial calcium uniporter." Nature **476**: 336-340.

DeLuca, H. and G. Engstrom (1961). "Calcium uptake by rat kidney mitochondria." Proc Natl Acad Sci **47**: 1744-1750.

Gunter, K. and T. Gunter (1994). "Transport of calcium by mitochondria." J. Bioenerg. Biomembr. **26**: 471-485.

Gunter, T., L. Buntinas, et al. (2000). "Mitochondrial calcium transport: mechanisms and functions." Cell caclium **28**: 285-296.

Gunter, T., D. Yule, et al. (2004). "Calcium and mitochondria." FEBS Lett **567**: 96-102.

Hansford, R. (1981). "Effects of micromolar concentration of free calcium ions on thre reduction of heart mitochondrial NAD (P) by 2-oxoglutarate." Biochem J **194**: 721-732.

Hansford, R. and D. Zorov (1998). "Role of mitochondrial caclium transport in the control of substrate oxidation." Mol cell Biochem **184**: 359-369.

Haycock, J. and J. Meligeni (1977). "Neurotransmitter accumulation and calcium-dependent release from different regions of rat brain." Life Sciences **21**: 1837-1843.

Hill, E. and P. Kats (2007). "Role of Membrane Potential in Calcium Signaling During Rhythmic Bursting in Tritonia Swim Interneurons." Journal of Neurophysiology **97**: 2204-2214.

Igbavboa, U. and D. Pfeiffer (1988). "EGTA inhibits reverse uniport-dependent calcium release from uncoupled mitochondria. Possible regulation of the calcium uniporter by a calcium binding site on the cytoplasmic side of the inner membrane." J Biol Chem **263**: 1405-1412.

Kann, O. and R. Kovacs (2006). "Mitochondria and neuronal activity." American Journal of Physiology **292**: C641-C657.

Kirichok, Y., G. Krapivinsky, et al. (2004). "The mitochondrial calcium uniporter is a highly selective ion channel." Nature **427**: 360-364.

Krieger, C. and M. Duchen (2002). "Mitochondria calcium and neurodegenerative disease." Eur. J. Pharmacol. **447**: 177-188.

Kroner, H. (1986). "Calcium ions, an allosteric activator of calcium uptake in rat liver mitochondria." Biophysics **251**: 525-535.

Loeffler, M. and G. Kroemer (2000). "The mitochondrion in cell death control: certainties and incognita." Exp Cell Res **256**: 19-26.

Mailer, K. (1990). "Superoxide radical as electron donor for oxidative phosphoryaltion of ADP." Biochem Biophys Res Commun **170**: 59-64.

Martin, L., C. Blackstone, et al. (1993). "AMPA glutamate receptor subunits are differentially distributed in rat brain." Neuroscience **53**: 327-358.

Matlib, M., Z. Zhou, et al. (1998). "Oxygen-bridged Dinuclear Ruthenium Amine Complex Specifically Inhibits Ca2+ Uptake into Mitochondria in Vitroand in Situ in Single Cardiac Myocytes." Journal of Biological Chemistry **273**: 10223-10231.

McCormack, J. and R. Denton (1993). "Mitochondrial calcium transport and the role of mitochondrial calcium in the regulation of energy metabolism." Dev Neurosci **15**: 165-173.

McCormack, J., A. Halestrap, et al. (1990). "Role of calcium ions in regulation of mammalian intramitochondrial metabolism." Physiological Review **70**: 391-425.

McCormack, J., A. Halestrap, et al. (1990). "Role of calcium ions in regulation of mammalian intramitochondrial metabolism." Physiol Rev **70**: 391-425.

Mitchell, P. and J. Moyle (1967). "Chemiosmotic hypothesis of oxidative phosphorylation." Nature **213**: 137-139.

Nusser, Z. (2000). "AMPA and NMDA receptors: similarities and differences in their

synaptic distribution." Current Opinion in Neurobiology **10**: 337-341.

Peterson, C. and G. Gibson (1983). "Aging and 3,4-diaminopyridine alter synaptosomal calcium uptake." The Journal of Biological Chemistry **258**: 11482-11486.

Pinton, P., A. Rimessi, et al. (2007). "Biosensors for the detection of calcium and pH." Methods Cell Biol **80**: 297-325.

Pinton, P., M. Wieckowski, et al. (2004). "Long-term modulation of mitochondrial calcium signals by protein kinase C isozymes." J Cell Biol **165**: 223-232.

Pralong, W., A. Spat, et al. (1994). "Dynamic pacing of cell metabolism by intracellular calcium transients." Journal of Biological Chemistry **269**: 27310-27314.

Rizzuto, R., M. Brini, et al. (1995). "Photoprotein-mediated measurement of calcium ion concentration in mitochondria of living cells." Methods Enzymol **260**: 417-428.

Rizzuto, R., P. Pinton, et al. (1998). "Close contacts with the endoplasmic reticulum as determinants of mitochondrial calcium responses." Science **280**: 1763-1766.

Rizzuto, R. and T. Pozzan (2006). "Microdomains of intracellular calcium: molecular determinants and functional consequences." Physiol Rev **86**: 369-408.

Rottenberg, H. and A. Scarpa (1794). "Calcium uptake and membrane potential in mitochondria." Biochemistry **13**: 23.

Rottenberg, H. and A. Scarpa (1974). "Calcium uptake and membrane potential in mitochondria." Biochemistry **13**: 4811-4817.

Saavedra-Molina, A., S. Uribe, et al. (1990). "Control of mitochondrial matrix calcium: studies using fluo-3 as a fluorescent calcium indicator." Biochem Biophys Res Commun **28**: 148-153.

Saavedra-Molina, A., S. Uribe, et al. (1990). "Control of Mitochondrial matric calcium: studies using fluo-3 as a fluorescent calcium indicator." Biochemical and Biophysical Research Communications **167**: 148-153.

Santo-Domingo, J. and N. Demaurex (2010). "Calcium uptake mechanisms of mitochondria." Biochim Biophys Acta **1797**: 907-912.

Xiong, J., A. Verkhratsky, et al. (2002). "Changes in mitochondrial status associated with altered Calcium homeostasis in aged cerebellar granule neurons in brain slices

" The Journal of Neuroscience **22**: 10761-10771.

Chapter Four: Effects of the Over-Expression of Neuronal Glutamate Dehydrogenase (GLUD1) on Brain Mitochondrial Reactive Oxygen Species Generation

10. INTRODUCTION

Reactive Oxygen Species

Reactive oxygen species are highly reactive chemical species which contain an unpaired electron in their valence shell. These species include oxygen ions and peroxides. The generation by mitochondria of superoxide ($O_2^{\bullet -}$) and hydrogen peroxide (H_2O_2) is well documented (Gomez, Monette et al. 2009) (Kumaran, Subathra et al. 2004) (Ontko 1966). Once the ROS are produced, they are involved in a variety of cell functions that can benefit or harm the cell. The ROS formed in cells are involved in many signaling networks such as redox signaling, in the mediation of apoptosis, cell homeostasis, and induction of host defense genes (Liu, Fiskum et al. 2002).

Cells normally defend themselves against the harmful effects of ROS through the action of cellular antioxidants. These include enzymes such as glutathione peroxidases, superoxide dismutases, catalases, lactoperoxidases, peroxiredoxins, and alpha-1-microglobin. All of these enzymes function in a similar manner and prevent damage by ROS species through the scavenging of free radicals. Due to their damaging effects on the cell, ROS levels are maintained relatively low (Wirtz and Schuelke 2011) through the activities of these antioxidants.

The source of ROS in cells

The primary source of ROS is the electron transport system (ETS) in the mitochondria (Raha, Myint et al. 2002) (Maj, Raha et al. 2004). The major ROS produced as a by-product of the ETS is $O_2^{\bullet-}$ through the process of mono-electronic reduction of O_2. The generation of $O_2^{\bullet-}$ can occur at very fast rates when the electron transport system activities are increased in response to a demand for more ATP generation, thereby establishing a relationship between metabolic conditions and ROS generation. Many enzyme complexes within the ETS have been documented to directly generate ROS. Specifically, ubiquinone oxidoreductase (complex III) and ubiquinone oxidoreductase (complex I) have been shown to lead to $O_2^{\bullet-}$ and ROS gneration (Mailer 1990) (Choksi, Nuss et al. 2011) (Gnaiger 2009).

ROS and aging

There is a documented increase in ROS production in the mitochondria and a subsequent increase in oxidative damage to cells during the aging process (Sarnoska 2002) (Wang, Zaidi et al. 2009). These observations have led to the belief that an accumulation of oxidative damage as a result of ROS is a factor that contributes to the aging process. In support of this idea, genetic studies where mutant fly or worm models are resistant to oxidative damage have been shown to have extended life spans (Budd and Nicholls 1996). In addition, mice which have had $O_2^{\bullet-}$ dismutase 1 (SOD1), the enzyme with breaks down $O_2^{\bullet-}$,

knocked down have a 30% decrease in lifespan; whereas, over-expression of this enzyme results in an increase in lifespan (Khodorov 2003).

Differential neuronal vulnerability to oxidative stress

The damaging effects of oxidative stress that result from excess ROS formation has been well documented in studies of aging and age-associated diseases. Of particular interest is the observation that neurons express differential vulnerability to oxidative stress. In the brain, the hippocampus is divided into four regions, CA1 through CA4, and these regions respond to oxidative stress differently. When exposed to oxidative stress, cells in the CA1 region have very low survival rates, while cells in the CA3 region are almost completely insensitive to ROS-induced damage (Wilde, Pringle et al. 1997) (Wang, Pal et al. 2005) (Sarnoska 2002). Also agents that induce oxidative damage also cause massive cell death of neurons in the cerebellar granule cell layer, but not in the cerebral cortex area (Wang, Zaidi et al. 2009).

Mitochondrial calcium and membrane potential as regulators of ROS generation

As discussed in chapter three, Ca^{2+} can exert an overall positive effect on mitochondrial bioenergetics by up-regulating the TCA cycle and ETS activities through stimulation of specific dehydrogenases. As necessary as this function is at times when a high ATP output is needed, increased ETS activity may also lead to increased ROS generation, and thus a potentially negative effect on cell

survival. ROS generation parallels metabolic rate (Brookes, Yoon et al. 2004). In Figure 1 the possible effects of intra-mitochondrial accumulation of Ca^{2+} on the generation of ROS by the ETS are shown.

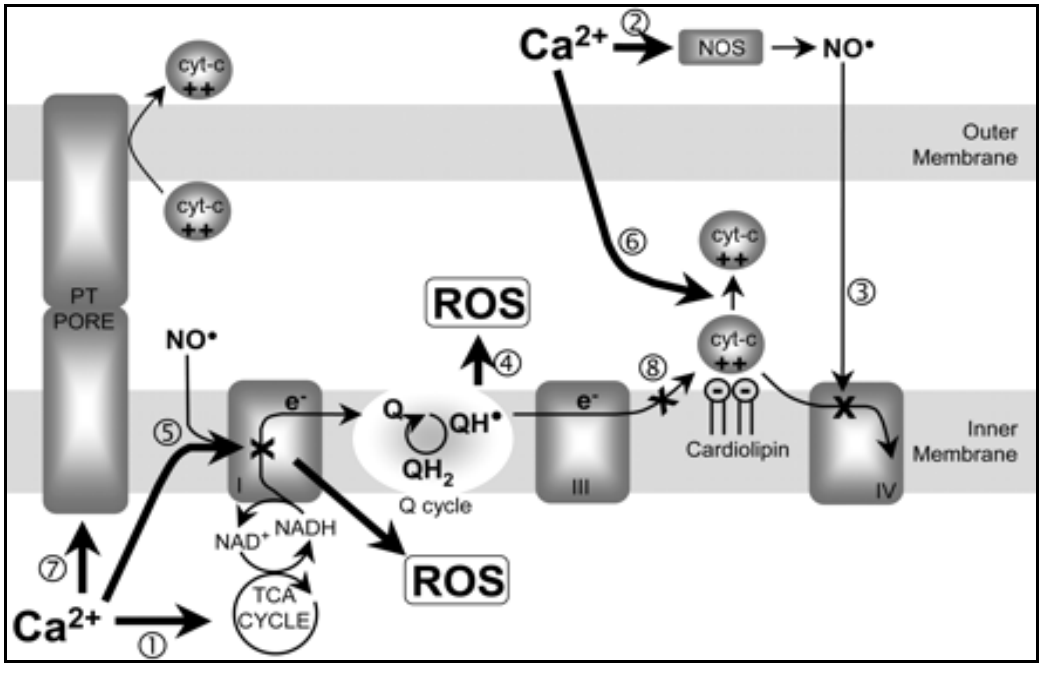

Figure 1 "Mechanisms for Ca^{2+} stimulation of mitochondrial ROS generation. Ca^{2+} stimulation of the TCA cycle (*1*) will enhance electron flow into the respiratory chain, and Ca^{2+} stimulation of nitric oxide synthase (NOS) and subsequent nitric oxide (NO·) generation (*2*) would inhibit respiration at complex IV (*3*). These events would enhance ROS generation from the Q cycle (*4*). In addition, NO· and Ca^{2+} can inhibit complex I, possibly enhancing ROS generation from this complex (*5*). Ca^{2+} also dissociates cytochrome *c* (cyt-c) from the inner membrane cardiolipin (*6*) and at high concentrations triggers PTP opening and cytochrome *c* release across the outer membrane (*7*). The subsequent inhibition at complex III (*8*) would enhance ROS generation at the Q cycle (*4*)"

The tight regulation of Ca^{2+} homeostasis within the mitochondria is required to ensure that the "positive" effects of Ca^{2+} and metabolic activation are exerted on the cell.

In addition to Ca^{2+}, another regulator of ROS generation in mitochondria has been shown to be the Ψ_m. Specifically, the generation of ROS is exponentially related to the magnitude of the Ψ_m (Brookes, Yoon et al. 2004).

In chapter two we demonstrated that the ETS activity that is stimulated by succinate is increased in the Tg mice at 9 mos of age, but this differential activation is lost by 15 and 22 mos of age. In chapter three it was shown that at 9 mos $[Ca^{2+}]_m$ was the same in wt and Tg mice, but increased at 22 mos in mitochondria from cerebellum and cortex. Thus, there was no direct correlation between ETS activity and $[Ca^{2+}]_m$. Furthermore, succinate did not activate excess Ca^{2+} uptake, whereas glutamate/malate caused both an increase in $[Ca^{2+}]_m$ at 22 mo old cerebellum and hippocampal neurons and stimulated Ca^{2+} uptake at 9 mos in cerebellum and cortex. Finally, though mitochondria from all three brain regions of the Tg mice maintained much higher Ψ_m, it was difficult to assign a specific ETS contribution to such differential in Ψ_m. Therefore, it was difficult to predict whether mitochondria from Tg or wt mice would be likely to produce more ROS or how such ROS formation might differ from brain region to brain region or across the aging process.

2. MATERIALS

All materials were purchased from Sigma-Aldrich unless otherwise noted. MitoSOX red dye was purchased from Molecular Probes, Catalog

#M36008. An Amplex Red Hydrogen Peroxide/Peroxidase Assay kit was purchased from Invitrogen, Catalog # A22188.

3. METHODS

Isolation of mitochondrial pellets

Mitochondrial samples from three different brain regions cerebellum, frontal cortex, and hippocampus were isolated as described in chapter two.

Measurement of O_2 and H_2O_2 levels in isolated mitochondria

Superoxide ($O_2^{\bullet -}$) levels were measured in mitochondria isolated from the brain of Tg and wt mice at 9, 15, and 22 months. The same three brain regions as in the other studies were the source of the mitochondria. MitoSOX red dye was used for the measurement of $O_2^{\bullet -}$. The assays were performed in 100 μL per reaction volume. Mitochondrial samples (10 μg protein) were incubated with 5 μM MitoSOX dye in the presence or absence of either 5 mM glutamate/malate or succinate. The mixture of mitochondria plus dye was incubated for 10 mins in the dark at 37 ^{o}C and at the end of this incubation period, was measured for 240

secs in a BioTek Synergy spectrofluorometer (excitation 510 nm; emission 580 nm).

Measurement of hydrogen peroxide levels in isolated mitochondria

Hydrogen peroxide levels were measured in the same mitochondrial preparations as those used for $O_2^{\bullet -}$ measurements. An Amplex Red Hydrogen Peroxide/Peroxidase Assay kit was used for the assays. Prior to the conduct of these assays, standard curves were generated in order to determine the dynamic range of H_2O_2 and of protein concentrations in the assay. A linear relationship between protein concentration and peroxide generation was obtained.

From the standard curves we determined that the protein concentration for the H_2O_2 measurements to be used was 10 μg per well. Mitochondrial samples (10 μg protein) were diluted in 1X reaction buffer provided in the kit. A positive control was run in each assay and consisted of 10 μM H_2O_2 in 1x reaction buffer. A negative control that contained only reaction buffer was used with no H_20_2 present. Fifty microliters of control and experimental samples were loaded into the individual wells in triplicate. Next a working solution was prepared which contained 100 μM Amplex red reagent and 0.2 U/mL horseradish peroxidase (all solutions are part of assay kit) in a 50 μL total reaction volume. This working solution (50 μL) was added to the protein solution (50 μL) for a total of 100 μL final reaction volume. The microplate was incubated at room temperature for

30 minutes, protected from light to allow the H2O2 and Amplex dye to react and form the red-fluorescent oxidation product, resorufin. After incubation a one time point measurement of fluorescence was obtained on a BioTek Synergy spectrofluorometer (excitation 520 nm; emission 590 nm). The values derived from the negative control were subtracted from those of each sample containing mitochondria from those of each sample containing mitochondria or known amounts of H_2O_2.

4. RESULTS

Baseline concentration of $O_2^{\bullet-}$ in the mitochondria from wt and Tg mice

Baseline generation of $O_2^{\bullet-}$ by mitochondria in the absence of any substrates was measured using the dye MitoSOX red. This dye is selectively targeted to the mitochondria and exhibits increased red fluorescence when oxidized by $O_2^{\bullet-}$. Therefore, an increase in the fluorescence signal corresponds to an increase in $O_2^{\bullet-}$ levels. This probe is oxidized by superoxide only and not by any other ROS (http://products.invitrogen.com/ivgn/product/M36008). Baseline measurements were carried out for 3 mins at 15-sec intervals. An average of all those measurements was obtained in order to determine the average $O_2^{\bullet-}$ concentration at a resting state for the mitochondria. Across the three different brain regions and across the three ages of 9, 15, and 22 months, the mitochondria from the Tg mice had an almost 2-fold

higher $O_2^{\bullet-}$ concentration as compared with mitochondria from wt mouse brains. Both genotypes maintained steady superoxide levels across regions. Student's t-test conducted on SigmaPlot 11.0 revealed a genotype significant difference ($p \leq 0.001$) across all ages and regions (Fig. 2A-C). When all three brain regions are combined and plotted across advancing age three-way ANOVA analysis indicated a significant genotype ($p=0.002$), age ($p \leq 0.001$), and region ($p<0.001$) effect (Fig. 3). Student's t-test indicated significant genotype effects with the levels of superoxide being higher in the Tg mouse mitochondria across all ages and different brain regions.

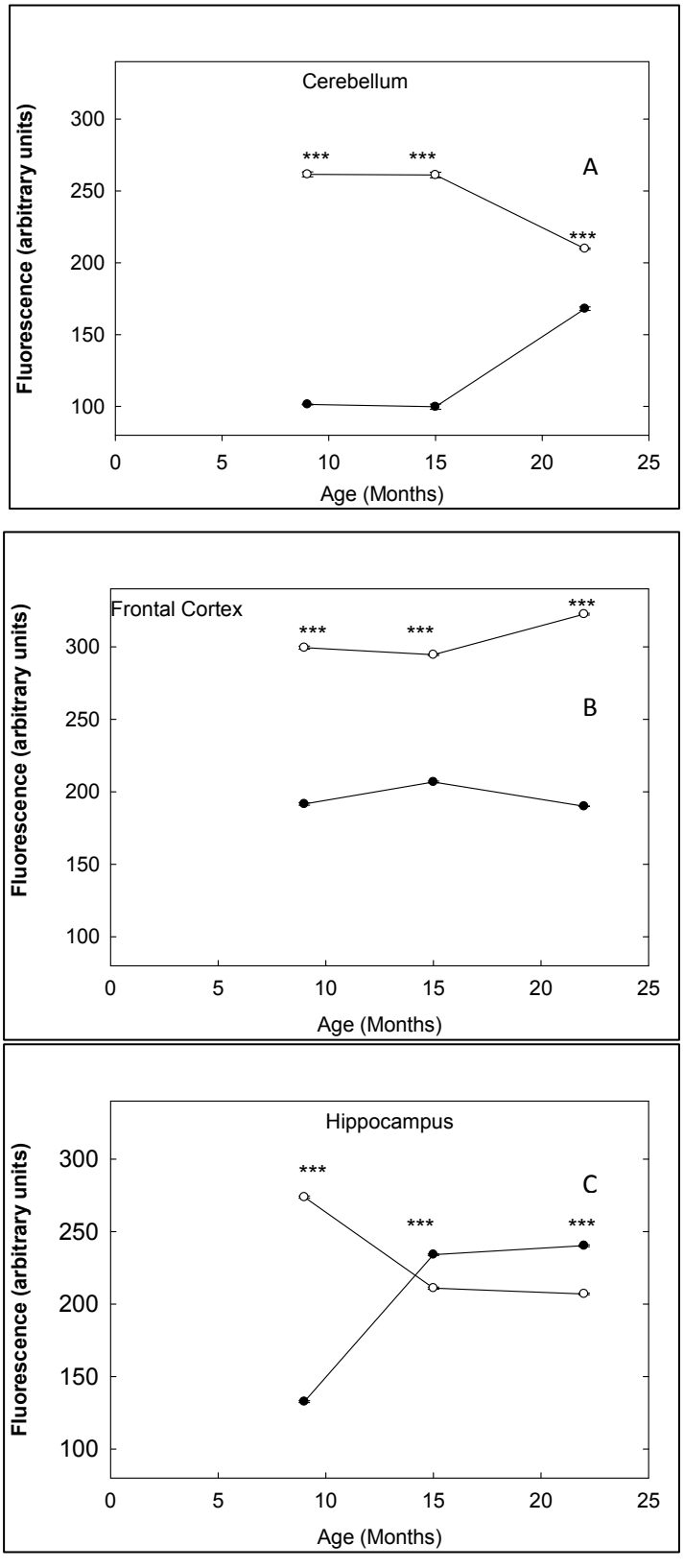

Figure 2 Superoxide levels across age of Tg and wt mice. Mitochondria were isolated from A) Cerebellum B) Frontal Cortex and C) Hippocampus. All experiments were performed using n=4 mice of each genotype. Dark circles indicate wt and open circles Tg mouse mitochondria. Students t-test indicated genotype significant effect*p≤0.001**

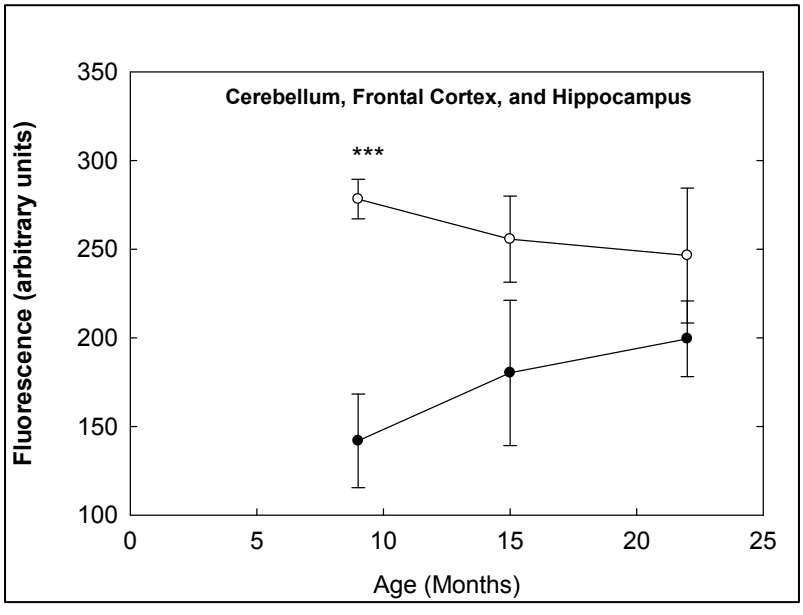

Figure 3 Superoxide levels across age of Tg and wt mice. Mitochondria were isolated from Cerebellum, Frontal Cortex, and Hippocampus and combined and treated as one sample. All experiments were performed using n=4 mice of each genotype. Dark circles indicate wt and open circles Tg mouse mitochondria. Three-way ANOVA analysis indicated a significant genotype ($p=0.002$), age ($p\leq0.001$), and region ($p<0.001$) effect.

Concentration of $O_2^{\bullet-}$ in the mitochondria from wt and Tg mice in the presence of glutamate/malate

ROS generation, a by-product of respiration, parallels metabolic rates (Brookes, Yoon et al. 2004). Having determined $O_2^{\bullet-}$ levels at baseline conditions, it was important to measure these levels after the addition of different substrates of the ETS. Our hypothesis was that energizing the ETS through either addition of glutamate/malate (NADH-generating) or succinate ($FADH_2$-generating) would lead to altered levels of $O_2^{\bullet-}$ as compared to baseline conditions and that brain mitochondria from Tg mice might respond differently compared to wt mice.

To estimate the amount of $O_2^{\bullet-}$ formed the average fluorescence measurements during the resting state were subtracted from the fluorescence values obtained at 240 secs of the kinetic assays and these measurements were plotted on a vertical bar graph (Fig. 4A-C). When the combined data from all regions and ages of the two genotypes were analyzed, the $O_2^{\bullet-}$ levels in the presence of glutamate/malate resulted in significant effects that were age ($p=0.003$), region ($p=0.049$) and genotype ($p=0.003$) dependent as determined by three-way ANOVA (Fig.4A-C). Only the mitochondria from the Tg mouse exhibited a significant age effect.

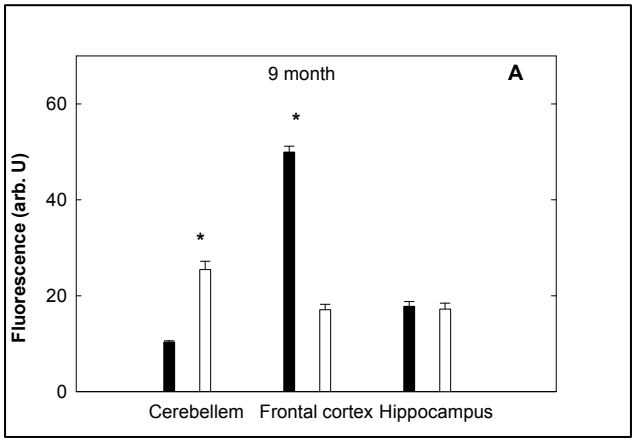

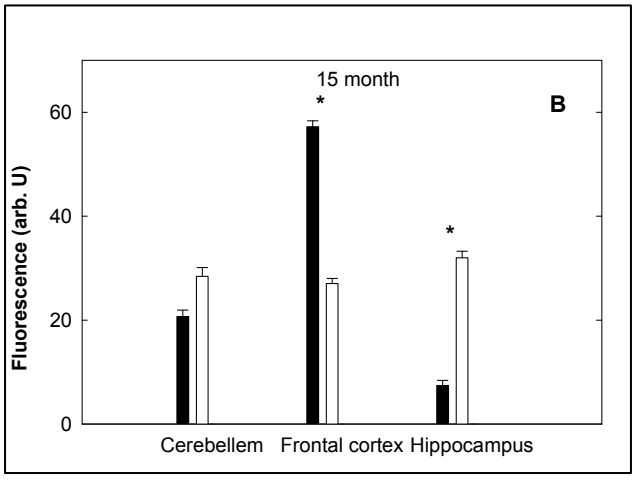

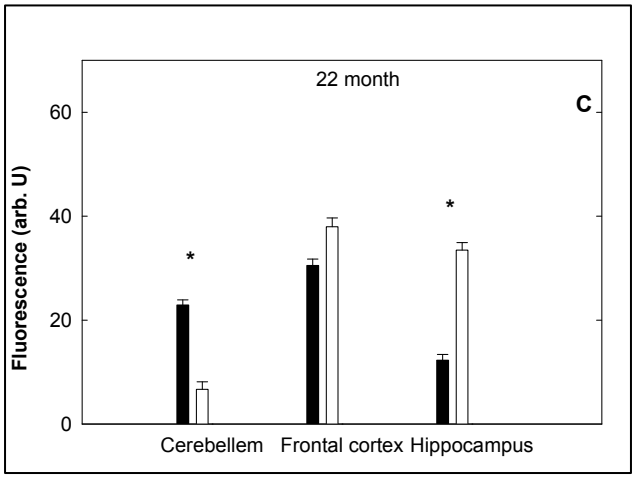

Figure 4 Superoxide levels in the presence of 5 mM glutamate/malate at A) 9 B) 15 C) 22 months. Mitochondria were isolated from cerebellum, frontal cortex, and hippocampus. All experiments were performed using n=4 of each genotype. Open bars indicate Tg and dark bars wt mouse mitochondria. Three-way ANOVA analysis indicated a significant genotype (p=0.003), age (p=0.03), and region (p=0.049) effect.

Concentration of $O_2^{\bullet-}$ in the mitochondria from wt and Tg mice in the presence of succinate

Superoxide fluorescence was also measured after the addition of 5 mM succinate for 3 min and at 15-sec intervals. The average fluorescence measurement during the resting state was subtracted from the values at 240 secs of the kinetic assays and these measurements were plotted on a vertical bar graph (Fig. 5A-C). Superoxide levels in the presence of succinate resulted in significant effects that were age ($p=0.008$), region ($p=0.032$) and genotype ($p=0.002$) dependent as determined by three-way ANOVA (Fig.5A-C). Both genotypes exhibited significant age effects and there were significant genotype differences dependent on the brain region. Student's t-test indicated significant genotype effect ($p<0.05$) in higher levels of $O_2^{\bullet-}$ in the mitochondria from Tg mouse as compared to wt at 9 month in the frontal cortex and hippocampus, at 15 months in the frontal cortex and at 22 months in the cerebellum. The mitochondria from wt cerebellum at 22 months had higher levels of $O_2^{\bullet-}$ as compared to Tg.

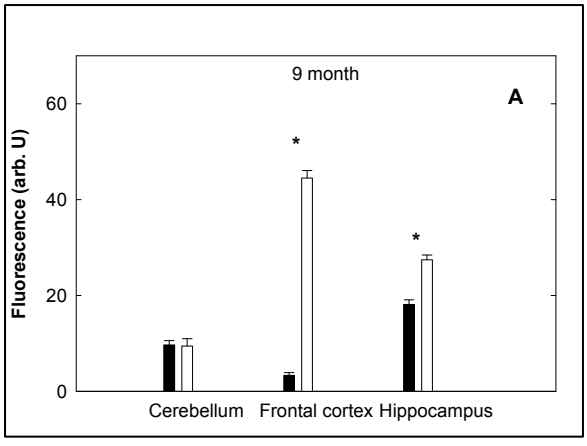

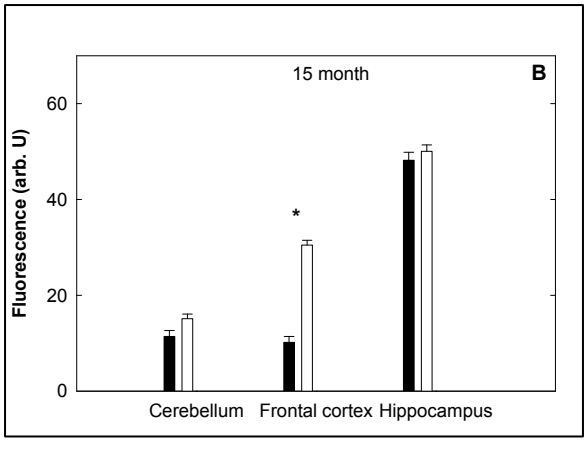

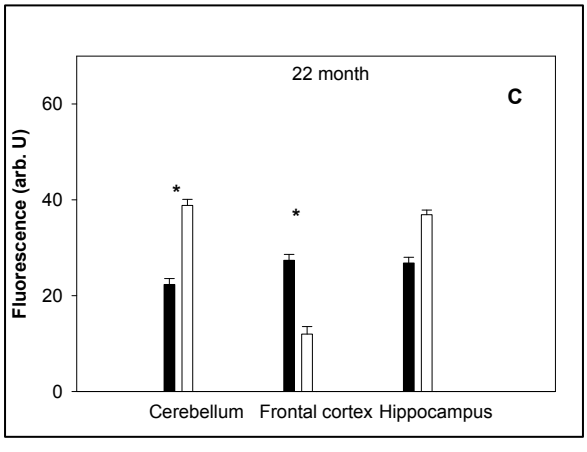

Figure 5 Superoxide levels in the presence of 5 mM succinate at A) 9 B) 15 C) 22 months. Mitochondria were isolated from cerebellum, frontal cortex, and hippocampus. All experiments were performed using n=4 of each genotype. Open bards indicated Tg and dark bards wt mouse mitochondria. Three-way ANOVA analysis indicated a significant genotype (p=0.002), age (p=0.008), and region (p=0.032) effect. Student's t-test p<0.05.

Baseline concentration of H_2O_2 in the mitochondria from wt and Tg mice

Hydrogen peroxide levels at resting conditions (no substrate addition) did not show any significant genotype differences. Both wt and Tg mice had similar levels and trends of H_2O_2 in the different brain regions and with advancing age. Both genotypes demonstrated a significant increase in H_2O_2 levels with advancing age as was determined by two-way ANOVA analysis (Fig.6A-C) ($p=0.014$). In addition, the levels of H_2O_2 were highest in the frontal cortex (Fig.6B) as compared to cerebellum and hippocampus (Fig.6A and 5C) ($p=0.027$).

Having determined H_2O_2 levels at resting conditions, these levels were also measured after the addition of different substrates of the respiratory chain. Activation of ETS through the addition of either glutamate/malate or succinate resulted in significant age, genotype, and region (Figs.4A-C & 5A-C) effects in O_2 levels; therefore, it was reasoned that H_2O_2 levels might also be altered. Both genotypes had a significant increase in H_2O_2 levels with advancing age as determined by three-way ANOVA ($p\leq0.001$).These increases were significantly region specific ($p\leq0.001$) for the different genotypes after the addition of glutamate/malate (5 mM) (Fig.7A-C). Specifically, the mitochondria from wt cerebellum mouse at 9 and 22 months had higher levels of H_2O_2 as compared to Tg and the mitochondria from wt hippocampus mouse at 9 months had higher levels as compared to Tg mouse. In the presence of succinate, significant

age (p=0.031), genotype (p=0.025), and region (p=0.047) effects were demonstrated by three-way ANOVA (Fig.8A-C). Specifically, both genotypes had significant increases in levels of H_2O_2 with age, and in the cerebellum the mitochondria from Tg mouse had higher levels of H_2O_2 at 9 months as compared to wt mitochondria while in the hippocampus at 9 months the mitochondria from wt hippocampus had higher levels as compared to Tg.

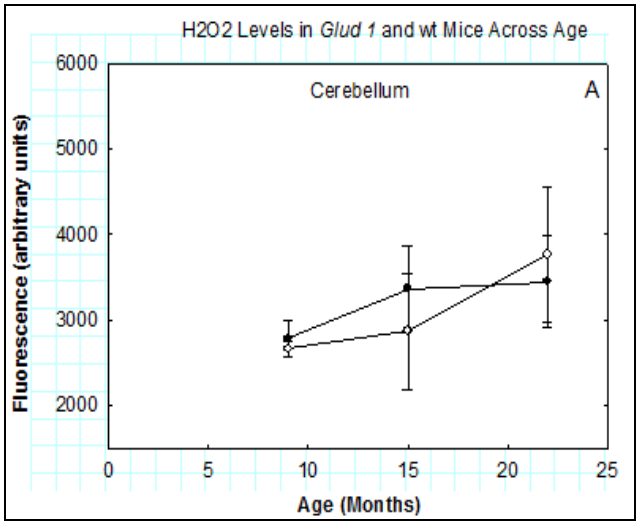

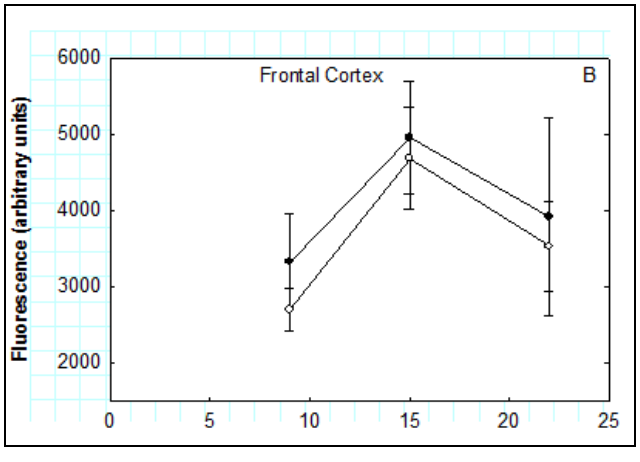

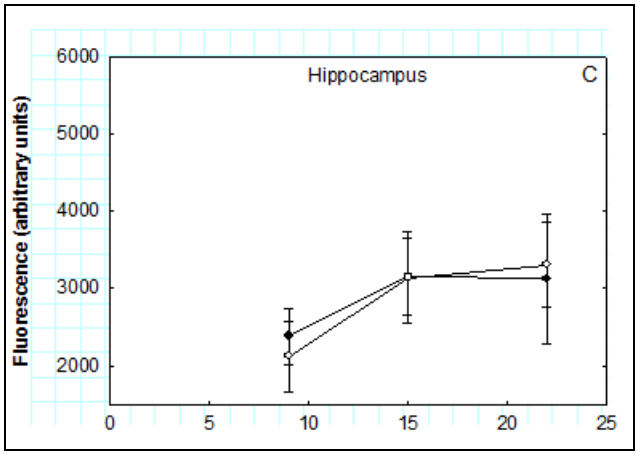

Figure 6 Hydrogen peroxide levels across age of Tg and wt mice. Mitochondria were isolated from A) Cerebellum B) Frontal Cortex and C) Hippocampus. All experiments were performed using n=4 mice of each genotype. Open circles indicate Tg and dark circles wt mouse mitochondria.

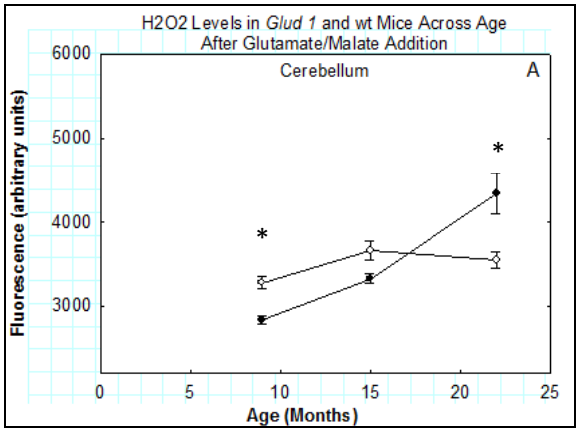

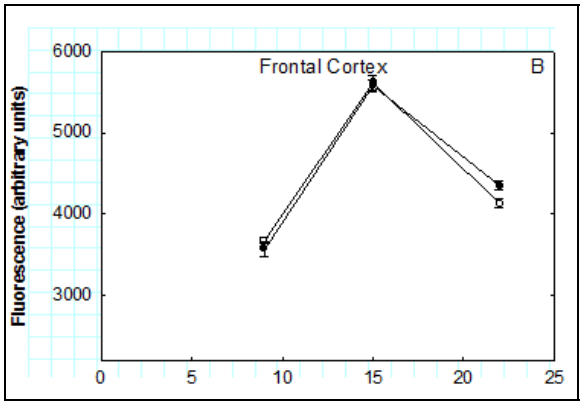

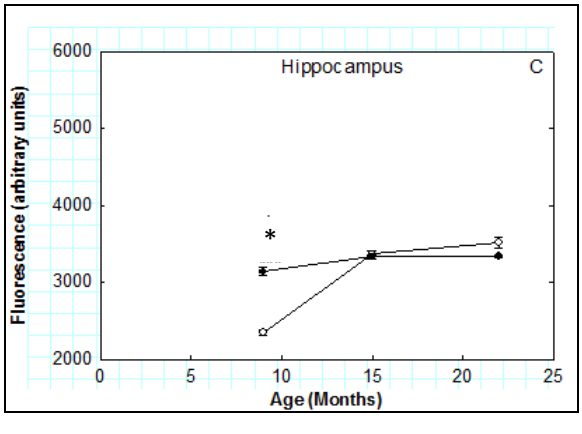

Figure 7 Hydrogen peroxide levels in the presence of 5mM glutamate/malate across age of Tg and wt mice. Mitochondria were isolated from A) Cerebellum B) Frontal Cortex and C) Hippocampus. All experiments were performed using n=4 mice of each genotype. Open circles indicate Tg and dark circles wt mouse mitochondria. Three-way ANOVA analysis resulted in significant increases in age ($p \leq 0.001$) in both genotypes and significant region effects ($p \leq 0.001$) in the mitochondria from cerebellum and hippocampus between wt and Tg mouse. Student's t-test* $p < 0.05$.

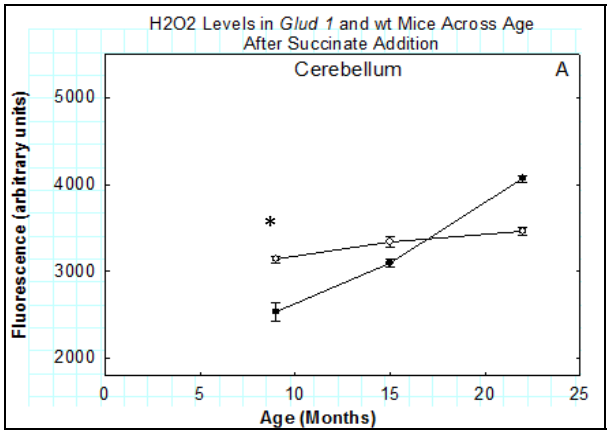

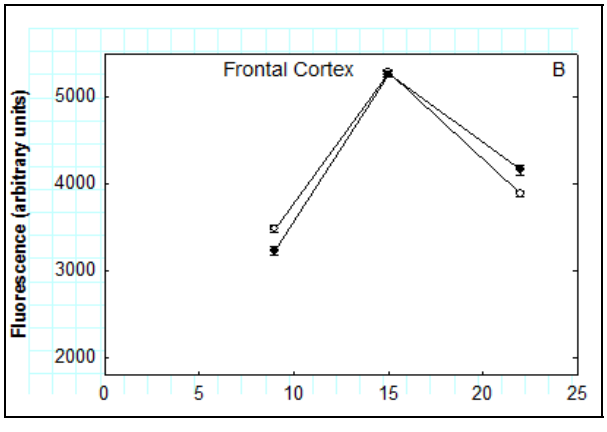

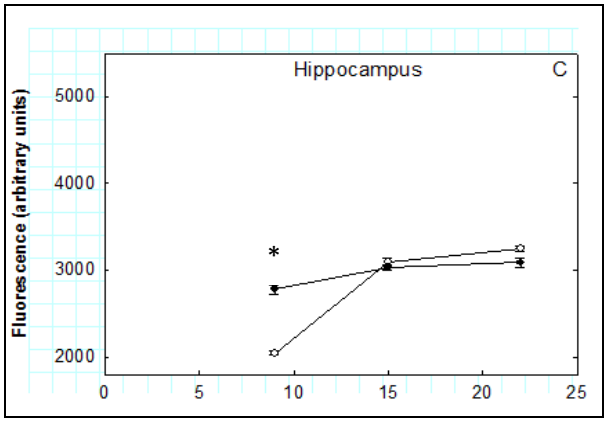

Figure 8 Hydrogen peroxide levels in the presence of 5mM succinate across age of Tg and wt mice. Mitochondria were isolated from A) Cerebellum B) Frontal Cortex and C) Hippocampus. All experiments were performed using n=4 mice of each genotype. Open circles indicate Tg and dark circles wt mouse mitochondria. Three-way ANOVA analysis resulted in significant increases in age (p=0.031) for both genotypes, significant region effects (p=0.047) and significant genotype effects (p=0.025).

5. DISCUSSION

Mitochondria are a main source of $O_2^{\bullet-}$ formation (Balaban and Ames 1998). Within mitochondria there are two main sites where $O_2^{\bullet-}$ generation occurs, complex I (NADH:ubiquinone reductase) (Turrens and Boveris 1980) and complex III (coenzyme Q : cytochrome *c* — oxidoreductase)((Boveris, Cadenas et al. 1976). With aging and in some age-associated diseases, there is an increase in ROS and the damage to cells associated with these processes might be a result of this increase (Balaban and Ames 1998) (Finkel and Holbrook 2000).

ETS activities, Ψ_m, and mitochondrial Ca^{2+} have been shown to be sources and regulators of ROS (Muller, Roberts et al. 2003) (Cleeter, Cooper et al. 1994) (Starkov and Fiskum 2003) (Turrens 1997) (St-Pierre, Buckingham et al. 2002). The over-expression of the GLUD1 protein lead to significant genotype differences in the bioenergetics of the ETS activities (chapter 2), mitochondrial Ca^{2+} homeostasis and Ψ_m (chapter 3); therefore we hypothesized that we would also observe differences in the levels of ROS. In addition, these significant differences were also demonstrated across age and different brain regions.

In chapter three we demonstrated significant genotype differences in Ψ_m. The generation of ROS has been shown to be exponentially dependent on Ψ_m (Starkov and Fiskum 2003). Chemical uncouplers have been shown to decrease ROS generation (Okuda, Lee et al. 1992)

and ROS has been shown to stimulate mitochondrial uncoupling (Echtay, ST-Pierre et al. 2002). These processes can function in a feedback loop (Brookes 1998) (Miwa and Brand 2003). Our results demonstrate that at baseline conditions (no substrate addition) there is a significant genotype difference in the levels of $O_2^{\bullet-}$ ($p \leq 0.001$) across all ages and regions. The Tg mice have higher levels of $O_2^{\bullet-}$ as compared to the wt mice. In our studies the levels of $O_2^{\bullet-}$ and the Ψ_m were two-fold higher in the Tg mitochondria as compared to wt and therefore support observations from other studies in which $O_2^{\bullet-}$ levels parallel Ψ_m (Fig. 9 and 10).

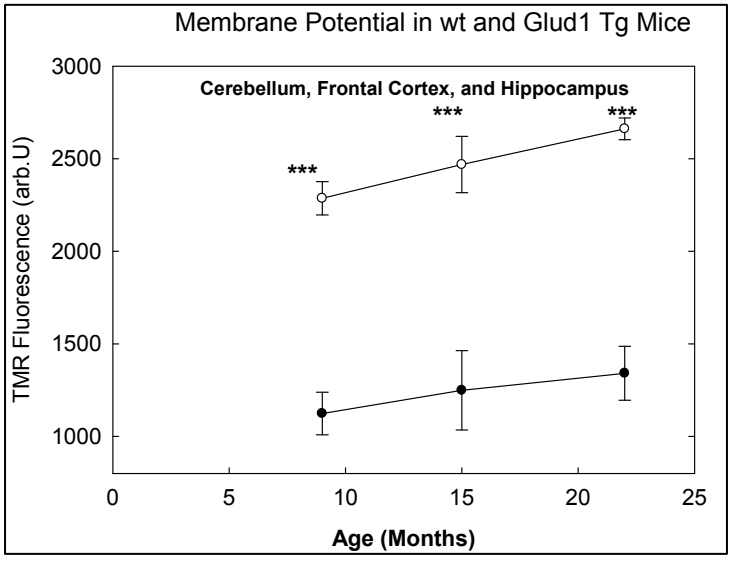

Figure 9 Membrane potential average across age of Tg and wt mice. Mitochondria were isolated from cerebellum, frontal cortex, and hippocampus and combined as one samples. All experiments were performed using n=4 mice of each genotype. Dark circles indicate wt and open circles Tg samples. ***=p≤0.001 (Student's t-test).

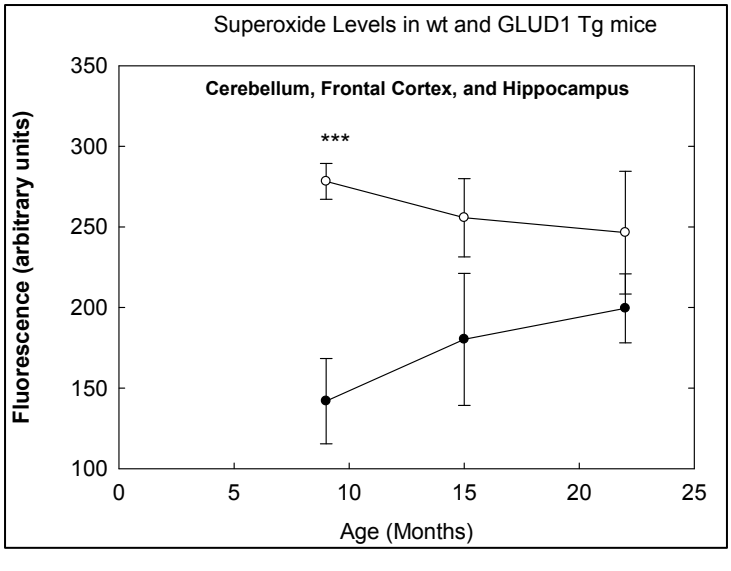

Figure 10 Superoxide levels across age of Tg and wt mice. Mitochondria were isolated from cerebellum, frontal cortex, and hippocampus and combined as one sample. All experiments were performed using n=4 mice of each genotype. Dark circles indicate wt and open circles Tg mouse mitochondria. ***=p≤0.001.

After the addition of either substrate, glutamate/malate or succinate, significant age, genotype, and region effects were demonstrated on superoxide levels. This data is similar to other studies where a correlation between respiration and ROS has been demonstrated. Specifically, increased activity of the ETS leads to increases in ROS as a result of mitochondrial ETC leak which occurs with the increased activity (Liu, Fiskum et al. 2002). However, our bioenergetic data did not correlate with our ROS data. A possible reason could be due that brain cells have adapted as a compensatory mechanism to reduce the generation of ROS, if there was to be an increase by increased respiration that is region specific.

Superoxide dismutase, which is the enzyme that catalyzes the dismutation of superoxide into oxygen and hydrogen peroxide, is differentially expressed in rat brain (Ledig, Fried et al. 1982). Specifically, it is expressed at higher concentrations in the cerebellum versus the frontal cortex or hippocampus. The lack of correlation between respiration state and ROS levels could be the result of differential superoxide dismutase expression.

It is known that the levels and activities of antioxidants increase with advancing age (Hussain, Slikker et al. 1995). If this is the case then any differences in $O_2^{\bullet-}$ levels between the genotypes observed at 9 months could be reduced with advancing age. In our data, we observed that with advancing age the Tg mitochondria $O_2^{\bullet-}$ levels decreased, while the wt mitochondria $O_2^{\bullet-}$ levels slightly increased (not

significant). These results might be the result of a compensatory mechanism exhibited in the Tg mitochondria to decrease $O_2^{\bullet-}$ levels, due to the already high levels. Integrated bioinformatics analyses studies conducted in our laboratory on transcriptomic data from Glud1 Tg mice revealed increased gene expression in genes associated with offering protection against oxidative stress (Wang, Bao et al. 2010).

In addition to using glutamate/malate as a substrate to energize mitochondria, we also measured $O_2^{\bullet-}$ levels in the presence of succinate which energizes electron transport chain activities through complex II. After addition of succinate in the 9 month mitochondria samples we noted no significant genotype differences, but we did observe significant region effects in the frontal cortex and hippocampus. In both of these regions there was a significant increase in the levels of $O_2^{\bullet-}$ indicating that there might be decreased antioxidant activity. In looking at our bioenergetics data (chapter 2) we observed significant genotype differences in complex II-III activity only in the frontal cortex and hippocampus as well. Specifically, in both of these regions the Tg mice had higher activity. Therefore, even though the Tg had higher electron activity this could have resulted in higher antioxidant activity as a protective mechanism of the cell. These data indicate that in the cerebellum activation of transport chain activities through complex II does not result in significant $O_2^{\bullet-}$ levels while activation of complex II in the frontal cortex and hippocampus leads to significant increases in the levels of $O_2^{\bullet-}$. In comparison to glutamate/malate which demonstrated

significant changes in superoxide levels across all brain regions. Providing for evidence that different brain regions are preferentially more susceptible to generation of $O_2^{\bullet-}$ through the activation of specific complexes.

In addition to measuring $O_2^{\bullet-}$ we measured H_2O_2 levels in the two genotypes, across the different brain regions, and in advancing age. At baseline conditions (no substrate) we observed no significant genotype differences. Studies have shown differential expression and activity of many antioxidants across different brain regions and with advancing age and therefore the concentration of $O_2^{\bullet-}$ are not parallel to that of H_2O_2. Specifically, an increase in $O_2^{\bullet-}$ will not necessarily result in an increase in H_2O_2. Overall, we did observe a significant increase in the levels of H_2O_2 at 15 months as compared to 9 month and again this could be attributed to an increase in antioxidant activity that has been documented with advancing age (Hussain, Slikker et al. 1995). After addition of glutamate/malate we observed significant genotype differences in the cerebellum and hippocampus at 9 months. We did not observe these differences at 15 or 22 months. In the cerebellum we did observe higher levels of $O_2^{\bullet-}$ in the Tg mice which could have led to the higher levels of H_2O_2. In addition, since antioxidant activity has been shown to be lowest at a younger age, then any significant genotype differences in $O_2^{\bullet-}$ levels in the younger age might disappear with advancing age due to an increase in antioxidant activity. The differential expression of antioxidants could also explain why there was

not a correlation between the $O_2^{\bullet-}$ data and the free intra-mitochondrial Ca^{2+} levels. In chapter three we demonstrated that free intra-mitochondrial Ca^{2+} levels only exhibited a significant genotype effect in one brain region at one age.

Overall, in chapter two we demonstrated significant genotypes effects in ETS activities and these effects were also demonstrated in chapter three with the Ψ_m measurements. However, there was not a direct correlation in the significant effects across different regions and ages as compared to the bioenergetics data. In chapter three we demonstrated that with advancing age free intra-mitochondrial Ca^{2+} levels increased, while mitochondrial Ca^{2+} uptake decreased. This type of opposite effect might be one of a compensatory mechanism of the cell to reduce the levels of free intra-mitochondrial Ca^{2+}; however, here was no correlation between the Ca^{2+} data and the $O_2^{\bullet-}$ data. In addition, the resting Ψ_m was two-fold higher in the Tg mitochondria as compared to the wt mitochondria and this data correlated with the $O_2^{\bullet-}$ data. Our data demonstrate that some correlations do exist; however, they are not consistent across regions or age. These differences could be due to one of the many compensatory and/or adaptive mechanism and/or pathways that the Tg mitochondria contain as a result of the lifelong exposure to glutamate. Our initial characterization of the Tg Glud1 mouse model in terms of bioenergetics, Ca^{2+} homeostasis, ROS generation together with our integrated bioinformatics analyses will help

elucidate further the adaptive and compensatory mechanism that exist and that are region and age specific.

OVERALL CONCLUSIONS

The following table lists a summary of the major differences between mitochondria isolated from wt and Tg mice, and among different brain regions.

1. Membrane potential higher in Tg vs. wt, across all regions and ages at resting conditions and tended to become higher during the aging process in the Tg mice.
2. Ca^{2+} uptake by glu/malate activated mitochondria and when Ca^{2+} concentrations were low (100 nM) decreased in all regions with advancing age and showed no genotype or regional differences.
3. Ca^{2+} uptake by glu/malate-activated mitochondria and when extra-mitochondrial Ca^{2+} concentrations were high (1 μM), as may occur in hyperglutamatergic states, was significantly more active in tg vs. wt in cerebellum and cortex, but declined substantially with age, reaching the same level of activity as that of wt mice at 22 mos.
4. There were no significant differences in Ca^{2+} uptake in glu/malate-activated mitochondria from the hippocampus when extramitochondrial

Ca^{2+} concentrations were at 1 μM.
5. There were no significant differences in any region in free Ca^{2+} concentration under resting conditions or when uptake was measured at low Ca^{2+} concentrations.
6. Superoxide levels at resting state were higher in Tg than wt across ages and tended to decrease with advancing age; hippocampus showed the least amount of differential superoxide accumulation.
7. Superoxide levels in tg mouse hippocampus increased with age in glu/malate-activated mitochondria, whereas they decreased with age in cerebellum and to some extent in frontal cortex.
8. Superoxide may be one of the signaling molecules in hippocampus and its source is likely from complex I and complex III.
9. ETS activities in Tg and wt mice that changed with age were: a) Complexes I-III decreased with age b) Complexes I-III had no significant genotype differences except at 9 mos in the cerebellum and cortex where the Tg mice had higher activity than the wt mice c) Complexes II-III increased with age and there was a genotype difference with the Tg mouse mitochondria being higher than the wt mitochondria, particularly at 9 mos in the cortex and hippocampus of the Tg mice d) Complex IV decreased with age but had no significant genotype or regional differences

The phenomenon of selective neuronal vulnerability refers to the differential sensitivity of neuronal cells to different types of stresses, i.e. glutamate induced toxicity. Specifically studies have demonstrated that hippocampal neurons are more sensitive or vulnerable to glutamate induced toxicity in comparison to other brain regions. Altered mitochondrial Ca^{2+} handling in the hippocampus as compared to other brain regions may be the mechanism resulting in the toxic effects. Our studies demonstrated that when a stress (1 μM excess mitochondrial Ca^{2+}) was applied to the mitochondria from hippocampal cells, Ca^{2+} uptake concentrations as compared to the cerebellum and frontal cortex regions were significantly lower. The inability of the mitochondria isolated from hippocampal neurons to take up Ca^{2+} may result in excess levels of Ca^{2+} in the cytosol and therefore toxic effects on the cell. The sensitivity of hippocampal neurons may be linked to the calcium handling. In addition, the age-related decreases in Ca^{2+} uptake, regardless of concentration of extra-mitochondrial Ca^{2+}, may be the determinant for age-related neuronal losses. The factor(s) that could be driving the differential Ca^{2+} regulation could be the result of significant genotype differences in membrane potential measurements as demonstrated in our studies. In addition, the differential formation of superoxide may be linked to altered sensitivity to the effects of Glud1 over-expression, especially by the fact that hippocampus neurons may be the ones that utilize superoxide for communication.

CITATIONS

Balaban, R. and B. Ames (1998). "The free radical theory of aging matures." Physiol Rev **78**: 547.

Boveris, A., E. Cadenas, et al. (1976). Biochem. J. **156**: 435-444.

Brookes, P. (1998). "Mitochondrial proton leak and superoxide generation: an hypothesis." Biochem Soc Trans **26**: S331.

Brookes, P., Y. Yoon, et al. (2004). "Calcium, ATP, and ROS: a mitochondrial love-hate triangle." Am J Physiol Cell Physiol **287**: C817-C833.

Budd, S. and D. Nicholls (1996). "Mitochondria, calcium regulation, and acute glutamate excitotoxicity in cultured cerebellar granule cells." J Neurochem **67**: 2282-2291.

Choksi, K., J. Nuss, et al. (2011). "Mitochondrial electron transport chain functions in long-lived Ames dward mice." Aging **3**: 1-14.

Cleeter, M., J. Cooper, et al. (1994). "Reversible inhibition of cytochrome c oxidase, the terminal enzyme of the mitochondrial respiratory chain, by nitric oxide. Implications for neurodegenerative diseases." FEBS Lett **345**: 50-54.

Echtay, K. R., D, J. ST-Pierre, et al. (2002). "Superoxide activates mitochondrial uncoupling proteins." Nature **15**: 96-99.

Finkel, T. and N. Holbrook (2000). "Oxidants, oxidative stress and the biology of ageing." Nature **408**: 239.

Gnaiger, E. (2009). "Mitochondrial Pathways through Complexes I + II: Convergent electron transport at the Q-junction and additive effect of substrate combinations." Mitochondrial pathways and respiratory control: 21-33.

Gomez, L., J. Monette, et al. (2009). "Supercomplexes of the mitochondrial electron transport chain decline in the aging rat heart." Arch Biochem Biophys **1**: 30-35.

Hussain, S., W. Slikker, et al. (1995). "Age-related changes in antioxidant enzymes, superoxide dismutase, catalse, glutathione peroxidase and glutathione in different regions of mouse brain." International Journal of Developmental Neuroscience **13**: 811-817.

Khodorov, B. (2003). "Glutamate-induced deregulation of calcium homeostasis and mitochondrial dysfunction in mammlian central neurons." Progress in Biophysics and molecular biology **86**: 279-351.

Kumaran, S., M. Subathra, et al. (2004). "Age-associated decreased activities of mitochondrial electron transport chain complexes in heart and skeletal muscle: role of L-cartinite." Chemicobiological interactions **148**: 11-18.

Ledig, M., R. Fried, et al. (1982). "Regional distribution of superoxide dismutase in rate brain during postnatal development." Developmental Brain Research **4**: 333-337.

Liu, Y., G. Fiskum, et al. (2002). "Generation of reactive oxygen species by the mitochondrial electron transport chain." Journal of Neurochemistry **80**: 780-787.

Mailer, K. (1990). "Superoxide radical as electron donor for oxidative phosphoryaltion of ADP." Biochem Biophys Res Commun **170**: 59-64.

Maj, M., S. Raha, et al. (2004). "Regulation of NADH/CoQ Oxidoreductase: Do phosphorylation events affect activity?" The Protein Journal **23**: 25-32.

Miwa, S. and M. Brand (2003). "Mitochondrial matrix reactive oxygen species production is very sensitive to mild uncoupling. ." Biochem Soc Trans **31**: 1300-1301.

Muller, F., A. Roberts, et al. (2003). "Architecture of the Qo site of the cytochrome bc1 complex probed by superoxide " Biochemistry **42**: 6493-6499.

Okuda, M., H. Lee, et al. (1992). "Comparison of the effect of a mitochondrial uncoupler, 2,4-dinitrophenol and adrenaline on oxygen radical production in the isolated perfused rat liver. ." Acta Physiol Scand **145**: 159-168.

Ontko, J. (1966). "Genesis of liver mitochondria in the neonatal rat." Life Sciences **5**: 817-825.

Raha, S., A. Myint, et al. (2002). "Control of oxygen free radical formation from mitochondrial complex I: roles for protein kinase A and pyruvate dehydrogenase kinase." Free Radic. Biol. Med **32**: 421-430.

Sarnoska, A. (2002). "Application of organotypic hippocampal culture for study of selective neuronal death." Neuropathol **40**: 101.

St-Pierre, J., J. Buckingham, et al. (2002). "Topology of superoxide production from different sites in the mitochondrial electron transport chain." J Biol Chem **277**: 44784-44790.

Starkov, A. and G. Fiskum (2003). "Regulation of brain mitochondrial H2O2 production by membrane potential and NAD(P)H redox state." Journal of Neurochemistry **86**: 1101-1107.

Turrens, J. (1997). "Superoxide production by the mitochondrial respiratory chain." Biosci Rep **17**: 3-8.

Turrens, J. and A. Boveris (1980). Biochem. J. **191**: 421-427.

Wang, X., X. Bao, et al. (2010). "Transcriptomic respoonses in mouse brain exposed to chronic excess of the neurotransmitter glutamate." BMC Genomics **11**: 1-19.

Wang, X., R. Pal, et al. (2005). "High intrinsic oxidative stress may underlie selectie vulnerability of the hippocampal CA1 region." Brain Res. **140**: 120-126.

Wang, X., A. Zaidi, et al. (2009). "Genomic and biochemical approaches in the discovery of mechanisms for selective neuronal vulnerability to oxidative stress." BMC Neurosci. **10**: 12.

Wilde, G., A. Pringle, et al. (1997). "Inflammation as a causative factor in the aetiology of Parksinon's disease." Br. J. Pharmacol. **150**: 963-976.

Wirtz, S. and M. Schuelke (2011). "Region-specific expression of mitochondrial complex I during murine brain development." PLoS ONE.

Chapter Five: Future Directions

1. CHAPTER TWO

In chapter two we measured electron transport system activities in the two genotypes, among different brain regions, and with advancing age. Three-way ANOVA analysis identified significant genotype effects in complex I-III activity in mitochondria from the frontal cortex and cerebellum at 9 months and complex II-III in the frontal cortex and hippocampus brain regions at 9 months. To determine specifically which complex was leading to the differences we measured complex I and complex II activities separately. At the current time; however, complex I and complex II activity was only assayed in 9 month cerebellum and frontal cortex samples. Looking at complex I and complex II activities separately in all of the ages and different brain regions needs to be carried out to determine which complex is involved in the altered bioenergetics and whether the separate complex activity is similar to the coupled complex activity. Once the exact complex/s leading to the altered bioenergetics between the two genotypes is determined further work should be carried out in determining the mechanism and pathway involved in the differential genotype dependent bioenergetics. One approach, which we preliminarily began to address, is to measure the protein levels of all of the protein complexes. We began this work by carrying out ELISA assays and measuring the protein concentration of Complex I across the different brain regions and with advancing age. This should also be carried out for the remaining protein complexes of the

ETS. If no differences in protein concentrations are observed then the differences in bioenergetics may be attributed to differences in enzymatic activity and not protein levels. The next step will be to investigate the pathway(s) leading to enzyme activity regulation. Studies have shown that there are several mechanisms which lead to regulation of electron transport system complexes including phosphorylation, substrate limitation, and calcium regulation (Maj, Raha et al. 2004) (Phillips, Covian et al. 2012). Taking our preliminary data showing altered Complex I-III, Complex I, and Complex II-III bioenergetics between the two genotypes, I feel that further work should be carried out investigating the mechanism of regulation of Complex I in the Tg mice versus the wt. My hypothesis is that complex I will be the major, if only contributor leading to the altered bioenergetics between the two genotypes. This hypothesis is based on our own findings and other research which has demonstrated that complex I is the main contributor in altering electron transport system activities and leading to Ca^{2+} and the generation of ROS. Based on these findings Complex I has been labeled a "pacemaker" of aging and thought to play a pivotal role in age-associated diseases (Maj, Raha et al. 2004). Specifically, a major mechanism of complex I activity is through post-translational modification processes such as phosphorylation. Studies have demonstrated that pyruvate dehydrogenase kinase (PDK) decreases complex I activity through phosphorylation while protein kinase A (PKA) increases its activity (Yadava, Potluri et al. 2008) (Phillips, Covian et al. 2012). Further worked should be carried out to determine phosphorylation states of complex I in the wt versus Tg sample. Specifically, *in vitro* phosphorylation of complex I in mitochondrial pellets can be carried out by

incubating the protein with [y-^{32}P]ATP in the presence and in the absence of cAMP and then analyzed by SDS-PAGE and autoradiography. If any significant differences are demonstrated in the levels of subunit phosphorylation then further work can be carried out to determine the levels of the kinases in the samples. Determining if any kinases, specifically PDK or PKA are up or down-regulated will aid in determining the kinases involved in the phosphorylation. Going even further into the mechanism of regulation, calcium has been shown to be involved in altering levels and activities of specific kinases (Phillips, Covian et al. 2012). Further work can be carried out where calcium concentrations are altered in the mitochondrial samples and then measure complex phosphorylation of complex I again. All of the experiments thus far all dive further into elucidating the mechanism of complex I regulation, however, one approach before beginning any of these experiments could be to ensure that bioenergetics are differentially altered in the two genotypes by another type of assay. Measuring electron transport chain activities in blue native polyacrylamide gel electrophoresis has been a very successful technique carried out by many laboratories (Jung, Higgins et al. 2000). Carrying out these assays will provide for further support for the altered bioenergetics we observed in our biochemical assays.

2. CHAPTER THREE

In chapter three we observed significant differences in calcium concentrations and calcium uptake in isolated mitochondrial samples under different conditions, baseline (no substrate) and after addition of a substrate (glutamate/malate or succinate). At this point all of these assays were carried out *in vitro* and further work should be carried out *in vivo.* It will be important to

determine whether these significant differences are also demonstrated *in vivo* since many studies have demonstrated differences in calcium concentrations based on the type of sample being used. Specifically, studies have shown that mitochondria in an *in vivo* setting respond more efficiently and faster to cytosol calcium concentrations due to their increased capacity to sense the calcium ions more efficiently in this type of setting. Therefore assays should be carried out where intra-mitochondrial calcium, cytosol calcium levels, and calcium uptake is measured in living cells using the calcium sensitive photoprotein aequorin specifically targeted to the mitochondria (Pinton, Rimessi et al. 2007) (Rizzuto, Brini et al. 1995) (Rizzuto, Pinton et al. 1998). If the calcium data *in vivo* supports what was demonstrated *in vitro* then further work should be carried out to determine if and how calcium is involved and leading to altered bioenergetics. Specifically, calcium is thought to stimulate or be involved in altering bioenergetics by allosteric activation of pyruvate dehydrogenase, isocitrate dehydrogenase, and alpha-ketoglutarate dehydrogenase (McCormack and Denton 1993). Assays should be carried out to quantitatively measure the activity of the above dehydrogenases in the different genotypes, across the different brain regions, and with advancing age. In addition, different concentrations of calcium can be added to determine the direct effect of calcium on the dehydrogenases activity, but more importantly to determine whether the two genotypes respond differently to the altered calcium levels.

In chapter three we also demonstrated significant genotype differences in the potential difference across the mitochondrial inner membrane. Further work should be carried out to determine the mechanism leading to the difference in

membrane potential. Specifically, many studies have demonstrated that calcium concentrations and calcium uptake contribute to the potential difference therefore assays should be carried out where the membrane potential is measured in the presence of varying concentrations of calcium (Brookes, Yoon et al. 2004).

3. CHAPTER FOUR

In chapter four we demonstrated that there were significant genotypes differences in the concentrations of reactive oxygen species. Further work should be carried to determine whether the results we demonstrated *in vitro* are also seen *in vivo.* Specifically, superoxide levels should be measured in cells using chemilumigenic probes (Li, Zhu et al. 1999). If the *in vivo* data supports the *in vitro* data then further work should be carried out to determine the mechanism or factors involved in the altered levels of ROS. Specifically, assays should be carried out where the concentrations of calcium are altered and the ROS levels measured. Many studies have demonstrated that calcium regulates ROS generation; therefore; it will be pivotal in determining whether this is also the factor leading to the altered ROS generation in the Tg mice (Yan, Wei et al. 2006). In addition, our studies demonstrated that across different brain regions and with advancing age there were significant differences in the generation and break down of superoxide across a kinetic time plot. Many studies have demonstrated that there are differences in the levels and activities of many antioxidants that are tissue and age specific (Hussain, Slikker et al. 1995). Further work should be carried out to determine whether the levels and activities of specific antioxidants, specifically superoxide dismutase, are altered across the

different brain regions, with advancing age, and between the two genotypes. Changes in the activities of these antioxidants will aid in elucidating the mechanism of action that cells in the Tg mice, in different brain regions, or with advancing age use to decrease the levels of ROS and therefore use as a compensatory mechanism to decrease damage to the cell.

CITATIONS

Brookes, P., Y. Yoon, et al. (2004). "Calcium, ATP, and ROS: a mitochondrial love-hate triangle." Am J Physiol Cell Physiol **287**: C817-C833.

Hussain, S., W. Slikker, et al. (1995). "Age-related changes in antioxidant enzymes, superoxide dismutase, catalse, glutathione peroxidase and glutathione in different regions of mouse brain." International Journal of Developmental Neuroscience **13**: 811-817.

Jung, C., C. Higgins, et al. (2000). "Measuring the quantity and activity of mitochondrial electron transport chain complexes in tissues of central nervous system using blue native polyacrylamide gel electrophoresis." Biochemistry **286**: 214-223.

Li, Y., H. Zhu, et al. (1999). "Detection of mitochondria-derived reactive oxygen species production by the chemilumigenic probes lucigenin and luminol." Biochimica et Biophysica Acta **1428**: 1-12.

Maj, M., S. Raha, et al. (2004). "Regulation of NADH/CoQ oxidoreductase: Do phosphorylation events affect activity?" The Protein Journal **23**: 25-32.

McCormack, J. and R. Denton (1993). "Mitochondrial calcium transport and the role of mitochondrial calcium in the regulation of energy metabolism." Dev Neurosci **15**: 165-173.

Phillips, D., R. Covian, et al. (2012). "Regulation of oxidative phosphorylation complex activity: effect of tissue specific metabolis stress within an allometric series and acute changes in workload." Am J Physiol Regul Integr Comp Physiol.

Pinton, P., A. Rimessi, et al. (2007). "Biosensors for the detection of calcium and pH." Methods Cell Biol **80**: 297-325.

Rizzuto, R., M. Brini, et al. (1995). "Photoprotein-mediated measurement of calcium ion concentration in mitochondria of living cells." Methods Enzymol **260**: 417-428.

Rizzuto, R., P. Pinton, et al. (1998). "Close contacts with the endoplasmic reticulum as determinants of mitochondrial calcium responses." Science **280**: 1763-1766.

Yadava, N., P. Potluri, et al. (2008). "Investigations of the potential effects of phosphorylation of the MWFE and ESSS subunits on complex I activity and assembly." The International Journal of Biochemistry and cell biology **40**: 447-460.

Yan, Y., C. Wei, et al. (2006). "Cross-talk between calcium and reactive oxygen species signaling." Acta Pharmacologica Sinica **27**: 821-826.